GEOMAR REPORT

GEOMAR

Helmholtz-Zentrum für Ozeanforschung Kiel

RV POSEIDON Fahrtbericht / Cruise Report POS518

Baseline Study for the Environmental Monitoring of Subseafloor CO_2 Storage Operations

Leg 1: Bremerhaven – Bremerhaven (Germany)
25.09.-11.10.2017

Leg 2: Bremerhaven – Kiel (Germany)
12.10.-28.10.2017

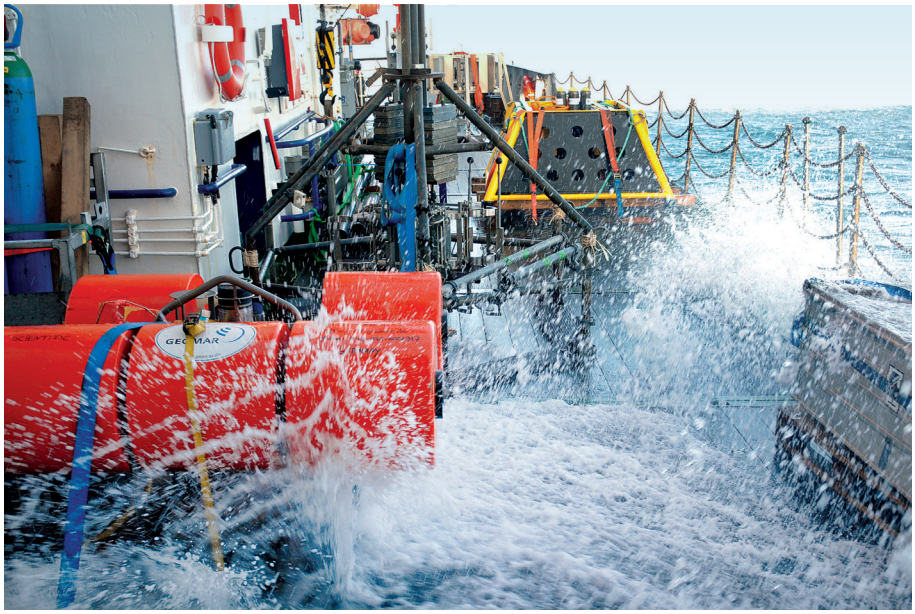

Berichte aus dem GEOMAR
Helmholtz-Zentrum für Ozeanforschung Kiel

Nr. 40 (N. Ser.)

January 2018

GEOMAR

Helmholtz-Zentrum für Ozeanforschung Kiel

RV POSEIDON Fahrtbericht / Cruise Report POS518

Baseline Study for the Environmental Monitoring of Subseafloor CO_2 Storage Operations

Leg 1: Bremerhaven – Bremerhaven (Germany)
25.09.-11.10.2017

Leg 2: Bremerhaven – Kiel (Germany)
12.10.-28.10.2017

Berichte aus dem GEOMAR
Helmholtz-Zentrum für Ozeanforschung Kiel

Nr. 40 (N. Ser.)

January 2018

GEOMAR
Helmholtz-Zentrum für Ozeanforschung Kiel

Das GEOMAR Helmholtz-Zentrum für Ozeanforschung Kiel ist Mitglied der Helmholtz-Gemeinschaft Deutscher Forschungszentren e.V.

The GEOMAR Helmholtz Centre for Ocean Research Kiel is a member of the Helmholtz Association of German Research Centres

Herausgeber / Editors:
Peter Linke and Matthias Haeckel

GEOMAR Report
ISSN Nr.. 2193-8113, DOI 10.3289/GEOMAR_REP_NS_40_2018

Helmholtz-Zentrum für Ozeanforschung Kiel / Helmholtz Centre for Ocean Research Kiel
GEOMAR
Dienstgebäude Westufer / West Shore Building
Düsternbrooker Weg 20
D-24105 Kiel
Germany

Helmholtz-Zentrum für Ozeanforschung Kiel / Helmholtz Centre for Ocean Research Kiel
GEOMAR
Dienstgebäude Ostufer / East Shore Building
Wischhofstr. 1-3
D-24148 Kiel
Germany

Tel.: +49 431 600-0
Fax: +49 431 600-2805
www.geomar.de

Table of Contents

1 Summary

Peter Linke, Matthias Haeckel

Poseidon cruise 518 (leg 1 and 2) took place in the framework of the Horizon 2020 project STEMM-CCS of the EU. The project's main goal is to develop and test strategies and technologies for the monitoring of subseafloor CO_2 storage operations. In this context a small research-scale CO_2 gas release experiment is planned for 2019 in the vicinity of the Goldeneye platform located in the British EEZ (central North Sea). Cruise POS518 aimed at collecting necessary oceanographic and biogeochemical baseline data for this release experiment.

During Leg 1 ROV PHOCA was used to deploy MPI's tool for high-precision measurements of O_2, CO_2 and pH in the bottom water at Goldeneye. In addition, ROV push cores and gravity cores were collected in the area for sediment biogeochemical analyses, and video-CTD casts were conducted to study the water column chemistry. The stereo-camera system and a horizontally looking multibeam echosounder, both, for determining gas bubble emissions at the seafloor were deployed at the Figge Maar blowout crater in the German Bight. Investigations were complemented by hydroacoustic surveys detecting gas bubble leakages at several abandoned wells in the North Sea as well as the Figge Maar. Surface water alkalinity as well as CH_4, CO_2, and water partial pressures in the air above the sea surface were measured continuously during the cruise.

During Leg 2 three different benthic lander systems were deployed to obtain baseline data of oceanographic and biogeochemical parameters for a small research-scale CO_2 gas release experiment planned for 2019. The first lander was equipped with an acoustic Doppler current profiler (ADCP), a CTD and an O_2 optode. It was deployed for 6 days close to Goldeneye to obtain high resolution data which can be linked to the long-term measurements of the NOC-Lander. This lander is equipped with a suite of sensors to monitor temperature, conductivity, pressure, current speed and direction, hydro-acoustic, pH, pCO_2, O_2 and nutrients over a period of about 10 months with popup telemetry units for data transmission via IRIDIUM satellite telemetry every 3 months. Two short-term deployments of the Biogeochemical Observatory (BIGO) were conducted to study the molar ratio between oxygen and CO_2-fluxes at the seafloor. Sediment cores obtained by gravity and multi corer were collected for sediment biogeochemical analyses and video-CTD casts were used to study the chemistry of the water column.

2 Research Programme / Objectives

Peter Linke, Matthias Haeckel

Natural marine ecosystems of shelf seas such as the North Sea are in constant flux as they respond to daily/seasonal environmental drivers (e.g. ocean currents, tidal variation, land-sea interaction, water column stratification, phytoplankton blooms, nutrient supply variations; e.g. Rovelli et al., 2016; Richier et al., 2014; Thomas et al., 2009, Turrel et al., 1992), stochastic natural (e.g. cyclonic events; e.g. Fettweis et al., 2012) and anthropogenic disturbances (e.g. trawling, oil and gas production, sand extraction, or Carbon Capture and Storage). These drivers also strongly affect biogeochemical exchange processes (fluxes) at the seafloor, within the water column, and at the sea surface (Wakelin et al., 2012). Moreover, the response of the natural system to even one single driver can be highly variable (Artioli et al., 2014). This can be demonstrated e.g. by the variability of the natural flux of CO_2 across the sediment-seawater interface. Due to benthic degradation of organic matter the flux can vary by several orders of magnitude (~ 1-1000 g CO_2 m^{-2} yr^{-1}; e.g. Luff and Moll, 2004).

Consequently, strong efforts are needed to determine an effective environmental baseline in order to provide the data needed to discriminate the potential direct signals of unintended CCS emissions from those caused by other natural or man-made drivers (e.g. Wallmann et al., 2015; Blackford et al., 2015). Cruise POS518 will help us to investigate the natural variability of subsea biogeochemical and oceanographic parameters in 2017.

Specifically, the following goals of STEMM-CCS are addressed:

(1) Define and measure sensitive, but robustly measurable environmental background parameters that are indicative for potential subsea CO_2 leakage.

(2) Provide water column measurements of trace gases, nutrients, and carbonate chemistry variables to assess baseline conditions in the study area and collect geochemical porewater data under natural (baseline) conditions to provide a quantitative, process-based interpretation of porewater and benthic fluxes by state-of-the-art numerical modelling. The baseline data is also needed for analysing the CO_2 release experiments, which will be conducted in 2019 in the same area.

(3) Test newly designed benthic chambers, novel sensors, and hydroacoustic detection systems for measuring benthic and pelagic carbon fluxes, i.e. by using lab-on-the-chip technology, optodes, membrane inlet mass spectrometry, 3D-visual bubble imaging, and multibeam echosounder quantification.

3 Participant Lists

3.1 Leg 1

Scientific Participants		**Crew of RV POSEIDON**	
Andrea Bodenbinder	Gas / water / sediment chemistry	Matthias Günther	Captain
Matthias Bodendorfer	ROV PHOCA	Hero Nannen	1st Officer
Christoph Böttner	Hydroacoustics	Sebastian Pengel	2nd Officer
Patrick Cuno	ROV PHOCA	Hans-Jörg Freund	Lead Engineer
Matthias Haeckel	Chief Scientist, Geochemistry	Carsten Pieper	2nd Engineer
Dirk Koopmans*	Eddy covariance tool	Volker Blunck	Electrician
Thorge Matthiessen	ROV PHOCA	Felix Meyer	Engine
Martin Pieper	ROV PHOCA	Ralf Meilung	Ship Mechanic
Mark Schmidt	gas + water chemistry	Frank Schrage	Bosun
Inken Suck	ROV PHOCA	Merlin Till Pleuler	Ship Mechanic
Tim Weiß	GasQuant, Bubble Box, Picarro	Ronald Kuhn	Ship Mechanic
		Bernd Rauh	Ship Mechanic
Affiliation:		Marius Kruse	Ship Mechanic
GEOMAR		Patrick Kosanke	Cook
*MPI Bremen		Bernd Gerischewski	Steward

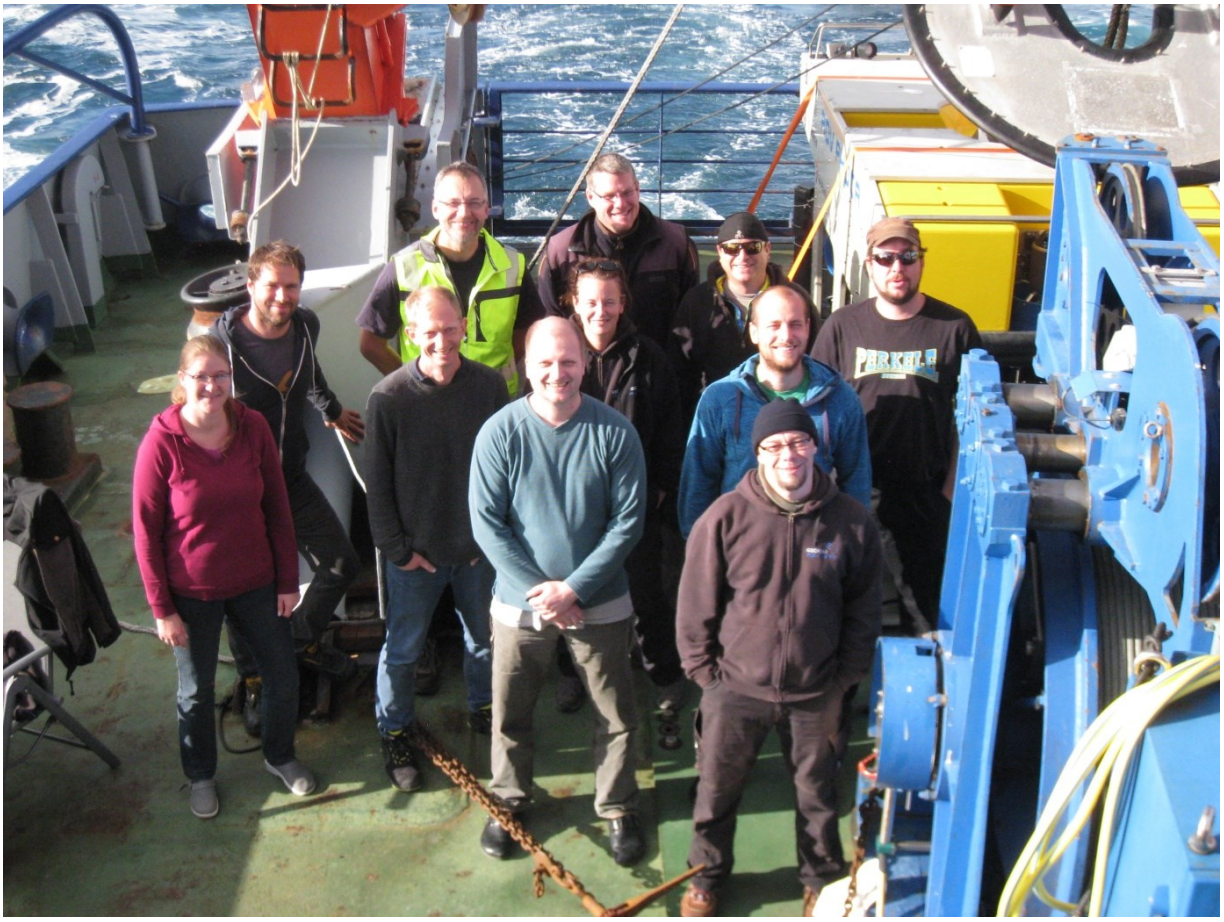

Fig. 1: Scientific participants of Leg 1.

3.2 Leg 2

Scientific Participants		**Crew of RV POSEIDON**	
Andy Dale	Sediment chemistry	Matthias Günther	Captain
Mario Esposito	Water chemistry, sensors	Helge Volland	1st Officer
Anita Flohr*	Sediment chemistry	Sebastian Pengel	2nd Officer
Dominik Jasinski	Water chemistry, sensors	Kurre Klaas Kröger	Lead Engineer
Peter Linke	Chief Scientist, Geochemistry	Carsten Pieper	2nd Engineer
Asmus Petersen	Lander, coring	Volker Blunck	Electrician
Gabriele Schüssler	Chemistry	Felix Meyer	Engine
Stefan Sommer	MIMS, chemistry	Ralf Meilung	Ship Mechanic
Regina Surberg	Chemistry	Frank Schrage	Bosun
Matthias Türk	Lander electronics	Merlin Till Pleuler	Ship Mechanic
Christine Utecht	MIMS, chemistry	Ronald Kuhn	Ship Mechanic
		Bernd Rauh	Ship Mechanic
Affiliation:		Magnus Kruse	Ship Mechanic
GEOMAR		Patrick Kosanke	Cook
*NOC		Bernd Gerischewski	Steward

Fig. 2: Scientific participants of Leg 2.

4 Cruise Narrative

4.1 Leg 1

Matthias Haeckel

The scientific party of leg 1 boarded RV Poseidon on Monday, 25th September to unload their equipment and install it in the ship's laboratories. Cruise preparations were concluded the next day with a harbour trial of ROV PHOCA and we set sail through the river Weser mouth on Wednesday morning at 7:00 UTC. Having a calm sea we went straight to our first stations for hydroacoustic investigations of possible gas seepage at abandoned wells in the German Bight. At the 54-year old blowout crater Figge Maar, located about 20 nm north of the island Juist, we saw indications for vigorous gas seepage in the hydroacoustic data, so-called flares. This blowout structure is about 17 m deep, relative to the surrounding seafloor, and about 500 m across. After mapping the seafloor feature overnight, we headed north to the "Entenschnabel", the outer part of Germany's EEZ in the North Sea, where we surveyed well B-11/3 for about 1 hour in the evening of 28th September. The survey included the nearby coordinate of a methane anomaly reported by Alan Judd several years ago, however, we did not see any gas flares in the multibeam data.

After midnight we crossed into the UK sector. On our way to the main working area in the vicinity of the Goldeneye platform, we surveyed more abandoned wells for gas emissions, which were evident by gas flares at the seafloor. In addition, a natural seep was discovered above a buried salt dome, next to wells 30/01a-7 and 30/01f-8. Around 6:00 UTC on Saturday, 30th September we arrived at Goldeneye. After two video-CTD casts and three gravity cores, the wave conditions had improved sufficiently in the afternoon around 13:00 UTC to allow diving with ROV PHOCA and deploy MPI's O_2/CO_2/pH eddy covariance tool. This short dive was followed by further hydroacoustic surveys around Goldeneye and at abandoned wells about 17 nm further east.

On Sunday, 1st October our research work had to be discontinued before lunch time because of the predicted bad weather conditions with strong winds up to 20 m/s and increasing wave heights. We headed westwards to take shelter in the Moray Firth in Scotland for 5 days until the multiple storm fronts had passed. Finally, on Friday, 6th October we could return into our working area to survey several more abandoned wells in the north-eastern part of our permit area in the British EEZ. On Saturday, we started to head back south towards the Figge Maar, where we arrived on Monday morning, 9th October. Here, we took a gravity core in the crater and conducted two dives with ROV PHOCA to deploy the GasQuant lander and the Bubble Box. Unfortunately, the electronics of GasQuant got wet and the system had to be brought back onto the deck. Around high-tide the gas bubbling in the Figge Maar ceased and we could not find a suitable site to place the Bubble Box. Finally, towards the end of the dive we managed to sample some of the emitted gas, but due to the strong bottom currents setting in after the tidal still water the deployment of the Bubble Box failed, because the ROV was pulled away from the Bubble Box by the ship and the rest of the dive was required to trace back the Bubble Box using its radar beacon signal. Overnight we surveyed the many bubble release sites in the crater once again. The work was concluded next morning with a yoyo-CTD at Figge Maar, before returning to Bremerhaven port in the evening of 10th October (cruise track in Fig. 3).

Wednesday, 11th October the ROV PHOCA was packed and unloaded from the ship and the scientific crew of leg 1 disembarked from RV Poseidon in the late afternoon.

4.2 Leg 2

Peter Linke

Eight participants of leg 2 boarded on Wednesday afternoon already to exchange information and take over for the last two and a half weeks of cruise POS518. The 2 trucks with the scientific equipment were unloaded the next day and the remaining 3 participants arrived to complete the scientific crew and helped to prepare the instrumentation on deck and install the scientific instruments in the ship's laboratories.

After the return of one deck hand from the doctor we left Bremerhaven and set sail through the river Weser mouth on Friday morning at 9:30 UTC. Starting with sun shine the weather changed already after passing the lighthouse "Roter Sand" towards overcloud with stronger winds of up to Bft. 6.

We arrived at Goldeneye on Sunday morning, 15th October at 11:00 UTC with strong winds (Bft. 7) and up to 4 m high waves. Under these weather conditions no deployment of scientific gear was possible. As the wind ceased during the night, we were able to perform a CTD and a multicorer cast and deployed the NOC-Lander, a satellite lander and the BIGO Lander at Golden eye in the morning of the 16th October. However, after this we headed westwards to take shelter in the Moray Firth in Scotland as Hurricane Ophelia approached Ireland and the United Kingdom.

In the early morning of the 18th October RV POSEIDON returned to the working area at Goldeneye. A CTD and a multicorer station were conducted before the BIGO Lander was retrieved successfully. It was prepared for the next deployment immediately as the weather forecast promised a short time window for a second deployment. In the morning the lander was deployed again and a gravity corer was taken for our colleagues at the NOC before the weather deteriorated. During the 20th October 3 CTD casts at the lander stations were performed. After this, an acoustic data link was established to verify that the NOC-Lander has started to record oceanographic and chemical data. Subsequently, the 2nd BIGO deployment came to its end and the lander was retrieved successfully despite a significant swell. At this lander's position a 4.5 m long gravity corer was taken before POSEIDON set sail for shelter in the Moray Firth.

In the morning of the 22nd October RV POSEIDON returned to the working area to retrieve the satellite lander and to perform a CTD cast within a large swell of sea. Since the weather forecast was favourable for the night and early morning only we headed for a position further to the east to take a CTD and a sediment core for our colleagues from WP3. The weather deteriorated rapidly to Bft. 7, but we were able to retrieve a 5.8 m long sediment core at the flank of the Scanner Pockmark to sample sediments of the Witchground Formation. After securing all instrumentation on deck RV POSEIDON set sail for a southerly course around the storm for the return to Kiel harbour. On Friday morning, 27th October we arrived at the east shore campus of GEOMAR, unloaded and disembarked the vessel (cruise track in Fig. 3).

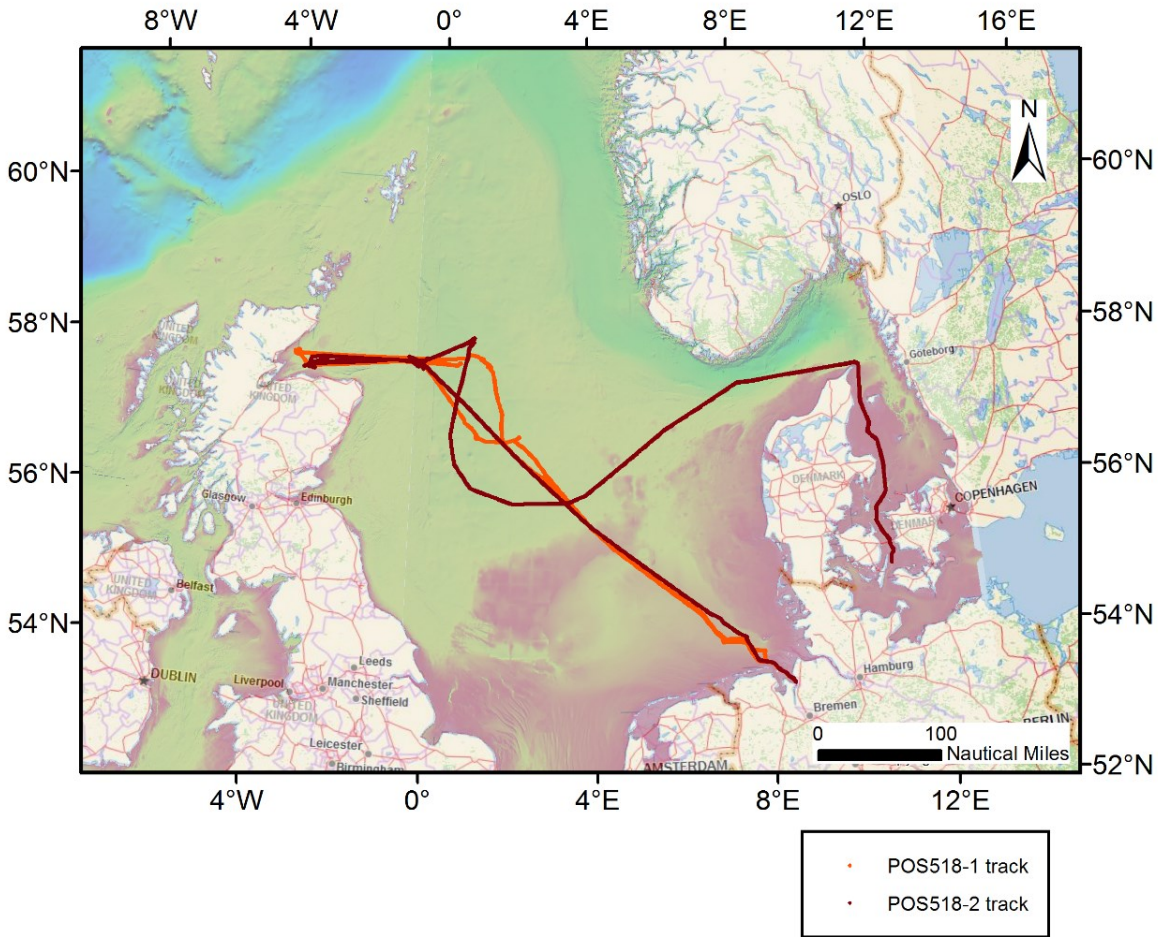

Fig. 3: Overview of cruise track POS518 starting from Bremerhaven and ending in Kiel.

4.2 Acknowledgements

We would like to express our gratitude for the excellent support by Captain Günther and his crew which enabled us to obtain valuable data despite the various storms during this cruise. The Technology and Logistics Centre (TLZ) at GEOMAR is acknowledged for the excellent logistic support. The cruise has received funding from GEOMAR and the STEMM-CCS project in the European Union's Horizon 2020 research and innovation programme under grant agreement No. 654462.

5 Methods

5.1 Hydroacoustic Systems

5.1.1 Wärtsilä ELAC SeaBeam 3050 MK II

Christoph Böttner

RV Poseidon is equipped with a hull-mounted 50 kHz multibeam SB3050 MKII with a 1.5° x 2° TX/RX aperture (Mills-Cross principle) manufactured by Wärtsilä ELAC Nautik GmbH, Germany. During POS518 we used it to acquire bathymetric and water column imaging (WCI) data. In single ping mode one transmission cycle is characterized by the formation of three simultaneously yaw and pitch stabilized transmit-sub fans with subsequent roll-stabilization during receive. The center transmit-sub fan has the frequency F1 slightly different from the respective outer sub fans with frequency F2 to foster reception signal separation. The system covers a maximum of 140° swath width. In multi ping mode, a second swath is formed also having three transmit sub fans with frequencies F3 and F4, respectively. 128 transmission and 64 reception staves transmit and record the echo signals, respectively. The transceiver electronic (SEE37) of the SB3050 then performs A/D conversion of the voltage and reception signal processing of the echo time series for further multibeam processing. 2 PCs perform real-time hybrid time-delay beam forming to generate up to 191 equi-angle beams (or up to 386 equi-distant beams). The beam formed data were processed in the bottom detection algorithm (BDA) and streamed to the “Operator PC” to display and store bathymetric data in the XSE file format and HYPACK/HYSWEEP.

The Wärtsilä ELAC SeaBeam 3050 MKII provides a fully automatic FM mode (FM – Frequency Modulation), utilizing linear FM pulses (CHIRPs) or CW (CW – Continuous Wave). In automatic mode, the system utilizes CW pulses for shorter pulse lengths and automatically switches over to FM pulses for longer pulse lengths without any user interaction required. The shallow water depth in the survey area did not allow automatic switch to FM transmission. Therefore, we manually set the pulse length to 3 ms to acquire FM data for dedicated surveys in order to test the results in post-processing. These dedicated survey data were stored in XSE, WCI and RAW (not beam-formed) format.

For accurate positioning and ship movement corrections the two Codaoctopus GPS antennas together with their IMU were used. The F180 GPS reference ellipsoid was set to WGS84. The data format sent by WERUM for the keel sound velocity was streamed to the multibeam system throughout the cruise. In addition vertical sound velocity profiles derived from CTD data were loaded via Hydrostar for sound speed dependent calculations (beam forming). Positions and heading as well as roll, pitch and heave data (TSS1, 25 Hz, F180 MRU) were streamed to the multibeam electronics and stored as RD-files for post-processing.

The latest Hydrostar control software V4.0.0 (built 3.348.1.467) was installed allowing pitch steering manipulation for enhanced bubble detection and automatic CW/FM mode. During medium weather conditions we faced major problems with the roll, pitch and heave correction of bathymetric data. The subsequent erroneous data is not feasible for seafloor mapping. Similar the full range of beams (140°) was never reached during the cruise as the outermost 10 beams showed low S/N-ratios and a systematic offset for the outermost port beams. Fortunately, the water column data, which was most important to achieve our scientific goal, was independent on these data corrections. Bathymetric data were streamed to the ship’s NAS server and processed,

gridded and displayed on a remote laptop. During the surveys we used HYPACK/HYSWEEP for online coverage display.

Water Column Imaging (WCI)

Besides bathymetric and sidescan data, uncompressed beam formed time series data of each beam were streamed to the “Processor PC” with a maximum sample rate of one half of the pulse length to visualize the water column backscattering data over travel time in each direction. We here analyze the full beam-formed time series of modern multibeam sonar records and for a few specific surveys we acquired raw stave data (not beam-formed). Water column imaging and logging was conducted during all surveys in a way not to lose the spatial coherence of potential rising and current-deflected gas bubbles streams (Schneider von Deimling & Papenberg, 2012). To exclude fish shoals as possible anomaly source signals all targets were crossed in two orthogonal profiles with low survey speed (~3 kn). All sounders (navigation sounders) of RV Poseidon were switched off, because they were found to significantly interfere with the SB3050. Single ping mode with auto ping rate and auto pulse width was chosen for valuable WCI results in shallow water. The transmission source level and receiver gain were set constant to auto mode. The water column data were streamed over a gigabit-ethernet controller to the WCI computer. Due to significant data transfer of up to 100 Mb/s the hard disk drive of the “Processor PC” was not able to display all necessary WCI echograms. For shallow water depth the high ping rate of 300 ms caused significant malfunction of the WCI Viewer software. This forced us to use only the beam-stack echogram for bubble identification. However, this procedure had no implication on the total data storage and investigations during post-processing.

We surveyed the Figge Maar starting on the 9.10.2017 to acquired three different data sets (CW, FM, pitch-steered) of the blow-out area for the SUGAR II project and subsequent development of the Wärtsilä ELAC Nautik GmbH SeaBeam 3050. We hope that these data sets help to enhance future development and help removing existing bugs.

Bathymetry Processing

Multibeam data were processed and evaluated on- and off-shore using the MBSystem Software, Fledermaus, Hypack/Hysweep, and MATLAB. The raw XSE data were imported with the MBSystem software for processing, pre-filtering, editing and visualization. A pre-filter was applied using MBSystem to remove the soundings outside a standard deviation threshold level, of 10 m bins and to get rid of the outermost ten beams from each side of the swath as these were found to be consistently erroneous (especially port side beams showed significant offset). In a later step data were evaluated in 3D using QPS Fledermaus software. NETCDF grids were created using a median filter with a grid size according to the local water depth and with respect to the 1.5° x 2° antenna beamwidth of the SB3050 on RV POSEIDON.

Aside from bathymetric measurements the SB3050 records backscatter and sidescan data in the XSE files. The poor data quality of bathymetric data made subsequent processing of these data not feasible.

WCI Processing

Water column data were processed on-the-fly via “range beam stack” function implemented in the WCIViewer 3.21 (Build 1.552) software developed within SUGAR

in cooperation between GEOMAR and Wärtsilä ELAC Nautik GmbH. This feature allows identifying gas seepage features online and within a time history of approximately 15 minutes at once, which highly facilitates the detection and localization of gas seepages during a survey. In post-cruise processing we will convert the data via „wci2gwc“ tool run on LINUX 64bit to generate QPS-IVS GWC file format (J. Schneider von Deimling, University Kiel). We used MATLAB to further investigate the sonar data and determine rough estimates for seep positions in the Figge Maar.

5.1.2 Imagenex 837B Delta T 260 kHz Multibeam System

Tim Weiß

In addition to the hull-mounted ELAC SB3050, an Imagenex 837B Delta T multibeam was used to detect flares in the water column in shallow waters. The Imagenex is a small-sized sonar and was installed in the moon pool of RV POSEIDON on the USBL system pole of the ROV PHOCA. The multibeam works at a frequency of 260 kHz. It has a transducer beam width of 120°x 3° and uses 120 beams. Because of the limited range of max. 100 m it was only used in shallow waters; a list of multibeam files obtained during leg 1 is provided in chapter 8.4 in the appendix. The water column data was recorded by the custom Delta T software in the raw (.837) format (Fig. 4).

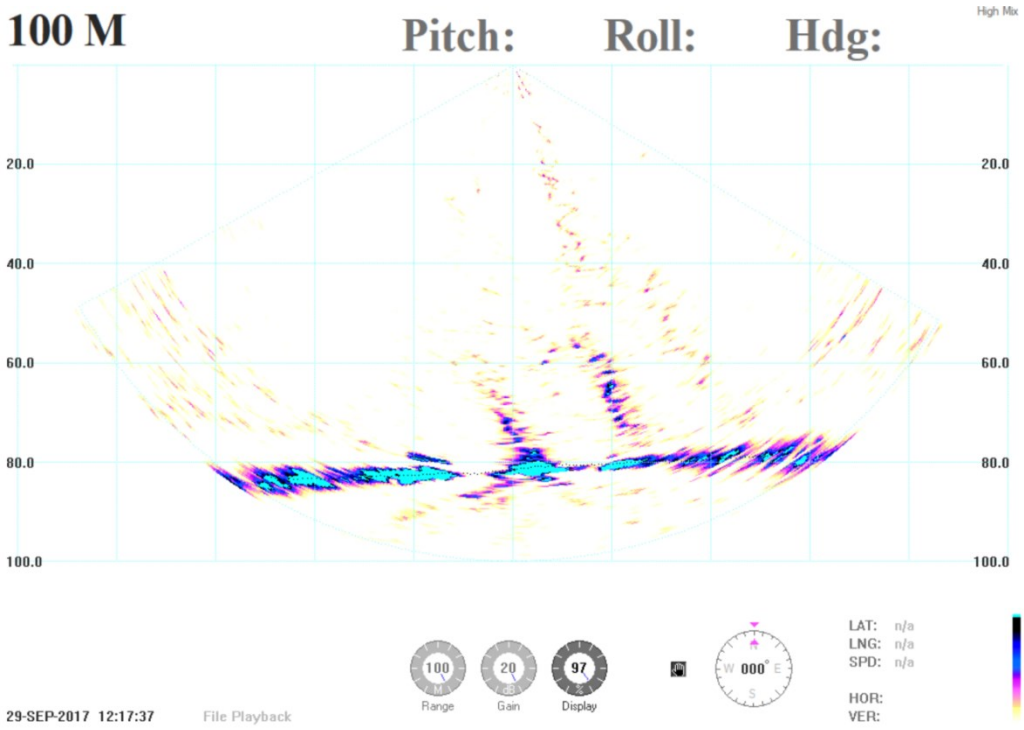

Fig. 4: Screenshot of Imagenex Delta T Software showing rising gas bubbles.

The GasQuant II lander system utilizes the Imagenex 837B Delta T for monitoring and quantifying marine gas releases. The multibeam is installed on top of a small tripod. The beams are aligned horizontally to the ocean floor in range of gas seepages to detect and monitor rising gas bubbles. The system was built as the successor of the Gas Quant I system (Greinert et al., 2008), which has been successfully used for tempo-spatial variability of gas releases in the past. The new system is lighter (ca. 43 kg), more energy efficient and designed for ROV deployments (Fig. 5). Hence, the

positioning of the system with respect to the bubble seepage could be much more improved.

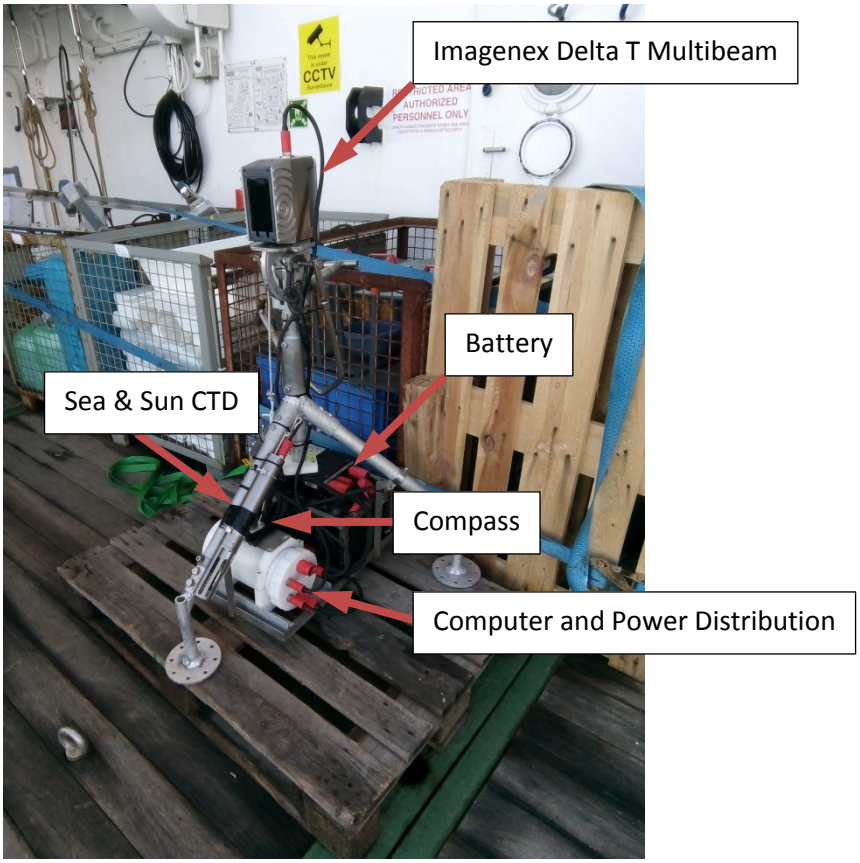

Fig. 5: The GasQuant II Lander

Besides the multibeam, the system consists of an Enitech battery system, a power and computer housing and a compass. In addition a Sea & Sun CTD was attached to the metal tripod. To record data a predefined script is started after switching power on. The script contains the start and end time, range and gain settings.

5.2 ROV PHOCA

Martin Pieper, Matthias Bodendorfer, Patrik Cuno, Torge Matthiessen, Inken Suck

ROV PHOCA (Fig. 6) is a 3000-m rated deep diving platform manufactured by SubAtlantic FET, Aberdeen, Scotland. It is based on commercially available ROVs, customized to our demands, e.g. being truly mobile. ROV PHOCA has previously been operated from the medium and large sized German research vessels POSEIDON, SONNE and ALKOR. As an electric work class ROV of the type Comanche, this is build No. 21.

During POS518, a midwater winch with a steel armoured fibre optic cable was used with a maximum length of 2700 m and a 19 mm diameter. The deck's setup during launch is shown in Figure 6.

The vehicle standardly carries various cameras: 1 HDTV Bullshark (which may be recorded permanently), 2 colour zoom video cameras (OE14H366) mounted on pan and tilt units, a digital stills camera (Imenco), 2 black and white observation cameras (OE15H108) and 1 color observation cam (Bowtech). Lighting for the video cameras

is provided by 4 MultiSeaLite Matrix LEDs (250 W) and 4 dimmable 250 W Deep MultiSeaLite halogen lights.

Fig. 6: ROV PHOCA after the harbor test of RV POSEIDON in Bremerhaven. Photo: M. Haeckel, GEOMAR.

Navigation was provided by an ORE Trackpoint USBL-Transponder (Edgetech) communicating to a transducer deployed through the ship moonpool, with a CDL TOGS fiberopics Gyro and an RD Instruments 1200 kHz Doppler Velocity Log. The vehicle also carried a FastCAT CTD SBE 49 manufactured by SeaBird. Real time observational logs are kept using OFOP (Ocean Floor Observation Protocol) by the scientists in the control van and the “show room” in a laboratory.

ROV PHOCA is based at GEOMAR, the Helmholtz Centre for Marine Sciences Kiel, Germany. For more details on the ROV system, please visit https://www.geomar.de/zentrum/einrichtungen/tlz/rovphoca/uebersicht/ (or see GEOMAR Helmholtz-Zentrum für Ozeanforschung Kiel, 2017).

ROV tasks during POS518

During this cruise, due to heavy weather, only three dives could be conducted. During the first dive near the Platform Goldeneye, the Eddy Covariance System of MPI Bremen (Fig. 7) was deployed. In addition, one pushcore was taken approximately 60 m west of the Eddy System.

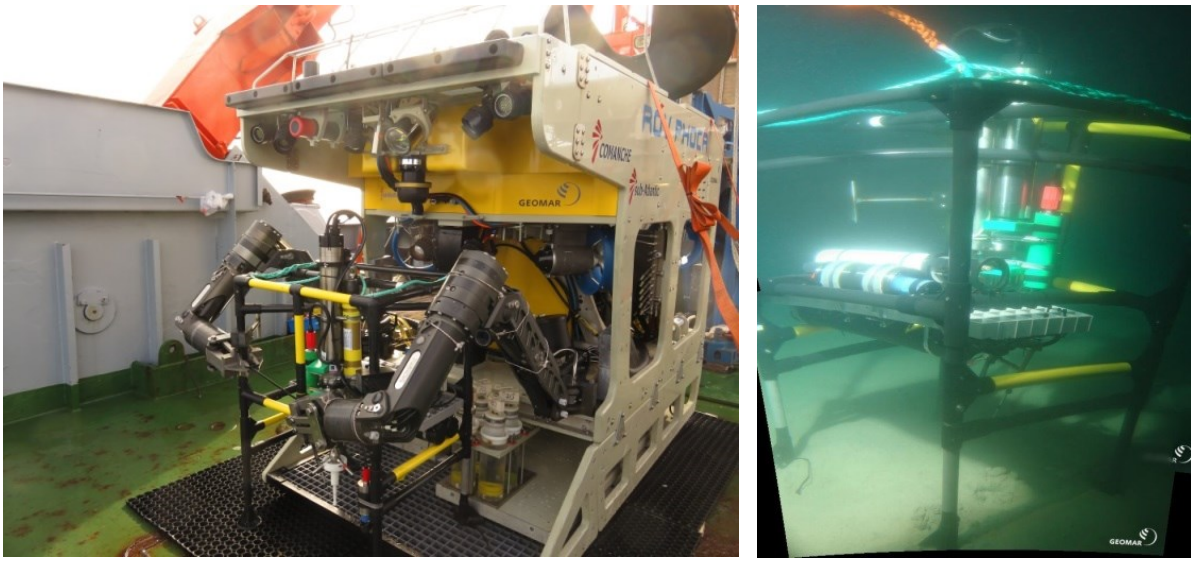

Fig. 7: (left) Eddy Covariance System on the porch of ROV PHOCA before the dive; **(right)** Eddy Covariance System after deployment at the seafloor (stitched image).

GEOMAR's GasQuant and Bubble Box were supposed to be deployed during two consecutive dives at the Figge Maar in the central German Bight. Unfortunately, GasQuant was malfunctioning at arrival at the seafloor and the first dive had to be ended. The objective of the second dive of the day was to deploy GEOMAR's Bubble Box (Fig. 8 left), sample gas using pressure samplers and take push cores. Visibility turned out to be very poor and only after several hours, gas bubbles were located and could be sampled with the gas sampler. One push core was taken (Fig. 8 right) to complement the gravity core taken prior to the dive (20 GC4).

During the dives, CONTROS CO_2 and CH_4 sensors were mounted on the ROV.

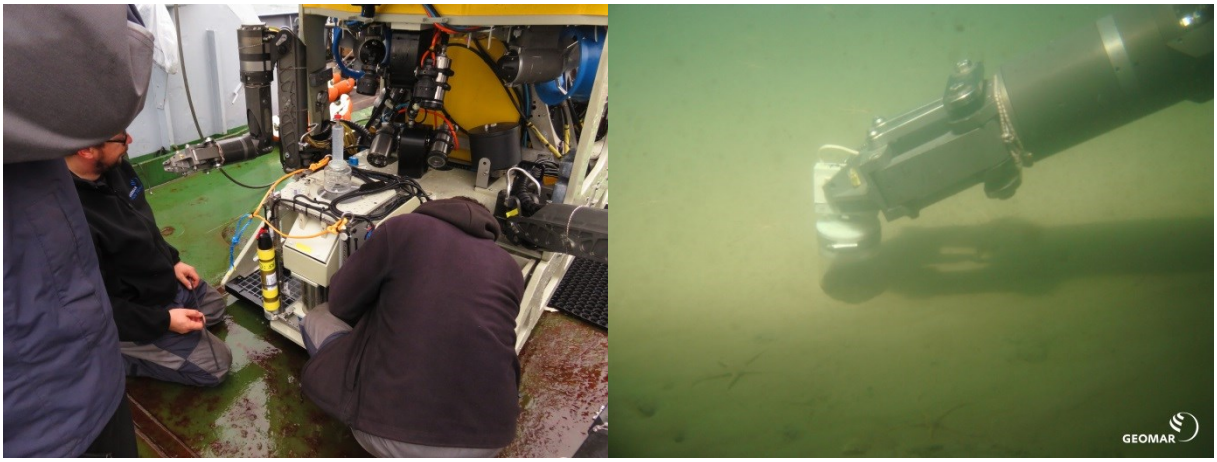

Fig. 8: (left) Bubble Box being fixed on the porch of ROV PHOCA before diving; **(right)** push core sampling in the Figge Maar crater.

During cruise POS518, 3 scientific dives (Tab. 1) were completed. Maximum bottom time was 07:12 hours and accumulated to approx. 9 hours (total dive time approx. 10 hours). For a more details on the dives, please refer to chapter 8.2 in the appendix.

Table 1: ROV station list during cruise POS518

Station Number POS518	Dive No.	Date (UTC)	Time Start (UTC)	At Bottom (UTC)	Off Bottom (UTC)	On Deck (UTC)	Location	Depth / m	ROV bottom time / h
Test	111	26.9.17	**Harbour Test Bremerhaven**						
13ROV01	112	30.9.17	13:33	13:37	15:22	15:40	Goldeneye	120	01:45
21ROV02	113	9.10.17	07:29	07:40	07:44	07:52	Figge Maar	44	00:04
21ROV03	114	9.10.17	08:56	09:06	16:18	16:30	Figge Maar	44	07:12
Total: 3 scientific dives									**09:01**

5.3 Eddy Covariance Technique for O_2, CO_2 (pH)

Dirk Koopmans

Overview

Our goal was to quantify benthic oxygen and dissolved inorganic carbon flux at the Goldeneye site. To accomplish this, engineers at the Max Planck Institute for Marine Microbiology (MPI) developed a prototype eddy covariance system based on a pH Ion Sensitive Field Effect Transistor (ISFET). This sensor was used by Long et al. (2015) to quantify benthic pH flux and the corresponding DIC flux in a coastal bay. The carbonate chemistry must be known for the pH eddy covariance technique to be effective for quantifying the CO_2 flux.

5.3.1 Eddy Covariance Technique

The eddy covariance technique relies on the simultaneous quantification of vertical velocity ad solute concentration at a single point in the water column. Turbulence is the dominant mechanism responsible for vertical mixing in flowing waters. This technique quantifies the vertical flux of solutes by the turbulent covariance of vertical velocity and the solute tracer of interest. Measurements are made at high frequency (5 Hz) to resolve turbulent fluctuations. Solute fluxes are calculated as

$$\overline{Solute\ flux} = \overline{V_Z{}'C'} \qquad \text{(Eq. 5.3.1)}$$

where V_z' is the fluctuating component of the vertical velocity and C' is the fluctuating component of the solute concentration (Berg et al., 2003). The overbar indicates averaging. The statistical distribution of turbulence ensures that flux contributions occur over a broad area. The eddy covariance flux footprint for sensors positioned 30 cm above the seafloor is approximately 10 m^2 (Berg et al., 2007). As the flow direction changes the sampled portion of the seafloor increases.

5.3.2 Eddy Covariance Instruments

Eddy covariance chemical sensors

Eddy covariance oxygen concentrations were determined with a 430 µm diameter FireSting optode (Fig. 9A; PyroScience, Gmbh). These minisensors have a 90% response time of 0.2 s. The light source and fluorescence detection were provided by a FireSting OEM module with a subport connector for underwater light transmission. Oxygen quenches the fluorescence of the optode membrane. Concentrations are determined by the phase shift in fluorescence that results from modulated excitation.

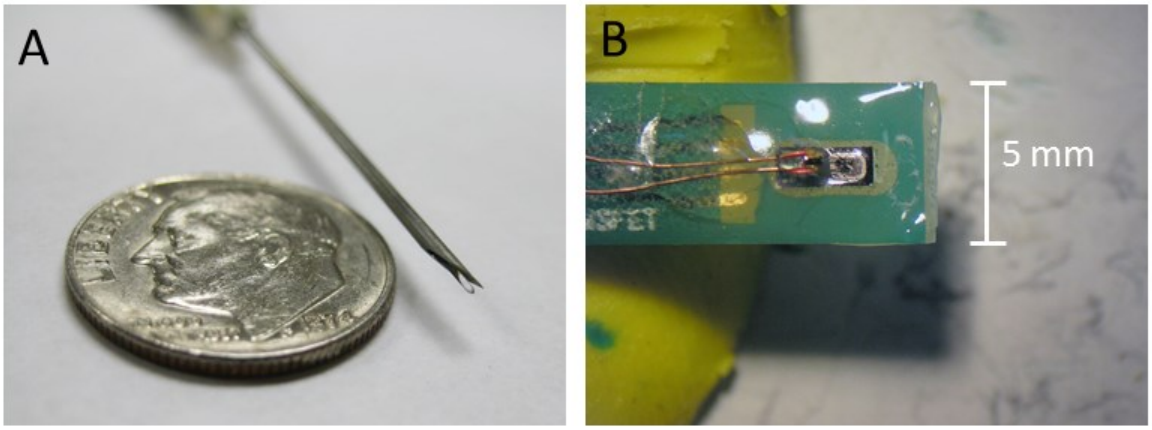

Fig. 9: (A) Oxygen mini-sensor and **(B)** pH-ISFET with added thermistor. The high precision and fast response times of these sensors makes them suitable for eddy covariance measurements of the turbulent fluctuations of solutes in the benthic boundary layer.

Eddy covariance pH was determined with a pH ISFET (Fig. 9B; Microsens CH). Briefly, as pH increases, the resistance to conduction across the transistor decreases due to a decrease in the strength of the electric field generated by the interfacial charge. ISFETS have a high precision and fast response time, making them good candidates for eddy covariance applications. One drawback of these sensors is that they are light-sensitive. To exclude light, the sensor was mounted inside of an opaque housing. Water was pumped from the measurement volume of the velocimeter through a thin intake tube and past the sensor and an adjacent reference electrode in a transparent housing (Fig. 10). To improve the reproducibility of pH fluxes, the ISFET signal was amplified, linearized, and also compensated for temperature changes.

Additional instruments

Water velocities were recorded by a Nortek Vector acoustic Doppler velocimeter (Nortek-AS). The ADV also recorded the signal output from the chemical sensors. Fluxes were measured at 32 Hz, at a height of 15 cm above the seafloor, with a nominal velocity of 0.3 m s^{-1}. The maximum frequency at which the chemical sensors can resolve flux is at 5 Hz. To minimize unnecessary data processing the resulting velocity signal was downsampled to 5 Hz for flux calculations.

To support the solute concentration measurements, we included two Aanderaa optodes and one RBR logger on the eddy covariance frame. The Aanderaa optodes measured temperature and dissolved oxygen at heights of 20 and 60 cm above the bed. The RBR logger measured oxygen concentration as well as pH and ORP.

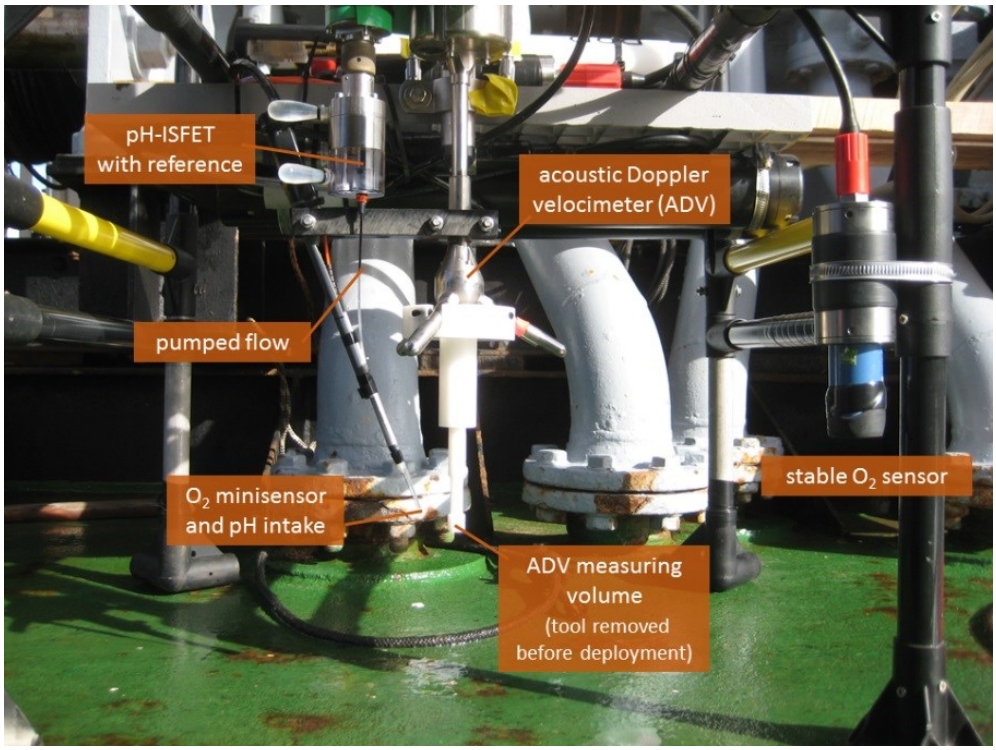

Fig. 10: The eddy covariance oxygen sensor and pH intake straw were arranged 1.5 cm outside the measuring volume of the ADV for simultaneous measurement of turbulent water velocities and solute concentrations at one location in the water column.

5.3.3 Eddy Covariance Deployment

Instrument frame

To deploy the eddy covariance instruments by ROV, they were mounted to a 1 m tall frame built from 3 cm O.D. fiberglass tubing (Fig. 11). This tubing maintains a surprising structural integrity even after splintering. Spare fiberglass tubing was useful for replacing damaged components and altering the frame to suit conditions. Stainless steel tubing was used in place of the legs at the ROV porch drawers.

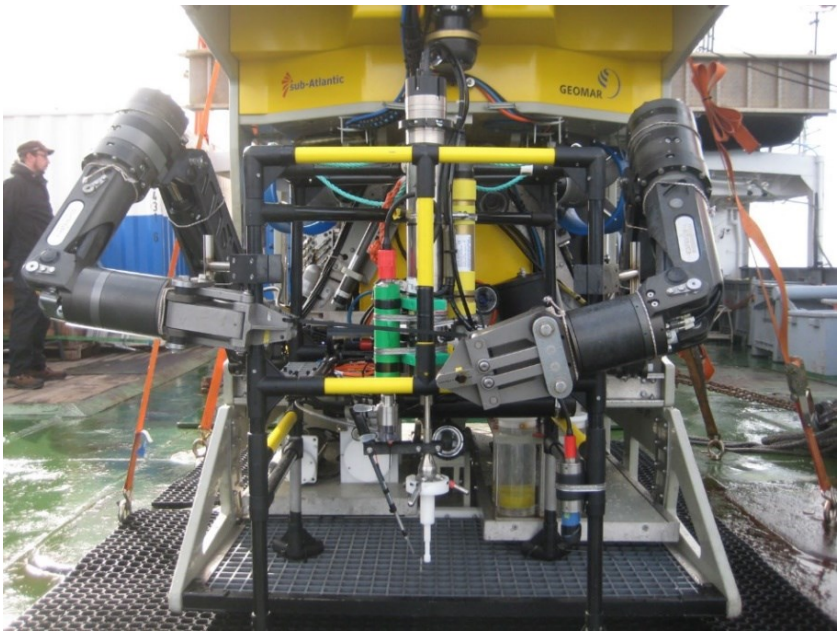

Fig. 11: The eddy covariance instruments on the ROV's porch just prior to deployment.

Ship and ROV telemetry

The eddy covariance frame was deployed by the ROV on 30.09.2017. Weather hindered the deployment. The sea state was too rough for deploying the ROV until 13:00 UTC, 15:00 local time. At 14:00 UTC, 16:00 local time the frame was placed on the seafloor. The ROV location system was ineffective, but the ship coordinates were 57:59.7 N and 0:22.389 W. The ship heading was 195.7, with the ROV positioned off of the aft, to the north of the ship. The frame was deployed in 116 m of water on 183 m of ROV cable. The eddy frame was recovered less than an hour later.

Conditions on the bottom

Water velocities at the site averaged close to 10 cm s^{-1}. Visibility at the bottom was poor due to sediment suspension. Sediments at the site have a high silt/clay content. Every time the ROV made contact with the seafloor, clouds of sediment were lifted into the water column. This made even simple ROV operations a challenge. For example, despite being less than five meters from the eddy frame, the ROV pilots primarily used sonar to get close enough to the frame to acquire it. Then they waited for the clouds of sediment to subside.

From my perspective, the deployment and recovery went well. In spite of rough weather during the deployment and the forces exerted on the instruments by the deployment and recovery of the ROV, the fragile sensors remained intact.

5.4 Bubble Box

Tim Weiß

For the assessment of bubble size distribution and bubble rise velocity, a bubble imaging box (Bubble Box) designed and constructed at GEOMAR in the project SUGAR II, received post processing routines (Jordt et al., 2015) in the project QUABBLE and significant technical improvement by the Deep-Sea Monitoring group.

The Bubble Box consists of a metal frame, which holds the camera systems, batteries, the backlit LED flash and an optional closing lid (Fig. 12). Two cameras take images at high frame rates (80-100 frames/second). The closing lid allows either undisturbed vertical flow-through, or precise flux measurements into predefined capture volumes. The gas in the capture volumes can be released using a physical ROV pull-switch to reset the measurement.

The lower front and sidewalls are made of transparent acrylic glass for ROV video observation, while the back wall is made of a white acryl glass acting as a light diffuser for backlit illumination of the gas bubbles. The green LED flash and the cameras are synchronised by a programmable trigger signal which controls the frame rate and the exposure time.

The time synchronisation between the cameras is achieved via a black (not illuminated) frame, which occurs every 5000 frames. The camera housing uses a dome port to minimise diffraction at the air/glass/water interface. The cameras were individually calibrated using checkerboards in a test tank at GEOMAR. This allows the determination of the exact position of the cameras towards each other.

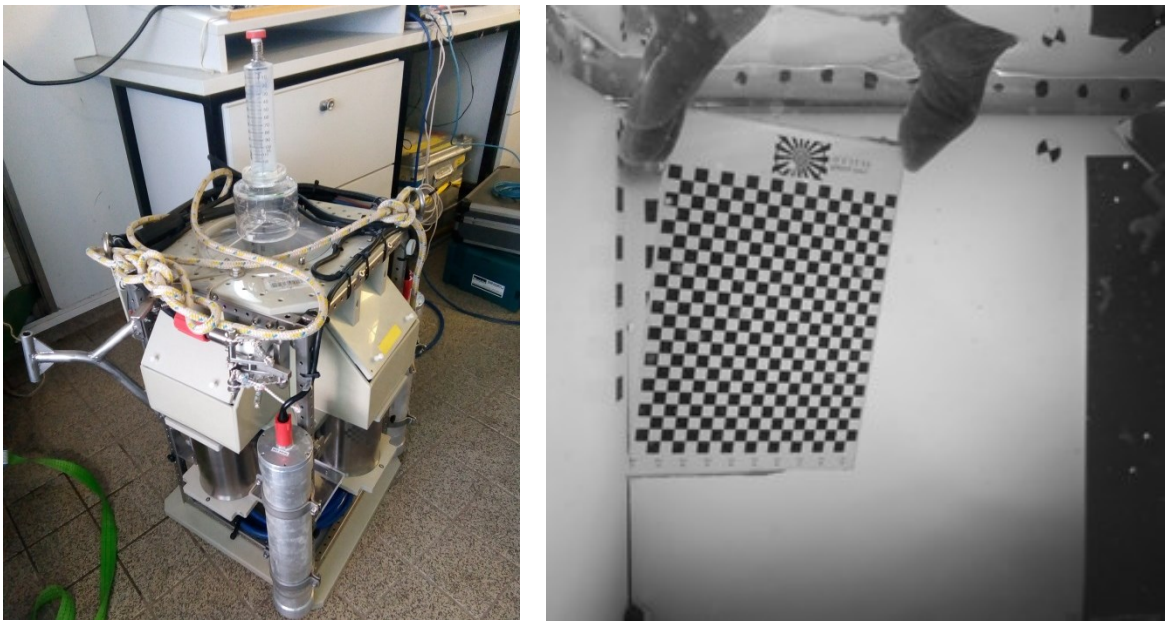

Fig. 12: BubbleBox before deployment and Checkerboard calibration in water before the POS 518 cruise.

The system was powered by two rechargeable battery sets with capacity of 17.5 Ah each. To save energy, but also data space, the system could be turned on/off using a physical ROV switch. Using the LED backlit flash, the system status can be observed by the ROV video cameras:

- 2 second flash: system power on (no bubble computer booted yet)
- 0.5 second flash: the master computer „bubble 2" booted
- 80 fps: both computer „bubble 2" and „bubble 1" booted and the system is recording data

The powerful LED flash allows exposure times of only 1 ms. This leads to detailed slow motion videos of bubbles without significant motion blur.

5.5 Picarro Atmospheric Gas Measurements

Tim Weiß

The atmospheric CO_2 and CH_4 concentrations were monitored during the cruise using a cavity ring down spectrometer (Picarro G2301-f) and GEOMARs 'Atmospheric Intake System' (AIS). The AIS pumps air from different air intakes into integrator volumes via aluminium tubings and then towards the Picarro analyzer. Three air intakes were installed on different elevation levels of RV POSEIDON to allow the calculation of concentration gradients for later sea-air gas flux assessments. Other parameters needed for such flux calculations, i.e. wind speed and water temperature were logged via the WERUM DVS data system throughout the cruise.

The long tubing between the AIS in the wet lab and the different air intakes (Fig. 13) caused time offsets between the air sampling and the actual gas measurement at the Picarro. Therefore each flow rate was adjusted according to the delay caused by the tubing. These delays where measured, by timing the arrival of a CO_2 peak generated by the breath of a second person at each air-intake.

The Picarro measured the different air intake sequentially one after each other. However, after the initial delay measurement, the flow rates were tuned to adjust the

delay of the different air intakes to make sure that the sequentially measured gas samples of the different air intakes originate from the same time point. Each intake was measured for one minute.

Air Intake No.	Position	Elevation	Delay	Calc. flow rate
1	Bow	7.25 m	65 s @ 2.389 l/min	2.389 l/min
2	Top Deck	10 m	103s @2.13 l/min	1.7551 l/min
3	Mast	13.4 m	89s @ 2.323 l/min	1.176 l/min

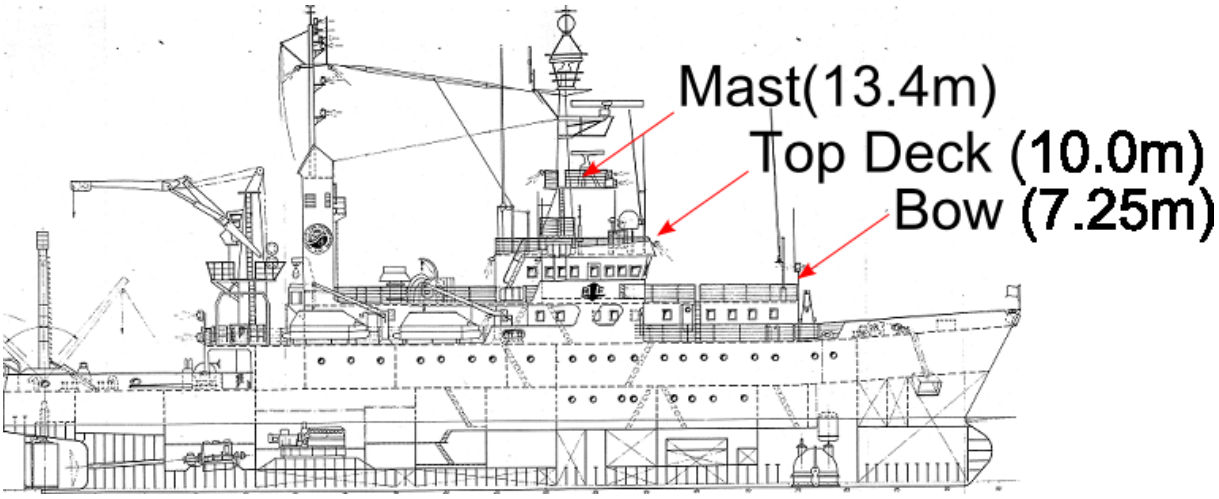

Fig. 13: Air intake locations on RV POSEIDON.

The Picarro analyzer software was running on the Picarro hardware. The CH_4 and CO_2 concentrations could be monitored in real time, and were logged for postprocessing. Additionally, OFOP (Ocean Floor Observation Protocol) software was running on a second computer. It was used to plot the gas concentrations onto a georeferenced map in real time (Fig. 14).

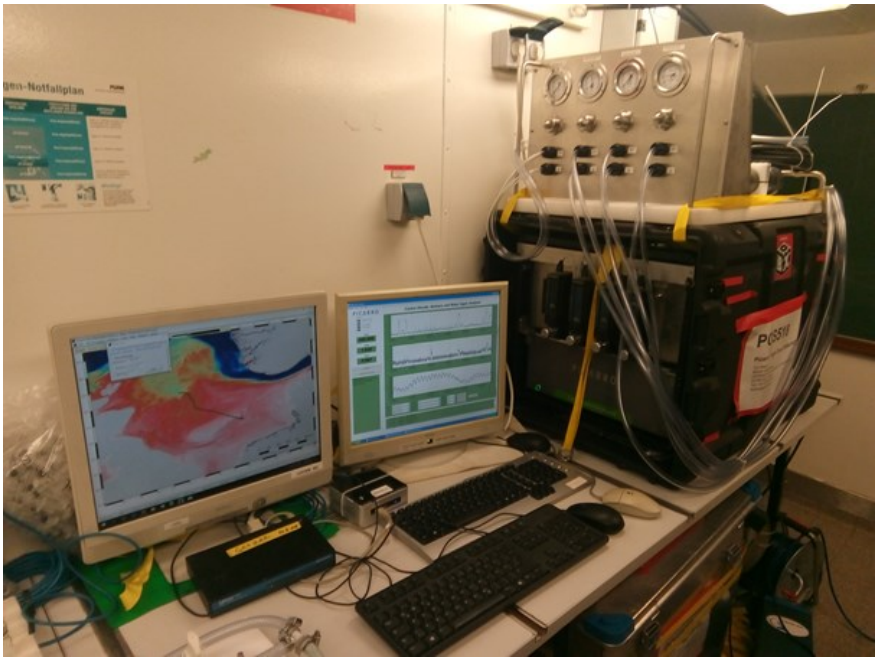

Fig. 14: Atmosphere Intake System (AIS) with the Picarro (right computer screen) and the OFOP data logging computer (left screen) in the wet-lab.

5.6 Water Column Sampling

Mark Schmidt, Andrea Bodenbinder, Mario Esposito, Anita Flohr, Peter Linke

5.6.1 "Multi-purpose" Rosette

A video-guided Water Sampler Rosette/CTD system (VCTD, Fig. 15a) was used to study environmental background water chemistry and hydrography in the working areas. The system was towed by winch 2 from the board site of RV Poseidon and water depths were controlled by pressure readings, altimeter and direct video observations near the seafloor. The digital video and data telemetry system (Linke et al., 2015) providing real-time monitoring of the seafloor was used to control the distance to the seafloor in "bottom view" mode. A HD-Video camera and light sources were attached to the lower part of the frame and are controlled by the telemetry deck unit via the coaxial cable (Fig. 15b). The VCTD rosette was equipped with additional sensors for pH and dissolved gases, i.e. CO_2 and CH_4, to monitor gas seepage near the seafloor (Schmidt et al., 2015).

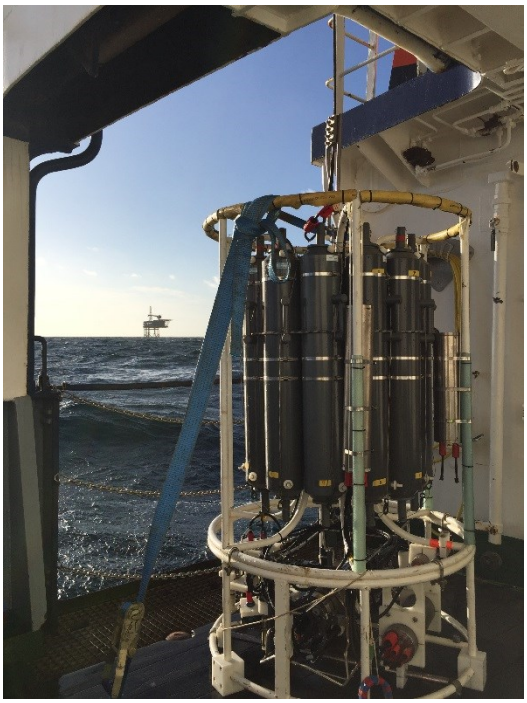

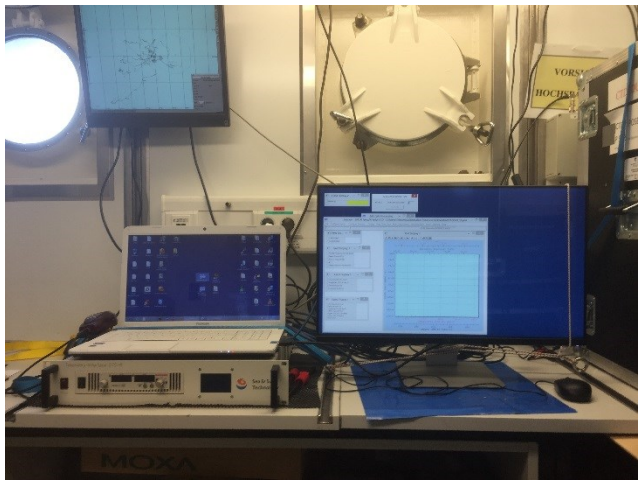

Fig. 15: (a) Water Sampler (12x10 L Niskin) Rosette including SBE9plus CTD, pH/O.R.P. sensor (SBE27), altimeter, external power-packs for HydroC^{TM}-CO2 and CH4. The telemetry pressure housing can be seen in the lower right of the rosette frame. **(b)** Telemetry deck unit with power supply, GPS unit, laptop and external screen for full control of video, lights, CTD data transmission and Niskin bottle firing.

SBE9plus CTD

The SBE 9plus underwater unit was equipped with pressure sensors, 2 temperature sensors, 2 oxygen sensors and 2 conductivity sensors. Furthermore, pH (SBE27) and altimeter sensors are attached. The SBE underwater unit and Niskin bottle carousel motor were powered via the winch's coaxial-cable by using the modem/power unit from SST (Linke et al., 2015). CTD data recording and triggering Niskin bottles were controlled with SEASAVE software (version 7.21) on an external laptop. CTD data were recorded with 24 Hz. GPS position data was logged parallel to the CTD and Video data from NMEA-string of RV Poseidon (Furuno GPS).

Hydro-casts and hydrographic data from towed CTDs were processed by using SBE software SBE7.22.1. Usually data files of 1 minute bins and 1 meter bins were created from raw data files and exported to ASCII. CTD is combined with data sets from external sensors by correlating with their UTC time stamps.

SBE27-pH/O.R.P. sensor

The pH-sensor (SBE27-0287) combines a pressure balanced glass-electrode, Ag/AgCl reference probe, and a platinum O.R.P. electrode (1200 m rated).

HydroC^{TM}-CO2 sensors

The HydroC-CO_2 (CO2-0412-005, Kongsberg) sensor, equipped with pumped (Seabird) sensor head, was integrated into the Video-CTD device (Schmidt et al., 2015). Same sensor was also operated with ROV Phoca during dives (Fig. 5.6.2). Measured pCO2-data is stored internally on SD card, however, the sensors reading is also monitored onboard by using one analogue 0-5V channel of the SBE9plus. When running in VCTD-mode, the HydroC^{TM}-CO2 is powered by an external NiMH-power unit (>10h at ~16°C). During ROV-dives the HydroC-CO2 is powered by ROV PHOCA (24V).

HydroC^{TM}-CH4P

A highly sensitive underwater methane sensor, i.e. HydroC-CH4P sensor (CH4P-1215-001, Kongsberg), was integrated into the Video-CTD or was operated on board ROV PHOCA (Fig. 16; Schmidt et al., 2013). When running in VCTD-mode, the HydroC^{TM}-CH4P is powered by an external NiMH-power unit. During ROV-dives HydroC-CH4P is powered by ROV Phoca (24V).

Fig. 16: HydroC-CO2 and HydroC-CH4P mounted to the front base plate of ROV PHOCA.

5.6.2 Water Sampling and Subsampling for Dissolved Gas and TA/DIC Analyses

Niskin water samplers were fired at selected water depths during CTD tracks and casts (Water depths between 5 and 120 mbsl). Video observation and CTD data were used for selection. After CTD recovery, seawater samples were transferred from Niskin bottles to 500 ml Schott glass bottles. The bottles were closed, after adding 100 µl saturated $HgCl_2$-solution, with a greased glass stopper leaving a headspace of about 3-5 ml. DIC and alkalinity determinations will be conducted at GEOMAR by using conventional titration methods (Dickson et al., 2007). The pCO_2 calculations will be performed according to Lewis and Wallace (1998). Calculated pCO_2 values will then be compared with calibrated HydroC-CO2 sensor data, and measured pH. Additionally, 100-ml glass bottles were filled with sampled seawater and stored for onboard TA-measurements with HydroFIA-TA.

100-ml glass vials were filled with water from Niskin samplers and were crimped with rubber stoppers. Then 10 ml of helium was added, replacing seawater of 10 ml, to extract dissolved gases into the headspace. Filled glass vials were poisoned with 50 µl of saturated $HgCl_2$-solution and stored after mixing for further gas chromatographic and stable isotope measurements of headspace gas.

30 ml of pre-cleaned plastic bottles were filled with filtered (0.2 µm) seawater which was then subsampled (1) into 3-ml plastic vials and acidified with 30 µl HNO_3 (6N) for ICP-OES analyses, (2) into 1.8-ml Eppendorf vials for ion chromatography measurements, and (3) into 3-ml cryo-caps (-20°C) for subsequent on board auto-analyzer measurements during leg 2.

On leg 2, additional DIC/TA samples were collected from CTD casts. Samples were drawn directly from the Niskin bottles into 250 ml Pyrex borosilicate glass bottles. Bottles were rinsed at least three times with the sampling water before filling. While filling, the bottles were rotated to ensure no bubbles accumulate inside and to avoid the persistence of any minute bubbles, overflowing was allowed. Samples were preserved by addition of 100 µl of 50% saturated $HgCl_2$ solution (Dickson et al. 2007). A thin layer of silicone grease was applied around the glass stoppers and after appropriate labelling, the bottles were sealed and stored in the dark for later analysis at GEOMAR. At selected stations dissolved oxygen was determined by Winckler titration.

Additionally, samples for dissolved inorganic carbon (DIC), total alkalinity (TA) and carbon isotope ($\delta^{13}C\_{DIC}$) analysis were filled into 40 mL borosilicate glass bottles (Thermo Scientific). The sampling followed standard procedures (Dickson et al., 2007). Duplicate samples were taken. The samples were preserved with mercury (II) chloride (10 µL of saturated $HgCl_2$ solution) directly after collection and stored cool and dark. The analysis of DIC, $\delta^{13}C\_{DIC}$ and $\delta^{13}C\_{DOC}$ will be performed using a TOC/TIC analyser (OI-Analytical, Aurora 1013W) in combination with a cavity ring-down spectrometer (PICARRO G2121-i) and the TA by titration (Metrohm, Titrino) both at the National Oceanography Centre in Southampton.

Samples for $\delta^{18}O$ analysis ($\delta^{18}O\_{DIC}$, $\delta^{18}O\_{H2O}$) and were filled into 12 mL Exetainer vials (LABCO) with no headspace. Duplicate samples were taken. To preserve the $\delta^{18}O$_DIC the samples were treated with 125 µL of a solution of 0.4 M $SrCl_2$ and 23 mM NaOH resulting in the precipitation of DIC as SrCO3. The $\delta^{18}O\_{DIC}$ and $\delta^{18}O\_{H2O}$ samples will be analysed at the Department of Earth Sciences in Oxford, England after the cruise.

The sampling of dissolved sulfurhexafluoride (SF6), trifluoromethylsulfurpentafluoride (SF5CF3) and dissolved noble gases was conducted at two stations from extra CTD casts. The sampling of SF6 and SF5CF3 followed the suggested procedures of the USGS Groundwater Dating Lab (https://water.usgs.gov/lab/sf6/). Duplicate samples were taken at selected depth levels. The samples were stored at a cool and dark place and will be analysed at the British Geological Survey (BGS) directly after the cruise. Samples for analysis of dissolved noble gases and their isotopes were filled into copper tubes and clamped following the suggested procedures (http://www.noblegaslab.utah.edu/how-to.html). Duplicate samples were taken. The samples will be analysed at the Department of Earth Sciences in Oxford, England after the cruise.

5.6.3 Underway Thermosalinograph

Underway temperature and salinity data were recorded during cruise PO518 by using the shipboard Thermosalinograph. Sub-surface waters were pumped from a port well at about 4 m water depth (inlet temperature is measured by SBE38), through a shipboard tubing system, to a flow-through tank, where temperature and conductivity is continuously measured with a SBE21 probe. Date recorded is shown on screen and can be downloaded via Dship (Fig. 17).

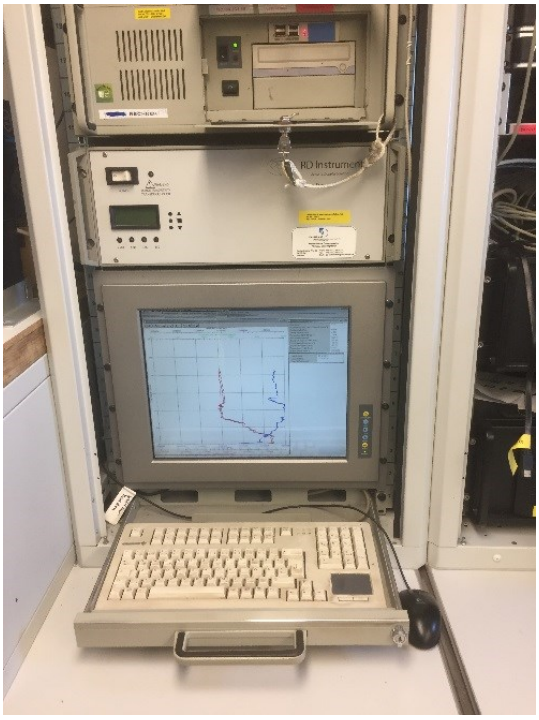

Fig. 17: Control unit of the Thermo-salinograph.

5.6.4 Underway Total Alkalinity (TA) Measurements

A newly developed underway TA-titration system (HydroFIA™-TA, Kongsberg) applies an acidic titration on a seawater sample of defined volume and measures related pH-change by optical absorbance measurements. The TA-System was set up in the wet laboratory together with the pCO_2 sensor (HydroC™-CO2) for continuous measurements of seawater pumped from the port of RV Poseidon, at 4 m water depth, to the wetlab (Fig. 17). Water tubes and pump are made of plastic or ceramic to reduce any artificial redox-reactions and pH changes. Before entering the inlet of the TA-system the water is filtered by a flow-through particle filter unit (Fig. 18). Seawater

bypassing the filter is ending in a flow through box containing the pCO_2 sensor. Wastewater from TA-titrations was collected in 20 l plastic canisters for onshore disposal.

The TA-system was also used for onboard determinations of TA of discrete 100 ml water samples derived from Niskin bottle subsampling.

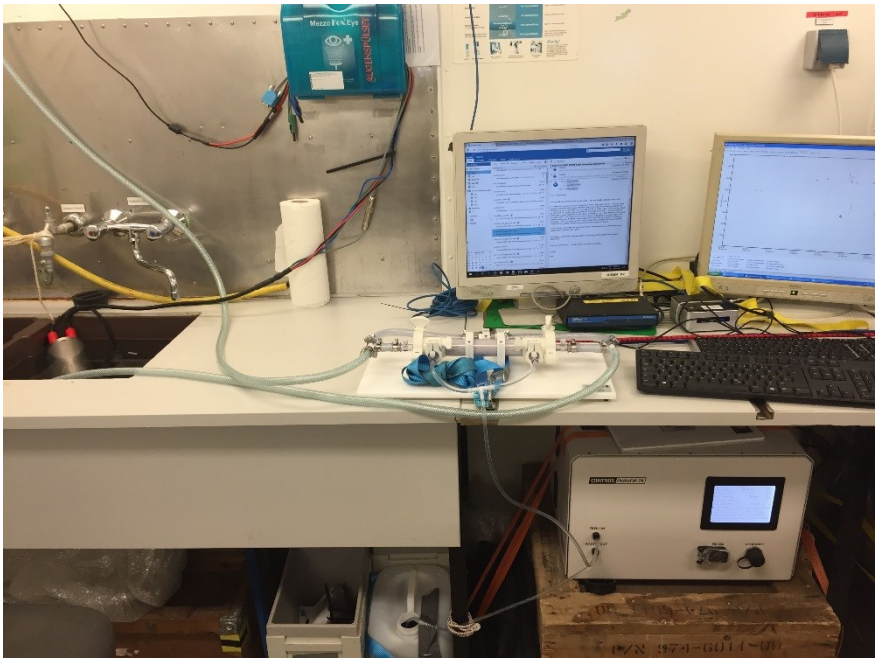

Fig. 18: Setup of the autonomous TA-System in the wetlab of RV Poseidon.

5.6.5 Gas Bubble Sampling

A gas-tight bubble sampler (stainless steel; funnel inlet; Fig. 19a) had been designed for free gas sampling at in situ pressure (max. 160 bar). The sampler was operated by ROV PHOCA for capturing gas bubbles emanating from the seafloor.

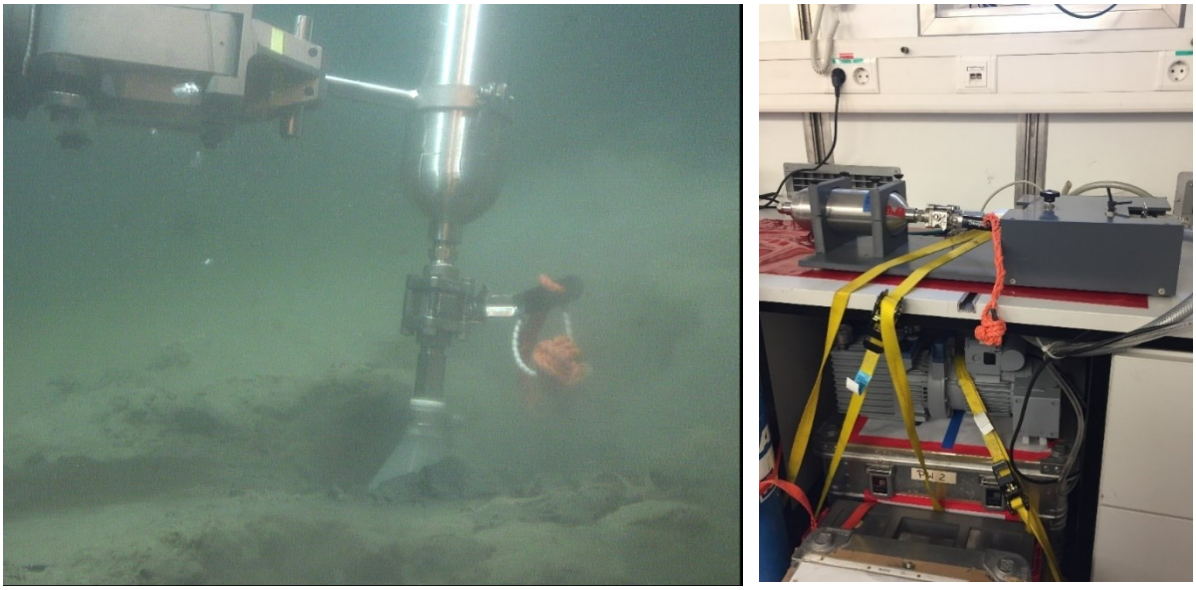

Fig. 19: (a) High-pressure Bubble Sampler with funnel inlet; **(b)** vacuum sub-sampling system for transferring high-pressure gas into headspace vials.

The gas bubble flux was calculated by monitoring the gas overflow from the sampler into the plastic funnel. The inlet valve of the sampler was closed at the seafloor after the volume was totally filled with gas. Onboard sub-sampling of the high-pressure bubble sampler was conducted in a vacuum system (Fig. 19b), which allowed pressure-controlled release of gas into headspace glass vials (up to 1.05 bar).

5.6.6 Dissolved Organic Carbon Sampling

Samples for dissolved organic carbon (DOC) were collected from CTD casts on POS518 leg 2. One end of a silicone tubing was connected directly to the tap of the Niskin bottle while at the other end a stainless steel filter holder was attached. Carbon cleaned 25 mm GF/F filters nominal pore size 0.7 µm (combusted at 450 °C for 4 hours) were placed into the filter holder for sampling. The filtered water was collected directly into pre-combusted 40 ml borosilicate glass vials. Samples were preserved by addition of 100 µl of 4M HCl to lower the pH of the solution to values less than 2. Vials were flame sealed and following appropriate labelling, they were stored in the cold and dark for subsequent analysis at GEOMAR.

5.6.7 Inorganic Nutrient Sampling

On POS518 leg 2, CTD casts were sampled for inorganic nutrients (nitrate/nitrite, phosphate, silicate and ammonium). Water samples were drawn directly from the Niskin bottles into acid washed (10% HCl) 200 ml Nalgene bottles. During sampling, latex gloves were worn in order to avoid contamination. Bottles and lids were rinsed at least 3 times with sampling water before filling. After appropriate labelling, the bottles were stored at -20 °C for later analysis. In selected water samples nutrients were measured on board with an autoanalyser following the method of Grasshoff et al. (1999). As CTD casts were performed in the area surrounding the NOC lander, measurements will be crucial for a first inter-comparison and potential re-calibration of the lander integrated chemical sensors.

5.7 Lander Deployments

Stefan Sommer, Mario Esposito, Peter Linke

Ecological habitats and biogeochemical processes at the seafloor and within the water column of shelf seas such as the North Sea are strongly affected by daily/seasonal natural environmental changes and anthropogenic disturbances. In the framework of the STEMM-CCS project, it is crucial to detect and discriminate changes caused by potential leakage at CCS sites from maxima in background signals. Our goal is to determine an effective environmental baseline in order to provide the data needed to define measurement strategies for a controlled sub-seabed CO_2-release experiment, which is planned for 2019.

5.7.1 NOC Lander

Mario Esposito

We deployed an autonomous in-situ seafloor lander equipped with a suite of sensors to monitor temperature, conductivity, pressure, current speed and direction, hydro-acoustic, pH, pCO_2, O_2 and nutrients over a period of about 10 months. The NOC lander is a submersible autonomous device manufactured by Develogic GmbH subsea systems according to our requirements. The NOC lander (Fig. 20) is composed of four main parts:

- A trapezoid shape trawl resistant frame
- A fully integrated solution with all mechanical and electrical components accessed and configured via interface connection or acoustic telemetry
- A recovery subsystem with 250 m tether reel connected to a ballast plate through a DW.R1000 titanium release
- A surface hydro-acoustic modem with a 35 m rugged Kevlar reinforced cable for real-time communication

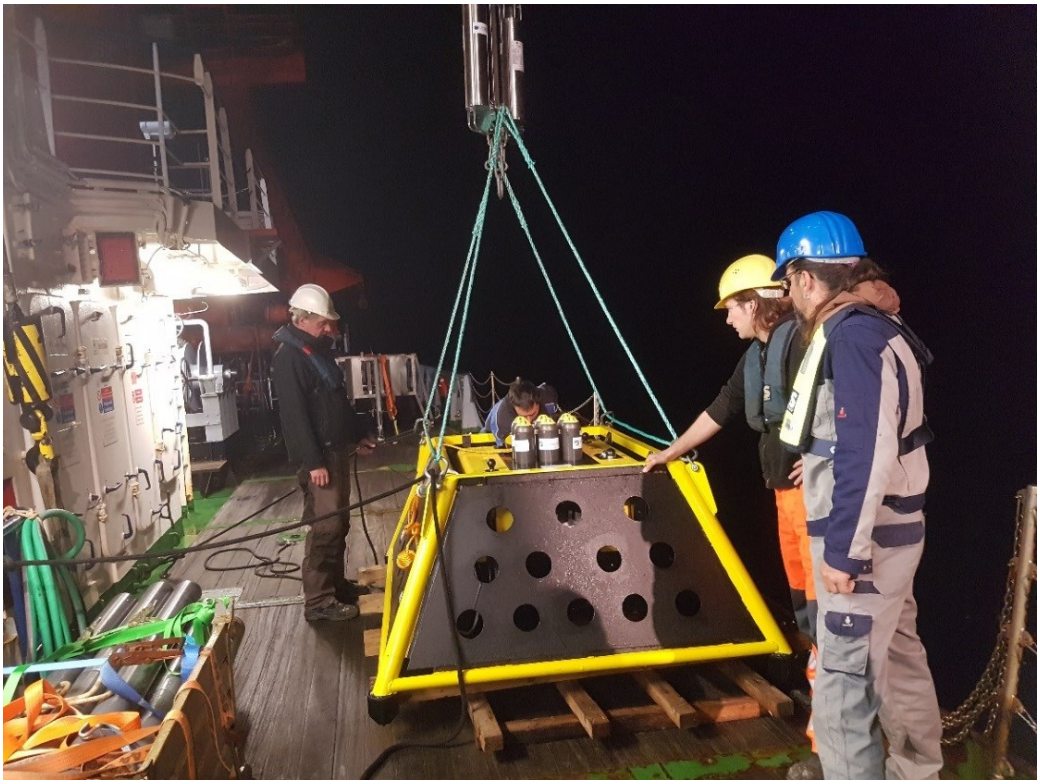

Fig. 20: NOC Lander ready for deployment.

The system has an integrated acoustic modem HAM.Base VHF for communication and data logging, a satellite recovery beacon DW.SRB for transmission of GPS position via IRIDIUM satellite telemetry at surface, an integrated Sono.Vault II HF acoustic recorder, an integrated depth sensor Keller PA33Xc, a conductivity and temperature sensor Seabird SBE37-SM and a set of 6 ECB popup telemetry units for data transmission via IRIDIUM satellite telemetry. The units contain an additional Port8 data logger fully integrated with a Seabird SeapHOx pH and O_2 sensor, 3 NOC Lab-on-Chip chemical sensors for inorganic nutrients (nitrate, phosphate) and pH and an Acoustic Doppler Current Profiler Nortek Signature 250. Three additional self-logging sensor devices for autonomous measurements of pH and pCO_2 were added. The loggers were provided by the Graz University of Technology.

Lander Configuration

In order to monitor the environmental conditions of the area, with focus on the bottom part of the water column, the suite of integrated attached sensors was configured in the following way:

ADCP Range = 40 m Resolution = 4 m cell Sample average interval = 180 sec Sampling interval = 20 min	*Lab-on-Chip NOC sensors* Nitrate sampling frequency = 6 hours Phosphate sampling frequency = 6 hours pH sampling frequency = 6 hours
Sono Vault Hydrophone Sampling every hour for a period of 10 minutes at 125 kHz	*Keller, SeaBird and SeapHOx* Sampling interval = 20 min
TUG self-loggers Sampling frequency = 1 hour	*Pop-ups release scheduled event* 1st pop-up on 01/12/2017 at 08:00 UTC 2nd pop-up on 01/03/2018 at 08:00 UTC 3rd pop-up on 01/06/2018 at 08:00 UTC

5.7.2 SLM Lander

Peter Linke, Stefan Sommer, Matthias Türk, Asmus Petersen

The Satellite Lander (SLM) is a low profile lander with a proven design by K.U.M. usually used for ocean bottom seismometers. During this cruise it was used to record oceanografic and chemical baseline values. For this purpose it was equipped with an ADCP (300 kHz, RDI), a storage CTD (SBE16plus, Seabird) and an oxygen optode (Aanderaa) with an autonomous data logger (A. Pinck, GEOMAR). A video-guided launcher was used for a smooth and targeted deployment at the seafloor (Fig. 20).

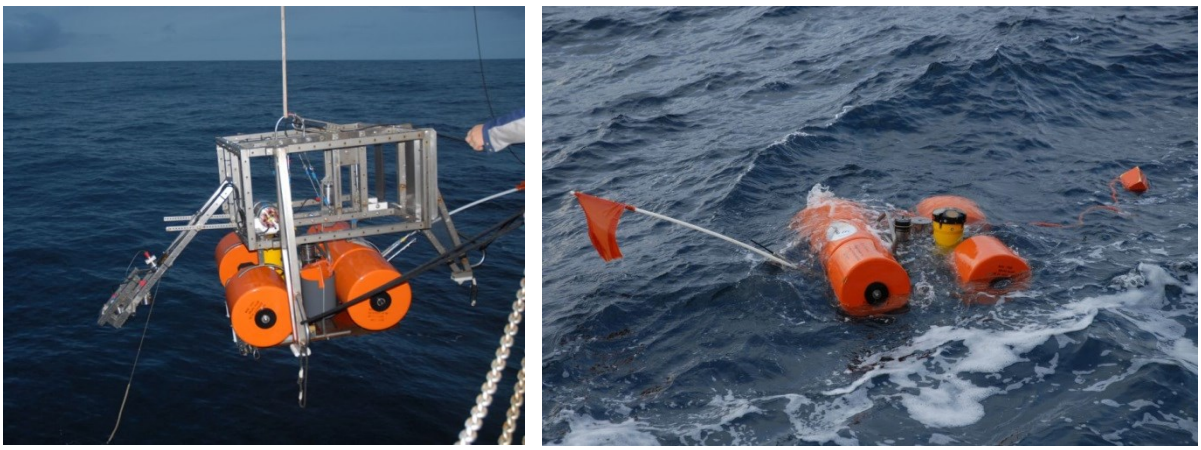

Fig. 21: Deployment and recovery of the Satellite Lander (SLM).

5.7.3 BIGO Lander

Stefan Sommer, Andy Dale, Peter Linke, Gabriele Schüßler, Regina Surberg, Christine Utecht

Major aim was to determine primarily the ratio between total oxygen uptake (TOU) and dissolved inorganic carbon (DIC) across the sediment water interface in the working area close to Goldeneye. The TOU to DIC ratio is considered as a biogeochemical tool

to detect possible CO_2 leakages from submarine CCS sites, indicated by strong deviations from the typical TOU to DIC ratio in this region. These fluxes including those of N_2/Ar, total alkalinity, nitrate, nitrite, phosphate, ammonium, and silica were measured in situ using the GEOMAR BIGO type lander (Biogeochemical Observatory). The BIGO has been described in detail by Sommer et al. (2016) (Fig. 22A). In brief, each BIGO contained two circular flux chambers (internal diameter 28.8 cm; surface area 651.4 cm^2). A TV-guided launching system allowed smooth placement of the observatories at selected sites on the sea floor. About 4 hours after the program of the observatory was started on deck the chambers were slowly driven into the sediment (~ 30 cm h^{-1}). During this initial time period where the bottom of the chambers was not closed by the sediment, the water inside the flux chamber was periodically replaced with ambient bottom water. The water body inside the chamber was replaced once more with ambient bottom water after the chamber has been driven into the sediment to flush out solutes that might have been released from the sediment during chamber insertion. To trace nitrogen, phosphate and silicate fluxes as well as total alkalinity 8 sequential water samples were removed with a glass syringe (volume of each syringe ~ 47 ml) by means of glass syringe water samplers (Fig. 22B). The syringes were connected to the chamber using 1 m long Vygon tubes with a dead volume of 5.2 ml. Prior to deployment these tubes were filled with distilled water. Another 8 water samples were taken from inside the two benthic chambers using an eight-channel peristaltic pump, which slowly filled glass tubes (quartz glass) (Figs. 22B+C).

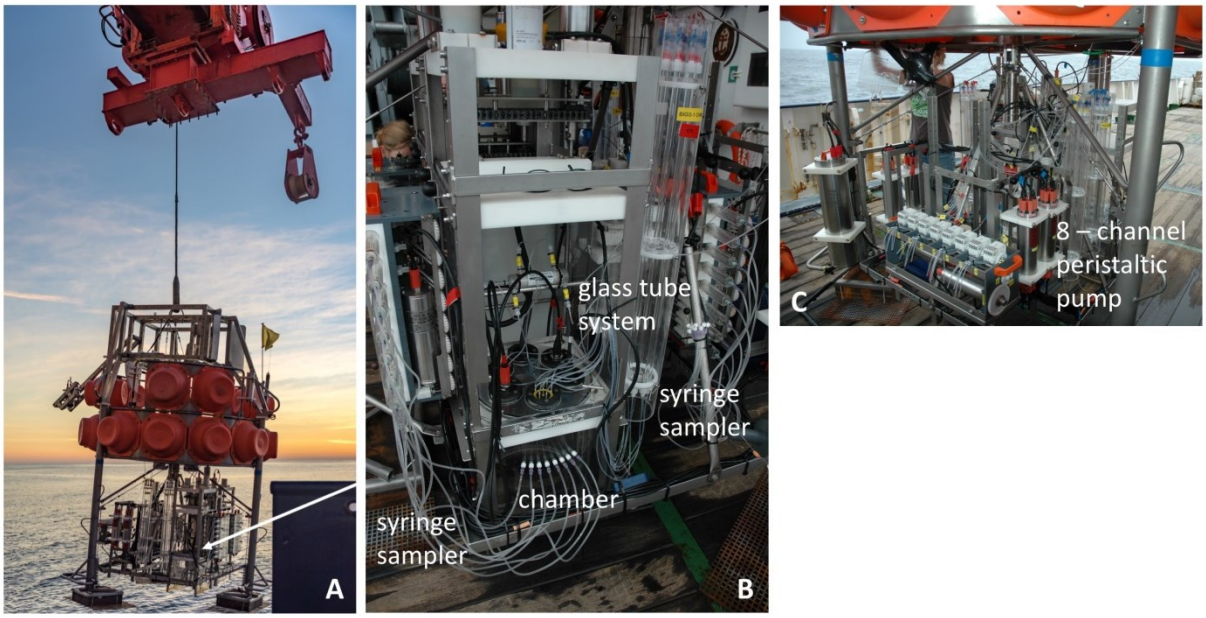

Fig. 22: A. Lander and launcher prior to deployment. **B.** Flux chamber with attached syringe water sampler and the glass tube system. **C.** 8-channel peristaltic pump for taking samples from the chamber and the ambient bottom water into the glass tubes (Photos: A, C. Rohleder, B and C, S. Sommer).

These samples were used for the gas analyses of N_2/Ar (Sommer et al. 2016) as well as DIC (Sommer et al. 2017). To monitor the ambient bottom water geochemistry an additional syringe water sampler and another series of eight glass tubes were used.

The positions of the sampling ports were about 30 – 40 cm above the sediment water interface. O_2 was measured inside the chambers and in the ambient seawater using optodes (Aanderaa) that were calibrated based on the O_2 time series recorded by the SLM lander, which was deployed during from the 16. – 22. Oct.17. O_2 data recorded by the lander were calibrated using CTD/water sampling rosette casts. Chamber two harboured two optical sensors for the measurement of pH and CO_2 (working group E. Achterberg).

5.8 Sediment Coring

Matthias Haeckel, Andy Dale

On Leg 1 sampling of sediments for geological and geochemical analyses was carried out with a gravity corer (GC), ROV-operated push cores (PC). On the 2nd leg a multi corer (MUC) was used to sample the sediment-water interface, in addition to further GC deployments.

Gravity coring

The GC, equipped with a weight of 1150 kg and a 3-m long core barrel, was operated by the large movebar. The GC was lowered into the sediment with a rope speed of 0.8 m/s in all deployments, resulting in only minimal core overpenetration in the generally silty-to-clayey surface sediments (see geochemistry chapter 6.3). After the retrieved GC was on deck the inner plastic liner (inner diameter of 110 mm) was pulled out and cut into 1-m long segments, which were each cut lengthwise into a sampling and an archive half. The geological core description and sediment photography was followed by sediment sampling for geochemical analyses in the ship's wet lab. Subsequently, the sampling and the archive half were transferred into D-tubes for long-term storage at GEOMAR's cooled core repository.

Push coring

The upper few decimetres of surface sediments were collected with ROV-operated PCs with a diameter of 60 mm allowing for sampling of an undisturbed sediment-water interface.

Multiple coring

The MUC is equipped with 6 Perspex liners 60 cm long and with an internal diameter of 10 cm. The MUC was lowered into the sediment with a speed of 0.3 m/s in all deployments and once on the seafloor the liners were pushed into the sediment under gravity by a set of lead weights. Due to the silty nature of the sediment, penetration did not exceed ca. 25 cm. Recovered sediments were immediately processed on board by sectioning with a depth resolution ranging from 1 cm at the surface to 4 cm in the deeper part of the cores.

Benthic chamber coring with BIGO

Sediments were also recovered in each benthic chamber of the BIGOs. These sediments are subject to artefacts after being incubated on the seafloor for up to 36 hrs. To check that the sedimentary geochemical distributions were broadly consistent with the main MUC data, one short push core (typical length 10 cm) was removed from one of the BIGO chambers and analysed in the same way as for the MUCs.

6 Preliminary Results

6.1 Gas Bubble Seepage

6.1.1 Hydroacoustics

Christoph Böttner

Vielstädte et al. (2015) proposed leakage at abandoned wells in the Central North Sea, where these pass through shallow gas accumulations. Significant amounts of this gas contribute to the North Sea methane budget and may reach the atmosphere (Vielstädte et al., 2017). The emitting gas (methane) is of biogenic origin and hence attributed to shallow gas pockets in the sedimentary succession. Leakage showed highest activity, where data indicated a seismic chimney in the subsurface. However, these studies were mainly based on evidence from three wells in the Norwegian sector of the Central North Sea. We set out to verify their findings in the UK sector of the Central North Sea and, if possible, to improve their statistics.

Prior to our cruise, we mapped all shallow gas accumulation over an extensive area of the UK Central North Sea. To achieve this goal we used the “MegaSurveyPlus” seismic survey, provided by Petroleum Geo-Services (PGS), and calculated the RMS amplitudes in between 50-700 ms two-way travel time (TWT) below the seafloor (Fig. 6.1.1). This time interval corresponds to approximately 1 km of the upper sedimentary succession. Prominent amplitude anomalies could be traced to the top-Pliocene horizon, also known as URU-R4 horizon. Based on this seismic evidence, we picked about 30 wells in the UK Central North Sea, of which half are located in an area with a seismic chimney and the other half without (Fig. 23**Fehler! Verweisquelle konnte nicht gefunden werden.**).

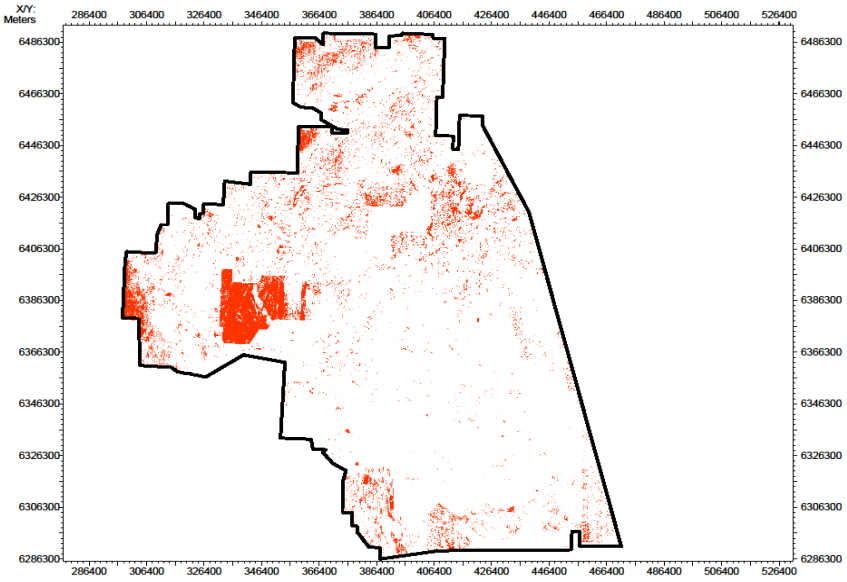

Fig. 23: Map showing regions with high RMS-amplitudes (red) of the interval between 50-700 ms below the seafloor. This interval corresponds to the upper 1 km of the sedimentary succession. The map is in UTM31N/ED50 projection. The underlying 3D seismic data set is compiled from various data sets and shows significant changes in min/mean/max amplitudes, resulting in varying RMS-amplitudes. However, for our pre-site survey we could derive valuable targets.

Water column imaging during our survey was done with approximately 3 kn ship speed to acquire high-quality data. We designed the surveys as orthogonal profiles across the abandoned wells to exclude the misinterpretation of fish shoals as flares.

German North Sea

In the German North Sea we conducted two surveys, which both did not show any signs of seepage above the well locations. Seismic data for pre-cruise analysis was not available. Therefore, we have no evidence for free gas in the upper 1 s TWT of the sedimentary succession.

UK North Sea

We conducted seven different surveys based on our RMS-amplitude map covering 21 abandoned wells in the UK sector of the North. 16 of 21 wells showed evidence for leakage (see Fig. 24, Table 2) into the water column expressed as flares in the water column image. The flares varied in ascend into the water column and spatial distribution. Both measurements are highly dependent on bottom water currents and flux from the well area. Our results suggest that crucial for leakage at abandoned wells are seismic RMS amplitude anomalies within the shallow sedimentary succession (below 1 s TWT). Major gas accumulations in this interval are found at the R4-URU horizon, corresponding to the top of Pliocene sediments.

Weather conditions severely influenced the quality of WCI data acquired with SB3050 MKII. Possible leaking wells might not have been identified due to bad weather conditions. However, most of our surveys were conducted in shallow to medium sea conditions.

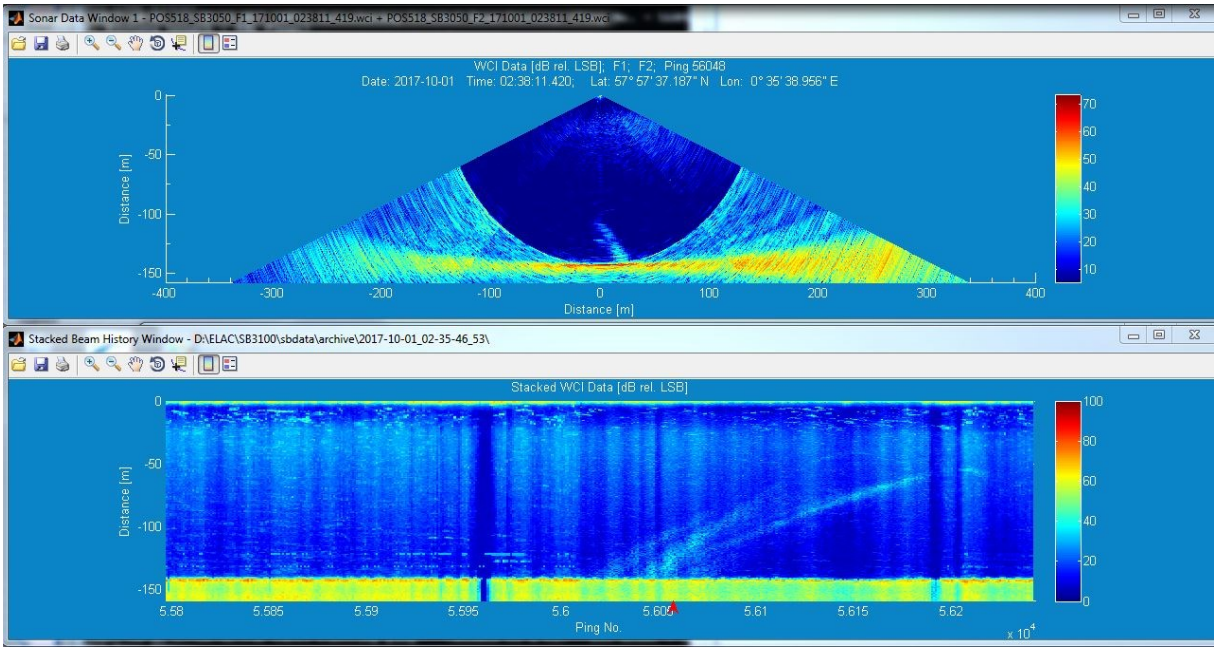

Fig. 24: (TOP) Fan view of ELAC SB3050 showing evidence for leakage at the seafloor in form of a flare. The graph shows distance in z-direction on the y-axis and range distance on the x-axis. **(DOWN)** Beam stack view with flare indicating leakage from well 21/03-2. The red arrow indicates the location of the fan view above. The plot shows range distance on y-axis and Ping numbers on the x-axis. The color bar is logarithmic from 0 to 100 dB.

Within the survey area around Goldeneye we conducted one survey covering 4 wells. None of the four wells did show any indications for leakage (Table 2). Pre-cruise analysis of seismic data did not show a RMS-amplitude anomaly within the first 0.6 s TWT.

Table 2: Table shows well identification number, latitude and longitude (WGS84), seismic chimney indicators and flare activity at the seafloor. Brackets mark uncertainties in the data.

Well ID	Lat [°dec]	Lon [°dec]	Seis. chimney	Flare (SB3050)	Flare (Imagenex)
21/03-2	57.96032265° N	0.59484599° E	No	Yes	No data
21/04b-5	57.98796563° N	0.64863782° E	No	Yes	No data
15/30-7	58.06849925° N	0.83968631° E	No	No	No data
15/30-1	58.08172147° N	0.83966628° E	No	Yes	No data
15/30-2	58.10242079° N	0.84184316° E	No	Yes	No data
15/30-11Z	58.11076772° N	0.84687348° E	No	No	No data
15/30-12	58.10081497° N	0.85885645° E	No	Yes	No data
14/29a-5	58.00539794° N	0.34646890° W	No	No	No data
20/04b-6	57.98907399° N	0.36719118° W	No	No	No data
20/04b-7	57.99142748° N	0.38766404° W	No	No	No data
14/29a-2	58.02437646° N	0.36792338° W	No	No	No data
30/01f-8	56.95494182° N	2.04974994° E	(No)	Yes	No
30/01a-7	56.99898931° N	2.16518431° E	Yes	Yes	Yes
23/26a-11	57.00510829° N	2.16473963° E	Yes	Yes	Yes
Natural seep	57.0011° N	2.1605844° E	Yes	Yes	Yes
29/01c-4	56.98680699° N	1.12869985° E	No	Yes	Yes
29/01c-9z	56.99149499° N	1.09466823° E	(Yes)	No	No
16/26-3	58.06173975° N	1.16689854° E	Yes	Yes	No data
16/27a-6	58.05366450° N	1.22586495° E	Yes	Yes	No data
16/27b-5	58.04533651° N	1.21006658° E	Yes	Yes	No data
16/26-24	58.04071637° N	1.18101603° E	(No)	No	No data
22/03a-2	57.94497112° N	1.43912433° E	(Yes)	Yes	No data
22/03a-3	57.93276731° N	1.42666349° E	Yes	Yes	No data
22/02b-15	57.94330722° N	1.38894170° E	No data	Yes	No data
22/02c-10	57.95075335° N	1.35554138° E	No data	No	No data

Figge Maar

The Figge Maar is located ~50 km north of Juist and is an anthropogenic blowout site in the German North Sea. After drilling into a gas pocket, fluids escaped with pressures of up to 200 bar and forced the rig “Mr. Louie” to end their drilling and abandon the blowout site. German newspapers report that the escaping fluids were identified as Nitrogen, while scientific publications refer to the Figge Maar as carbon dioxide blowout (Thatje et al., 1999). Due to these contradictory reports, the exact gas composition remains unknown. The drilling was conducted by consortium of 25 companies among

others including Deutsche Erdöl-Gesellschaft (DEA), Peussag-AG, Gelsenkirchener Bergwerks-AG.

Previous studies had a special emphasis on biological studies analysed the blowout crater and surrounding area. They found a 400 m diameter crater with a maximum water depth at the centre of ~ 50 m. Furthermore, they document high sedimentation rates of up to 50 cm per year (Thatje et al., 1999). Their bathymetric map of the Figge Maar shows a constant offset to our data of 300 m towards SW. Unfortunately, the Thatje et al. (1999) did not give information on the projection. So far, a reconstruction of the 300 m offset and a subsequent re-projection were not successful.

Our hydroacoustic survey, 54 years past the incidence, revealed a depression with 400 m in N-S and 500 m in W-E direction. The bathymetric data show an elliptical shape, which is 10-15 m deeper (max. ~45 m water depth) than the surrounding seafloor (avg. ~35 m water depth). The elliptical depression shows slightly increased slopes at the northern and western edges (Fig. 25).

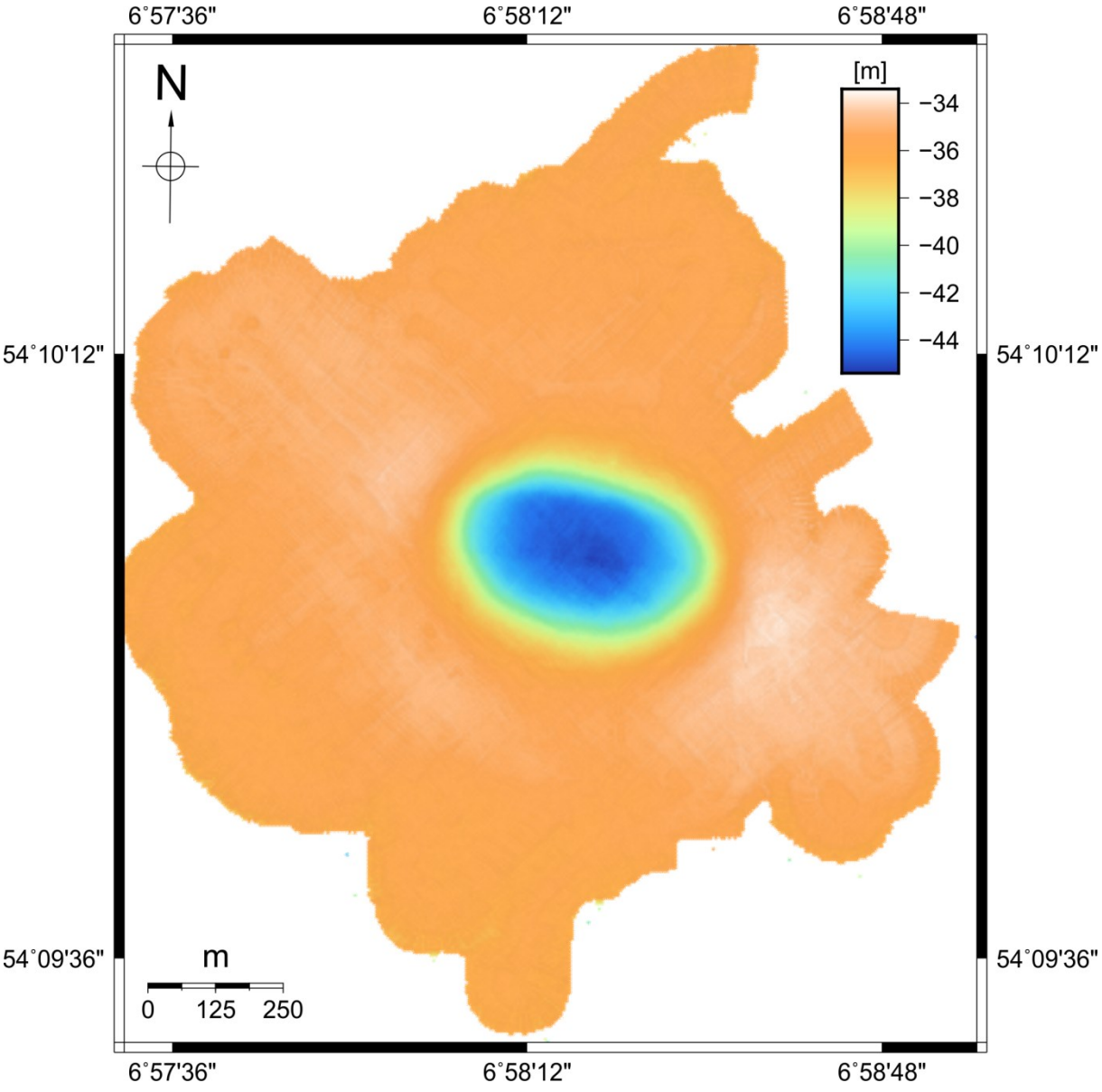

Fig. 25: Bathymetric map of the Figge Maar, a 10-15 m deep depression with a diameter of approximately 500 m.

We chose a very close line spacing of 50 m to enable post-cruise processing of water column data to identify seeps at the seafloor, track their trajectories, analyse the flare behaviour through the water column, and change of activity with time (e.g. tide currents). With our survey design (close spacing, orthogonal profiles), we are able to exclude shoals of fish as flare source signal.

We found abundant seepage sites inside Figge Maar. Seepage occurs widespread over the whole area of the Figge Maar. The seepage from the seafloor is highly dependent on the state of tide. During high tide, we saw no seepage activity in our multibeam data, while during low tide the system showed highest rates of activity.

6.1.2 Gas Composition and Gas Exchange into Atmosphere

Mark Schmidt, Tim Weiß

Atmospheric methane, water vapour, and CO_2-concentrations have been measured by the installed Picarro system during both POS518 legs (26.09.-28.10.2017; Fig. 26). Recorded data sets are separated into 1 hour files with a resolution of about 0.5-1 second. Unfortunately, the data sets exhibit numerous times of false signals or no signals as the internal detection unit of the Picarro had severe optical calibration issues (rough sea state?). Nevertheless, e.g. an interesting atmospheric data set of methane and CO_2 anomalies has been recorded on the 9th of October at the Figge Maar during a hydroacoustic survey (Fig. 27).

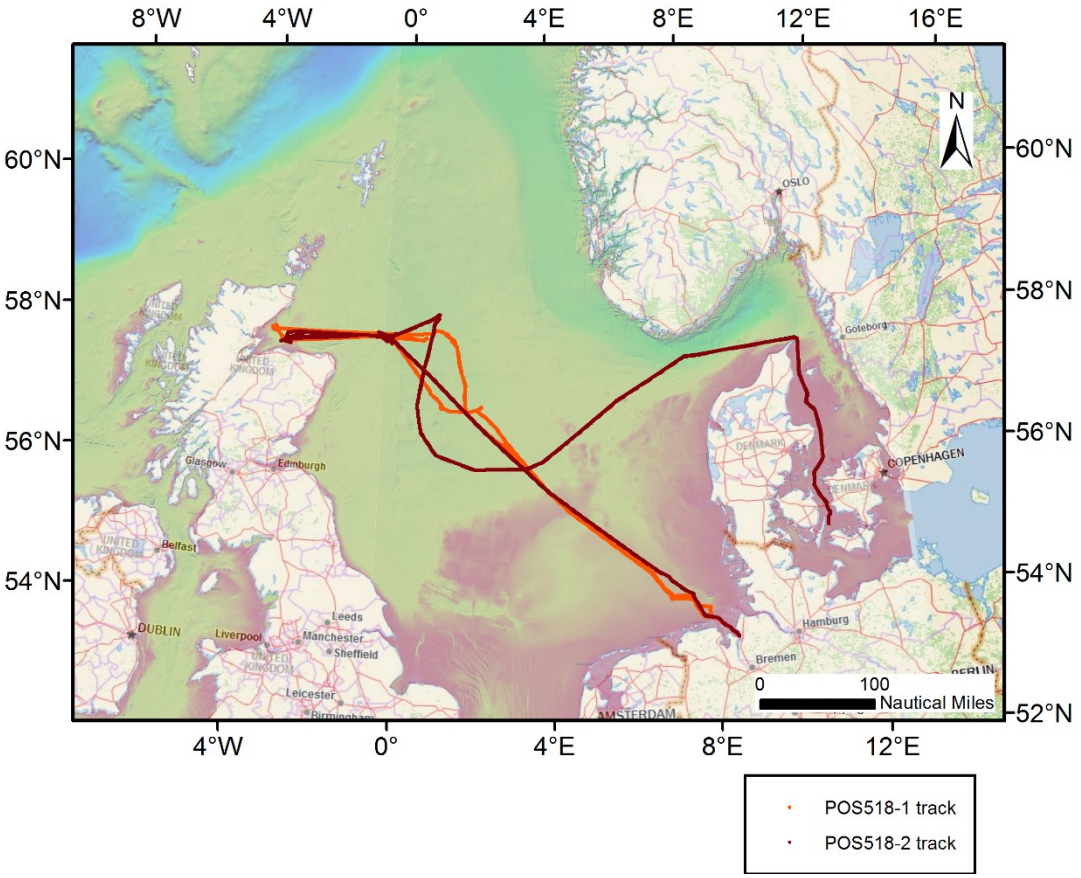

Fig. 26: Cruise track of Leg 1 and leg 2, where atmospheric gas composition was determined by using cavity ring down spectroscopy (Picarro).

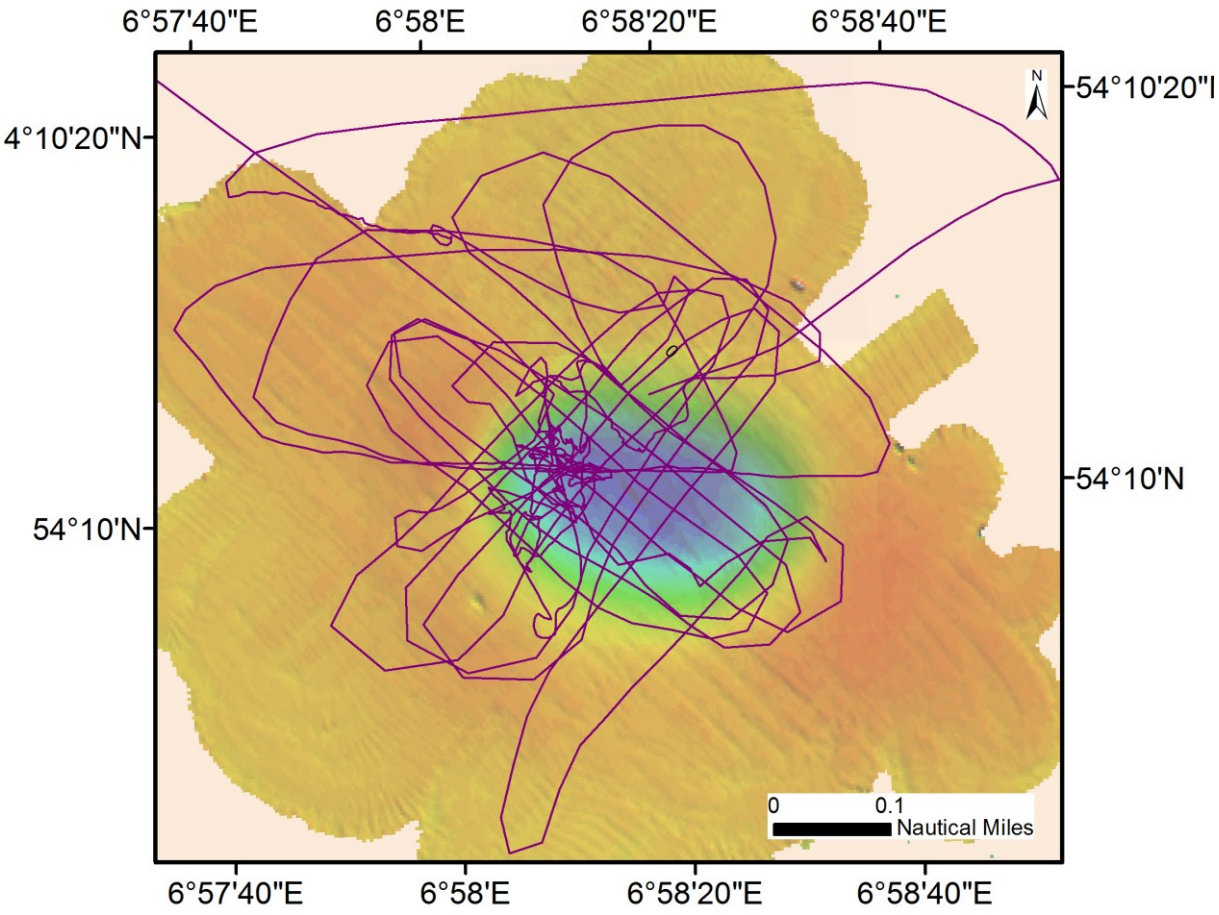

Fig. 27: Location (cruise track) where atmospheric CH_4, CO_2, and humidity was measured on the 9th of October 2017.

A clear relationship of gas seepage from the seafloor (30-40 mbsl) into the water column and to the atmosphere is not only indicated by hydroacoustic bubble imaging but also by atmospheric methane and CO_2 increase above the Figge Maar (Fig. 28). This increase of trace gases at 7.5 m above sea level strongly correlates with tidal changes. Means, that gas seepage can be clearly determined in the atmosphere at low tides only (Fig. 28).

First gas chromatographic results from determining gas composition of free gas bubbles, which were sampled at the seafloor of Figge Maar indicated methane concentrations >95 %-Volume.

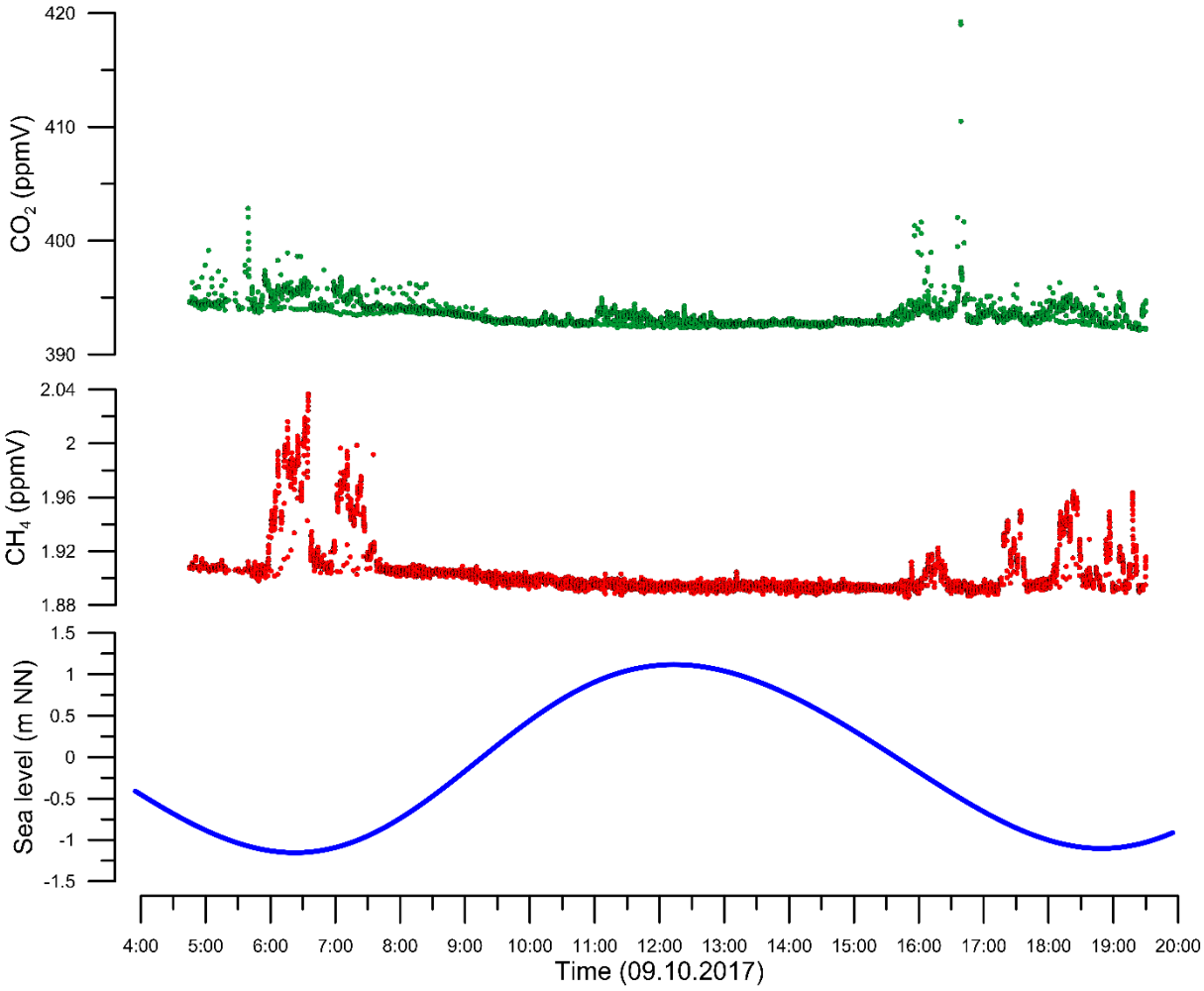

Fig. 28: Measured atmospheric methane and CO_2 concentrations at the Figge Maar are plotted with tide on 09.10.2017. For this date tidal changes (blue line) at Figge Maar are calculated by MB-system's OSU Tidal Prediction Software.

Dissolved methane and CO_2 concentrations measured by HydroC sensors during ROV dives 3 and 4 (St. 21-1, St. 21-2, 09.10.2017) and VCTD6 (St. 23-1 on the 10.10.2017 will also be processed for calculating methane and CO_2 fluxes at the Figge Maar.

Moreover, all measured data of pCO_2 (surface water), TA (surface water), atmospheric CO_2, pH (water column), dissolved CO_2 (water column), TA (water column), DIC (water column) will be used to identify a background scenario for inorganic carbon fluxes in the central North Sea, autumn 2017.

6.2 Hydrographic Investigations

6.2.1 Water Column Chemistry

Mark Schmidt, Stefan Sommer, Peter Linke, Anita Flohr, Christine Utecht

During leg 1, six CTD-stations were conducted in the German and British North Sea for hydrographic data recording and sound velocity calculations (Fig. 29). VCTD1, 2 and 5 were performed as hydrocasts, VCTD3, 4, and 6 were conducted in hydrocast and towed modus. Moreover, VCTD3 and 4 were used to sample the water column and benthic layer at Goldeneye (Fig. 30). In total 24 Niskin water bottles (NiBo) had been fired at selected depths and were subsampled for dissolved gas, carbon species, nutrients and chemical tracer studies (Table 3).

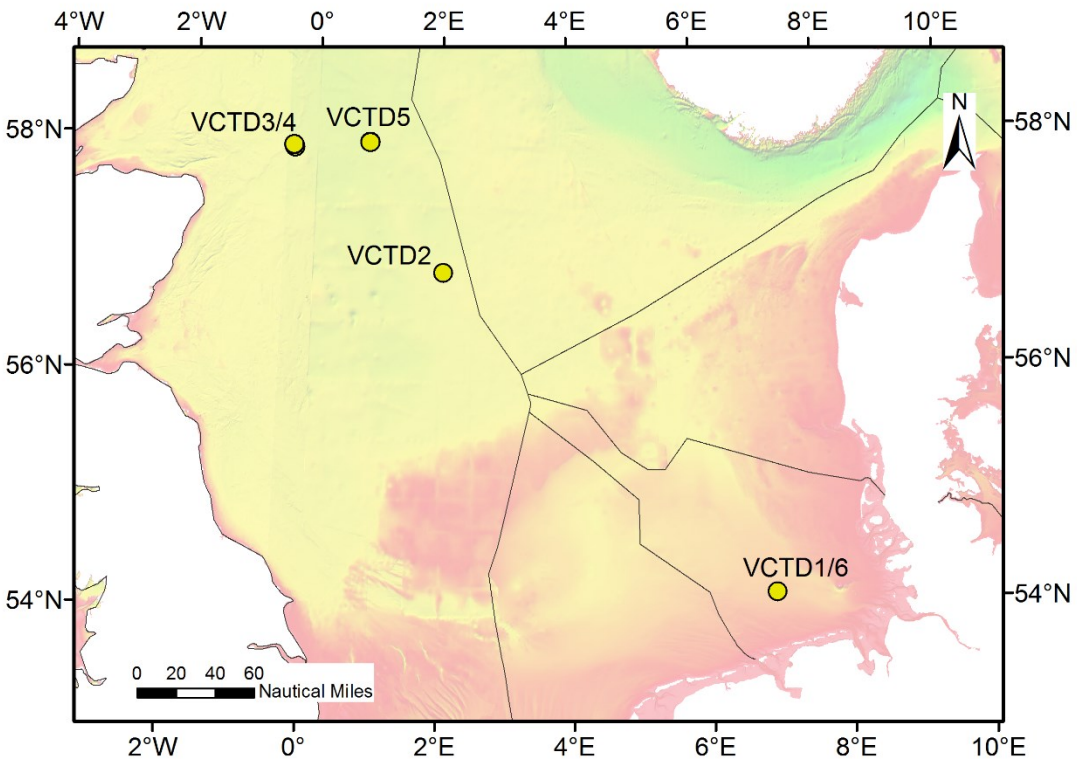

Fig. 29: Video-CTD (VCTD) stations conducted during cruise POS518/1 in the German and British sector of the North Sea.

Table 3: List of water samples taken during cruise POS518/1 for subsequent chemical analyses at GEOMAR.

	Methane	TA/DIC	TA_onboard	Nitrate/Nitrite	IC	ICP
8-VCTD03						
NiBo 1	x	X	X	x	x	x
NiBo 2	x	X	X	x	x	x
NiBo 3	x	X	X	x	x	x
NiBo 4	-	-	-	-	-	-
NiBo 5	x	X	X	x	x	x
NiBo 6	x	X	X	x	x	x
NiBo 7	x	X	X	x	x	x
NiBo 8	x	X	X	x	x	x
NiBo 9	x	X	X	x	x	x
NiBo 10	x	X	X	x	x	x
NiBo 11	x	X	X	x	x	x
NiBo 12	x	-	X	x	x	x
9-VCTD04						
NiBo 1	x	X	X	x	x	x
NiBo 2	x	X	X	x	x	x
NiBo 3	x	X	X	x	x	x
NiBo 4	-	-	-	-	-	-
NiBo 5	x	-	X	x	x	x
NiBo 6	x	X	X	x	x	x
NiBo 7	x	X	X	x	x	x
NiBo 8	x	X	X	x	x	x
NiBo 9	-	-	-	-	-	-
NiBo 10	x	-	X	x	x	x
NiBo 11	x	X	X	x	x	x
NiBo 12	x	X	X	x	x	x

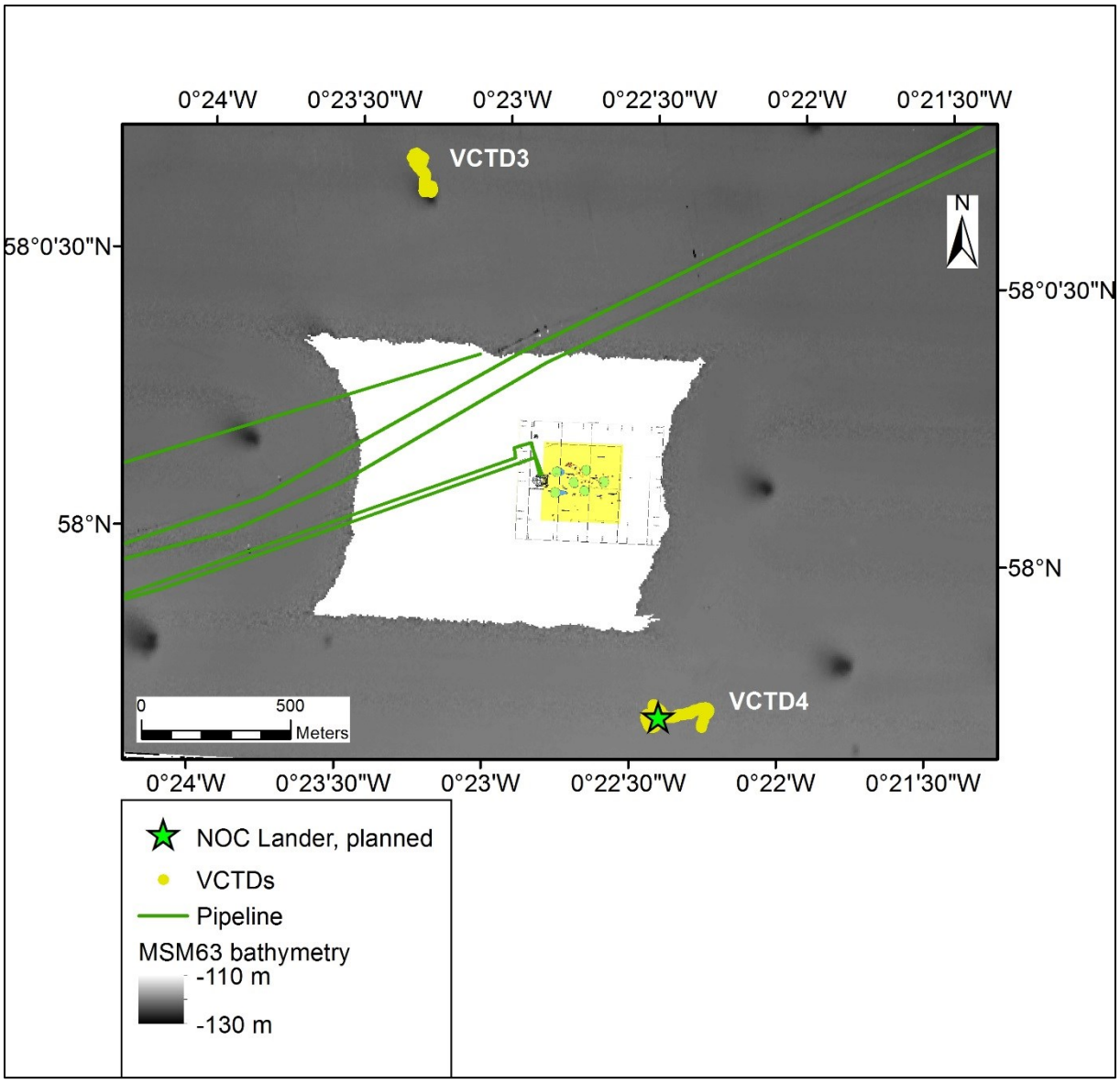

Fig. 30: Detailed view on tracks of towed VCTD3 and 4 in the Goldeneye area.

Recorded temperature, salinity, oxygen concentration, and pH are plotted versus water depth in Figures 31A-E. The southernmost station VCTD1 (St. 3) indicates a well-mixed water column at Figge Mare (German EEZ) from sea-surface down to the seafloor at about 35 mbsl. Deeper waters further north in the British EEZ show a distinct stratification with a thermocline at about 30-45 mbsl in VCTD2, station 5 (Fig. 31B). This prevents cold and saline waters, down to the seafloor at about 90 mbsl, from mixing with warm surface waters, even after several storm events, which had been taken place before starting PO518 expedition.

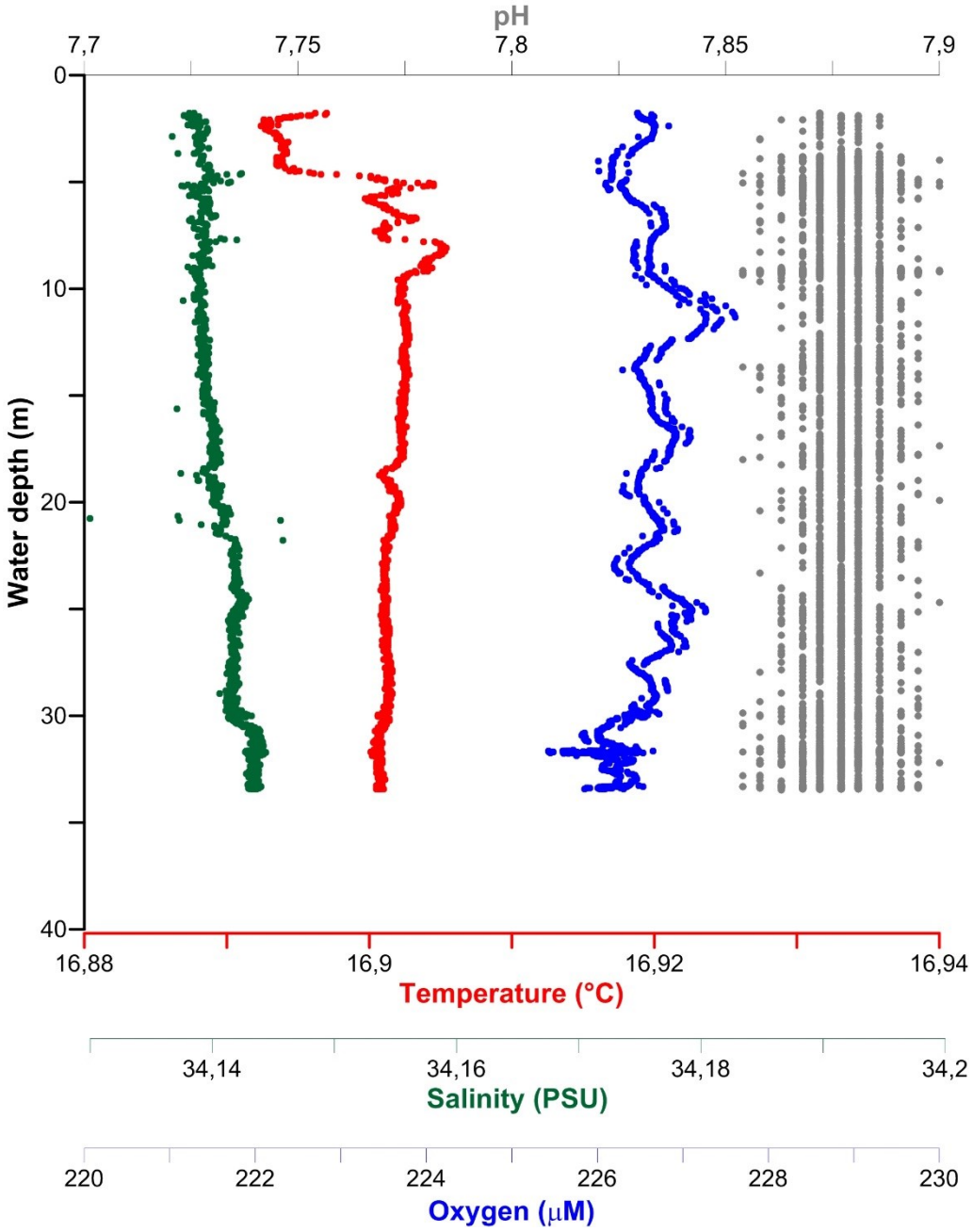

Fig. 31A: VCTD1 (Station 3, POS518/1) hydrocast is located in the Southern German North Sea (i.e. Figge Maar).

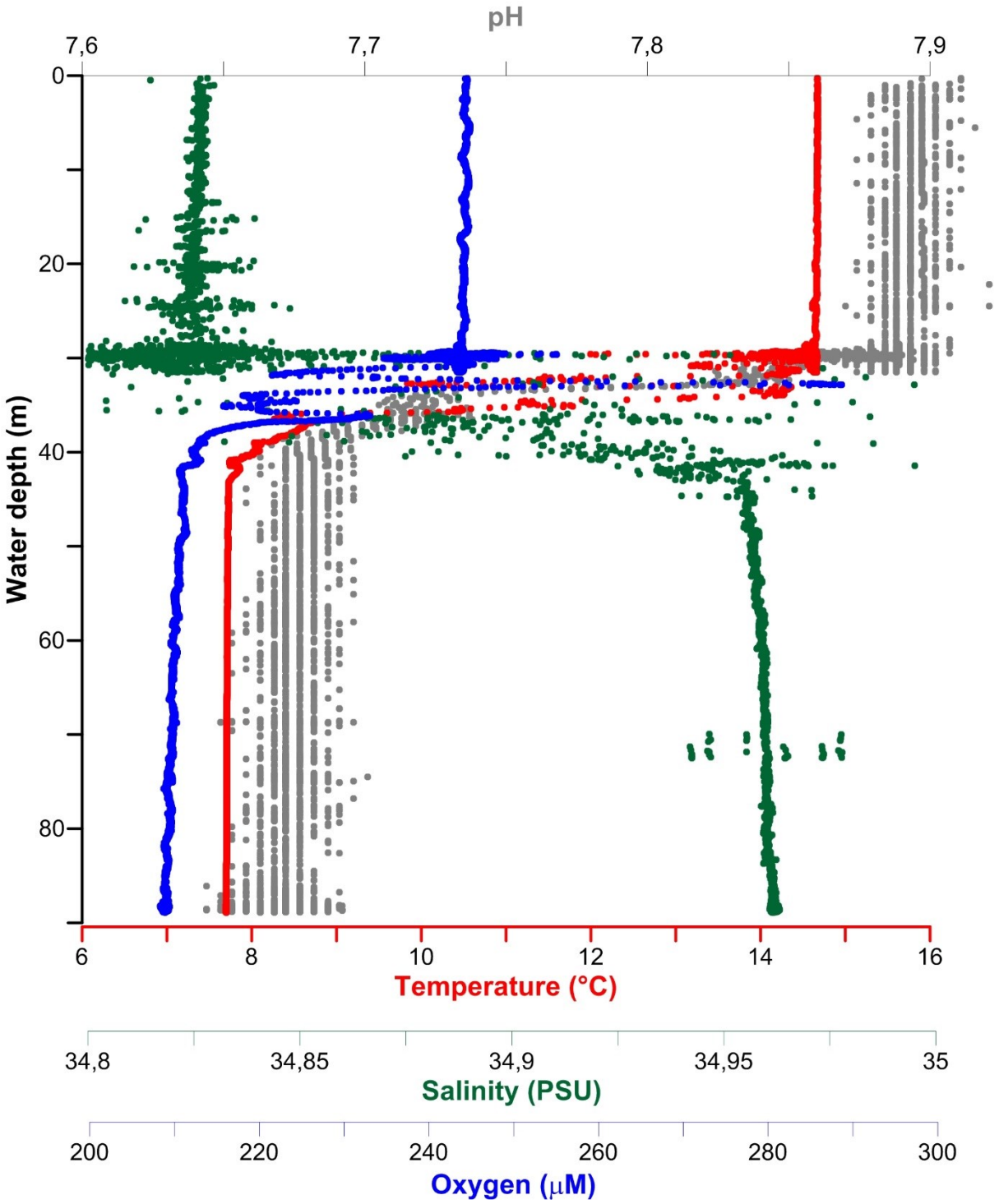

Fig. 31B: Station 5 (VCTD2, POS518/1) hydrocast is located in the British EEZ (central North Sea, Fig. 30).

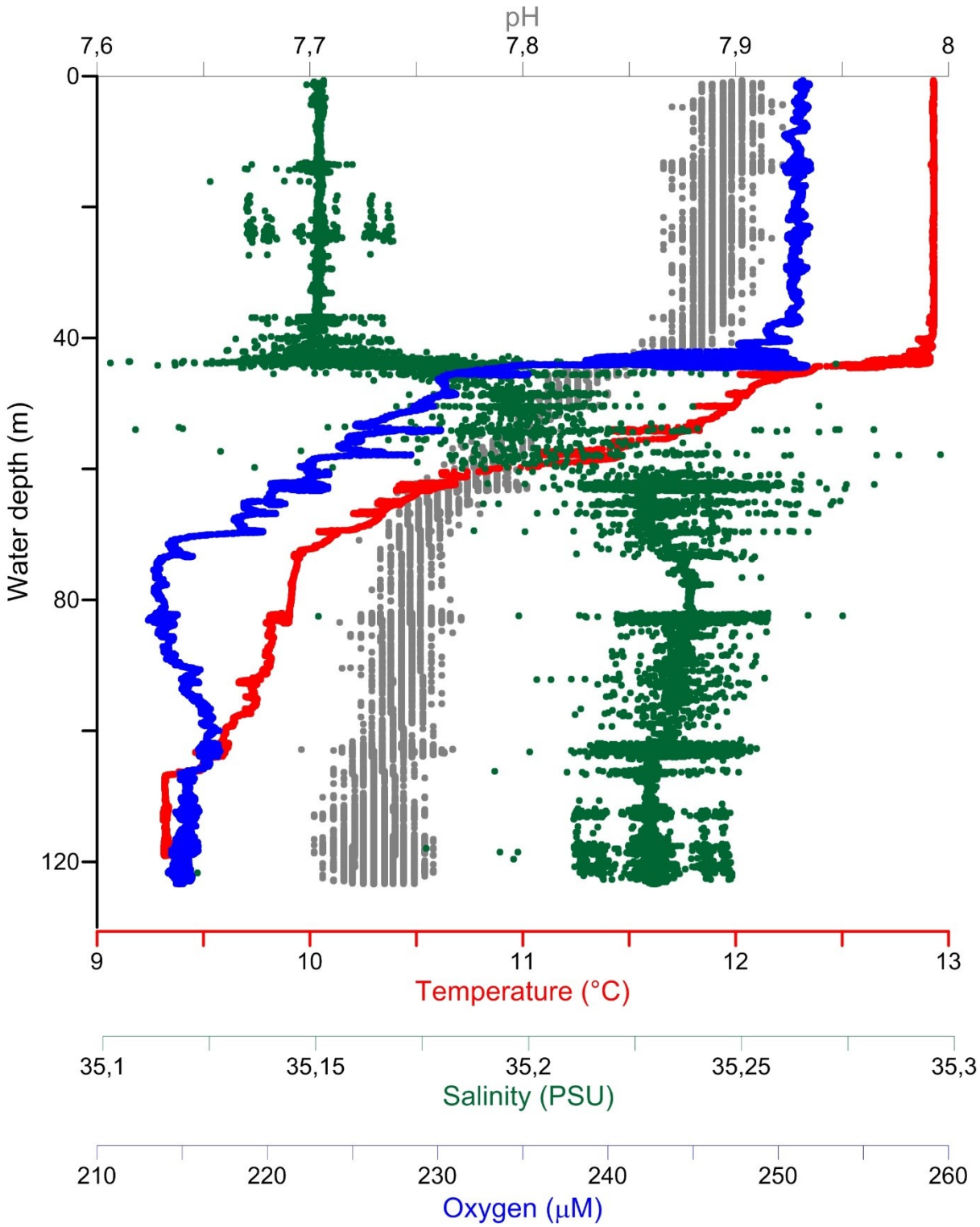

Fig. 31C: Station 8 (VCTD3, POS518/1) is located in the British EEZ (Pockmark structure, north of Goldeneye, Fig. 30). Water depth is about 125 m.

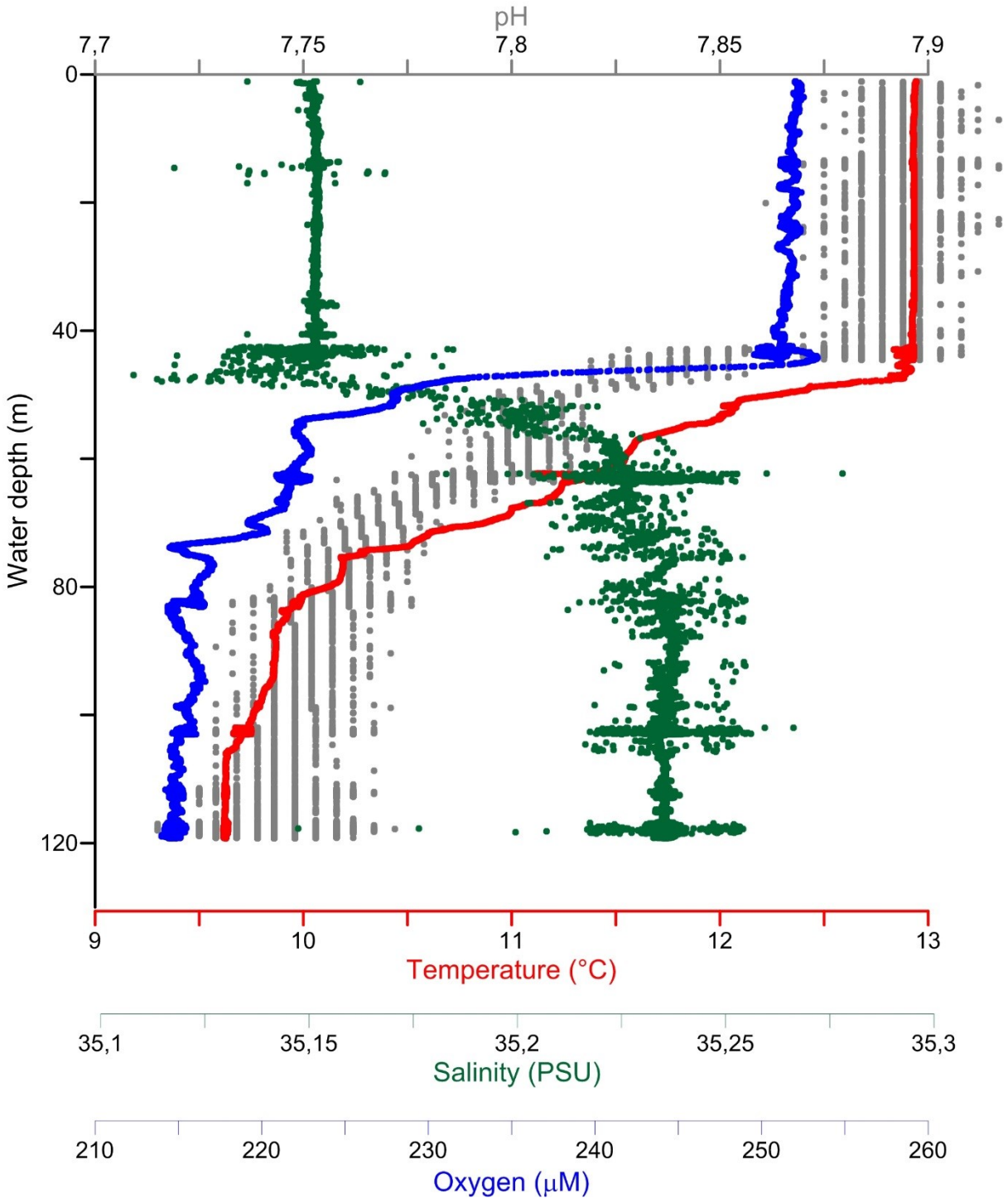

Fig. 31D: Station 9 (VCTD4, POS518/1) is located in the British EEZ (south of Goldeneye, Fig. 30). Water depth is at about 120 mbsl.

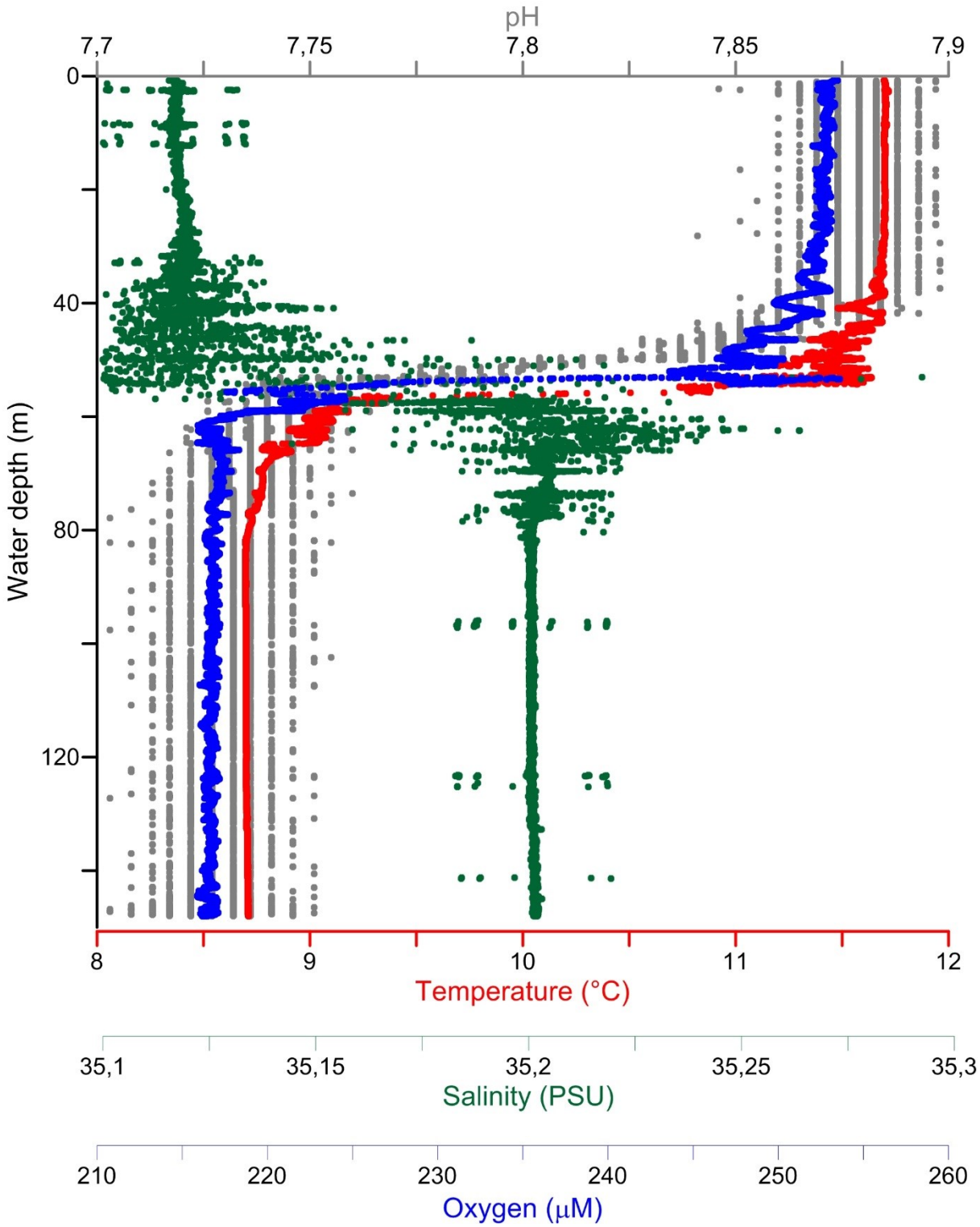

Fig. 31E: Station 16 (VCTD5, POS518/1) is located in the British EEZ (Fig. 30). Water depth is at about 150 mbsl.

During the 2nd leg of cruise POS518 a total of 8 vertical CTD hydrocasts was performed; 7 of them in the vicinity of the Goldeneye platform and one cast at the flank of the Scanner Pockmark. A list of water samples taken from these casts is provided in Table 4:

Table 4: List of water samples taken from VCTD casts during POS518/2.

Station	Area	DO onboard	Nutrients onboard	TA onboard	TA/ DIC	$\delta^{13}C_{DIC}$	DOC	$\delta^{18}O_{DIC}$ $\delta^{18}O_{H2O}$	DNG + isotopes	SF6, SF5CF3	TNT
1-VCTD 01	Goldeneye	X	X	X	X	X	X	X			X
4-VCTD 02	Goldeneye	X	X	X	X	X	X	X			X
7-VCTD 03	Goldeneye								X	X	
10-VCTD 04	Goldeneye				X	X	X	X			X
11-1-VCTD 05	Goldeneye				X	X	X	X			
11-2-VCTD 06	Goldeneye								X	X	
16-2-VCTD 08	Goldeneye	X			X	X	X	X			
17-VCTD 09	Scanner Pockmark	X			X	X	X	X			

DO = dissolved oxygen, TA = total alkalinity, DIC = dissolved inorganic carbon, DOC = dissolved organic carbon, DNG = dissolved noble gases, SF6 = sulfurhexafluoride, SF5CF3 = trifluoromethylsulfurpentafluoride, TNT = trinitrotoluene

During this cruise, we had the opportunity to observe the impact of the hurricane “Ophelia” on water column hydrodynamics and benthic oxygen fluxes. During its northwards passage the hurricane “Ophelia” weakened and has been categorized as a very strong gale. It passed over the working area during the night from Monday 16th to Tuesday 17th October. Whenever weather conditions were favorable, a CTD/rosette cast (V-CTD) was conducted at Golden Eye resulting in a total of 7 deployments.

Despite the storm, the water column was stratified and its vertical structure can be classified according to the scheme by Rovelli et al. (2016) into the four layers, i. mixed surface layer, ii. transition layer at the upper boundary of the thermocline, iii. interior layer of the thermocline, and iv. the BBL. It is remarkable that between the V-CTD #1 conducted before the storm passage (16. Oct. 2017 04:30) and the V-CTD#2 performed thereafter (18. Oct. 2017 11:25) the surface layer (salinity: 35.15 PSU; temperature: 11.4 to 12.0 °C) remained distinct from the bottom waters characterized by a higher salinity of about 35.25 PSU. Nevertheless, between the V-CTD #1 and V-CTD#2 a major deepening of the mixed surface layer from ~22 m to 56 m as well as an uplift of the thermocline was measured (Fig. 32). After the storm the thickness of the BBL increased to about 9 and 13 m associated with a compression of the interior layer of the thermocline. The BBL could not be resolved during V-CTD#1 prior to the storm. Vertical O_2 concentration profiles showed a similar trend as the temperature

with a sharp oxycline associated with the interior layer of the thermocline separating mixed surface layer concentrations of 263 µM from bottom water concentrations of about 230 µM (Fig. 32).

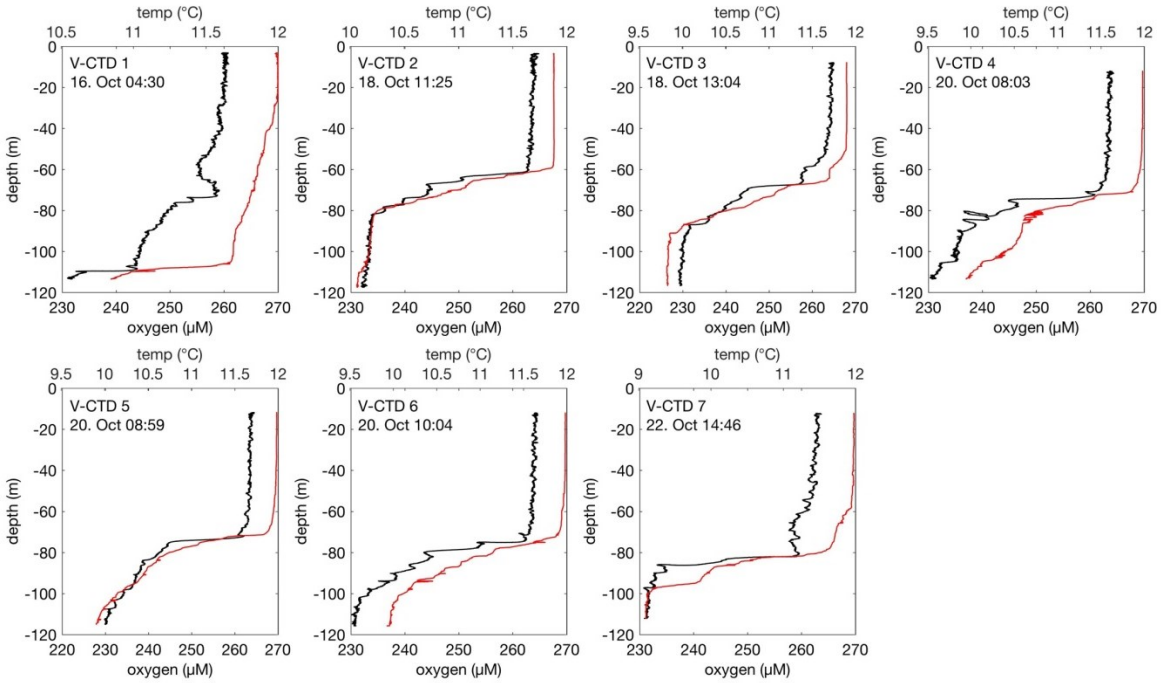

Fig. 32: Vertical oxygen (black line) and temperature profiles (redline) at 7 V-CTD casts at Golden Eye during POS518/2.

6.2.2 Oxygen, Carbonate System and pH at Goldeneye

Dirk Koopmans, Mark Schmidt

Measured pCO_2-concentrations during Leg 1 are ranging between 416 and 438 µatm near the seafloor at Goldeneye (Fig. 33). Total alkalinity concentrations determined onboard from Niskin bottle samples VCTD4 NiBo 1-5 (Table 3), are in the range of 2338 - 2346 µmol/kg. Near seafloor pH-value is about 7.5 (Fig. 30D).

Oxygen concentrations monitored near the seafloor during VCTD4 are about 215 µM (Fig. 31D), which corresponds to 76 % oxygen saturation.

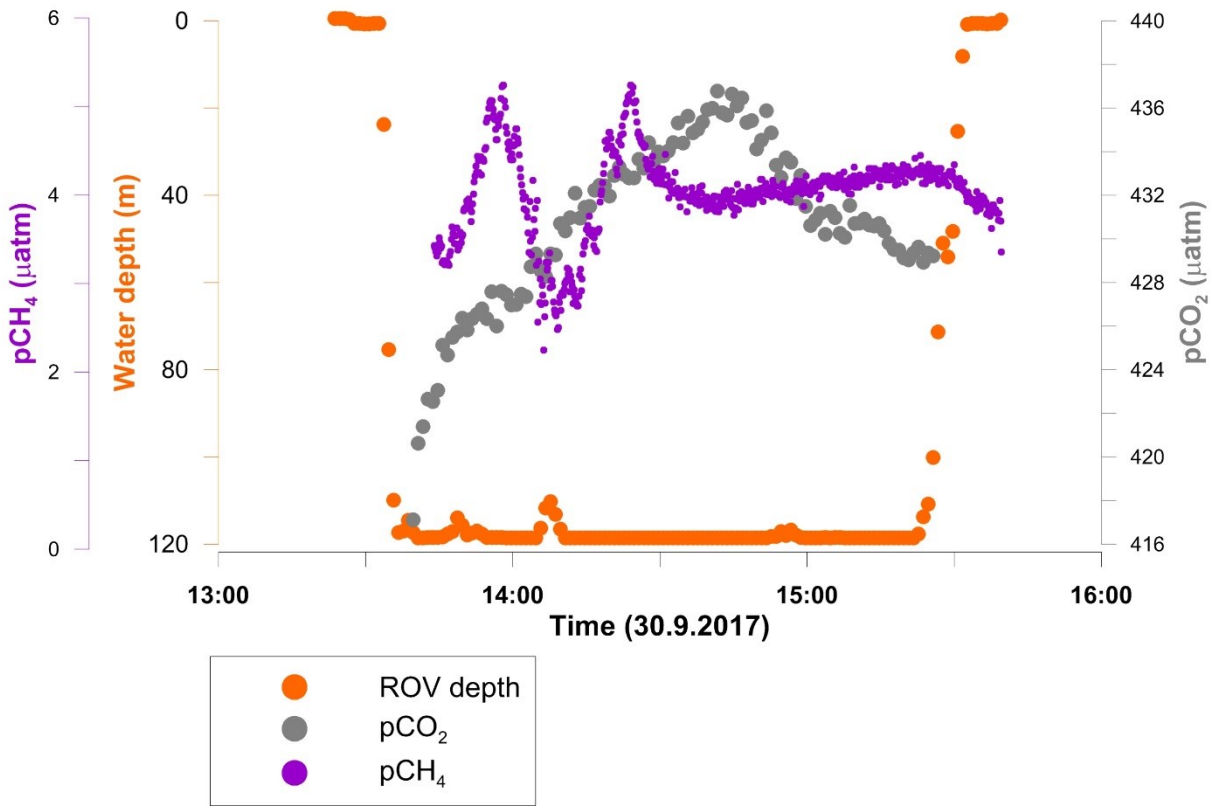

Fig. 33: Dissolved gas concentrations (pCO_2, pCH_4) were measured at the seafloor near Goldeneye during Eddy-correlation experiments with ROV Phoca (ROV-dive 1, St. 13; Fig. 34). Gas sensors (HydroCs) had been mounted to the plate of ROV Phoca. ROV-depth was monitored with the onboard SBE49-CTD.

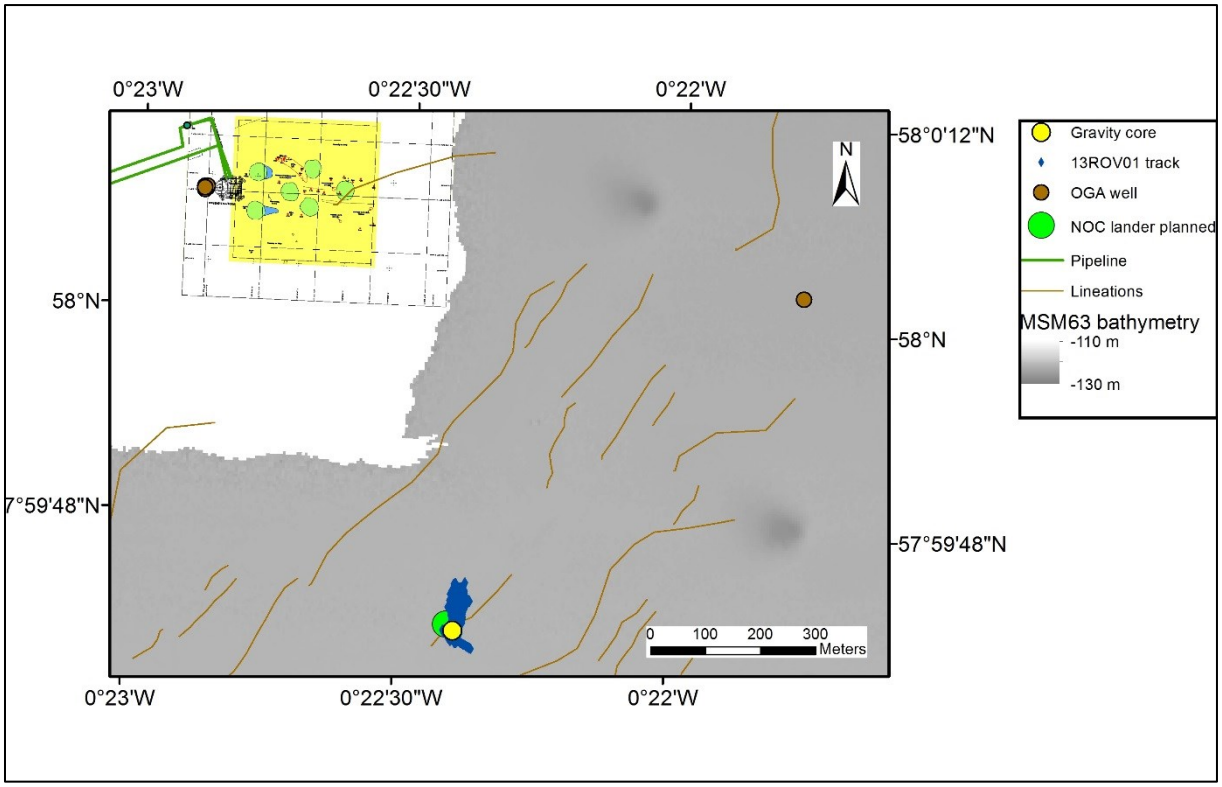

Fig. 34: Dive 1 of ROV PHOCA (blue dots) was conducted in the area south of Goldeneye.

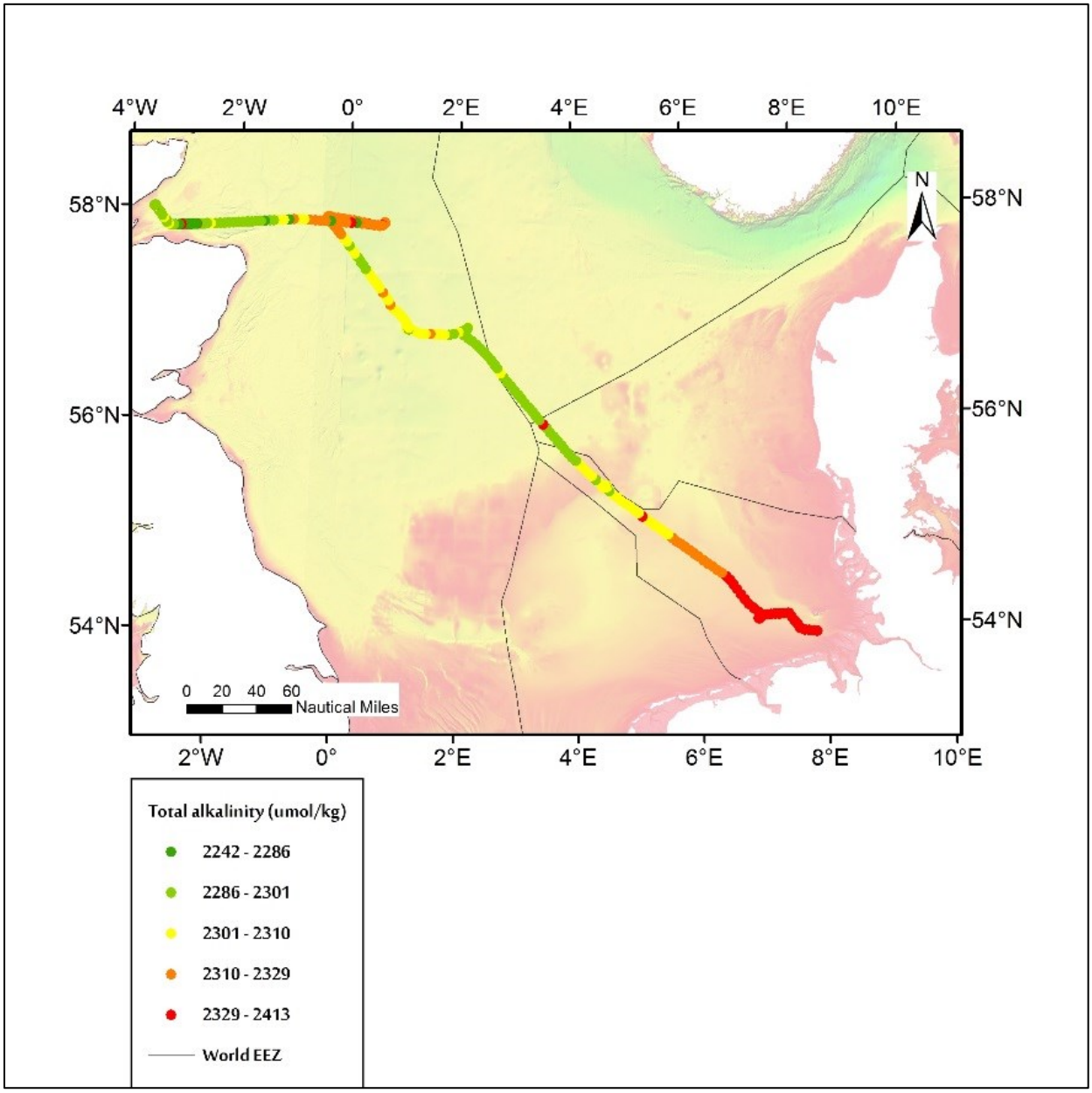

Fig. 35: All measured underway total alkalinity values (Leg 1) are plotted in a concentration heat map. Concentration variations probably reflect the general influence of North Atlantic inflow (Turrell et al., 1992) and coastal influences (southern North Sea).

Oxygen eddy covariance

Oxygen concentrations in bottom water were low, between 75 and 78% of saturation with our 3 stable oxygen sensors. The oxygen minisensor was not damaged by the deployment, but it may have been affected by the relatively high water velocities at the site. Dissolved oxygen concentrations were biased, with unexpected oscillations of 10 µM. Despite the bias, dissolved oxygen fluxes at the site were reproducible (Fig. 36). Oxygen fluxes were low, averaging about 5 mmol m^{-2} d^{-1}. At these low rates, we expect fluxes to be rough. These fluxes are one-fourth of the oxygen fluxes we would expect to find closer to shore in the German Bight.

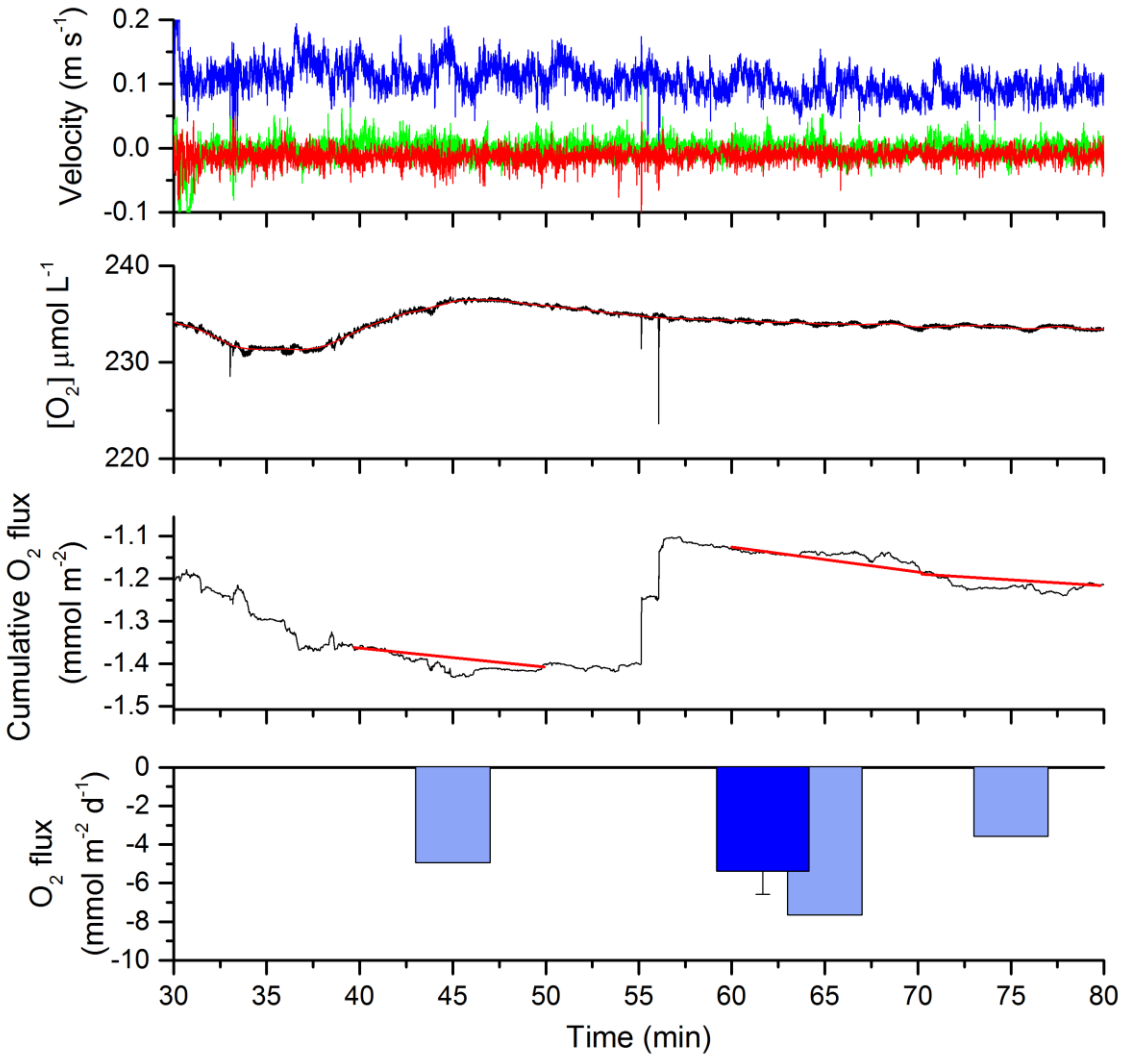

Fig. 36: The eddy covariance measurements of water velocity, oxygen concentration, cumulative oxygen flux, and oxygen fluxes for the deployment at Goldeneye. Negative values represent oxygen uptake by sediments. High frequency oxygen concentrations were offset from those measured by stable optodes (218 µM). Debris likely caused spikes in velocity and dissolved oxygen at minute 55.

pH eddy covariance

The pH of bottom water at the lander was 7.75 according to our RBR sonde. The pH ISFET eddy covariance technique performed well. Turbulent pH measurements were more stable than turbulent dissolved oxygen measurements. As a result, fluxes calculated from pH were also more reproducible than fluxes calculated from dissolved oxygen (Fig. 37). The proportion of hydrogen ions to CO_2 was calculated using the software CO2SYS. The input parameters were the in situ pH and the alkalinity determined by MAS (2342 µmol kg^{-1}). The mean benthic CO_2 production was 6.5 mmol m^{-2} d^{-1}, in agreement with oxygen consumption. Because this system was able to quantify CO_2 production at these low rates, it holds a lot of promise for quantifying CO_2 production during a scenario of abiotic release. Quantifying abiotic release will involve new challenges, however.

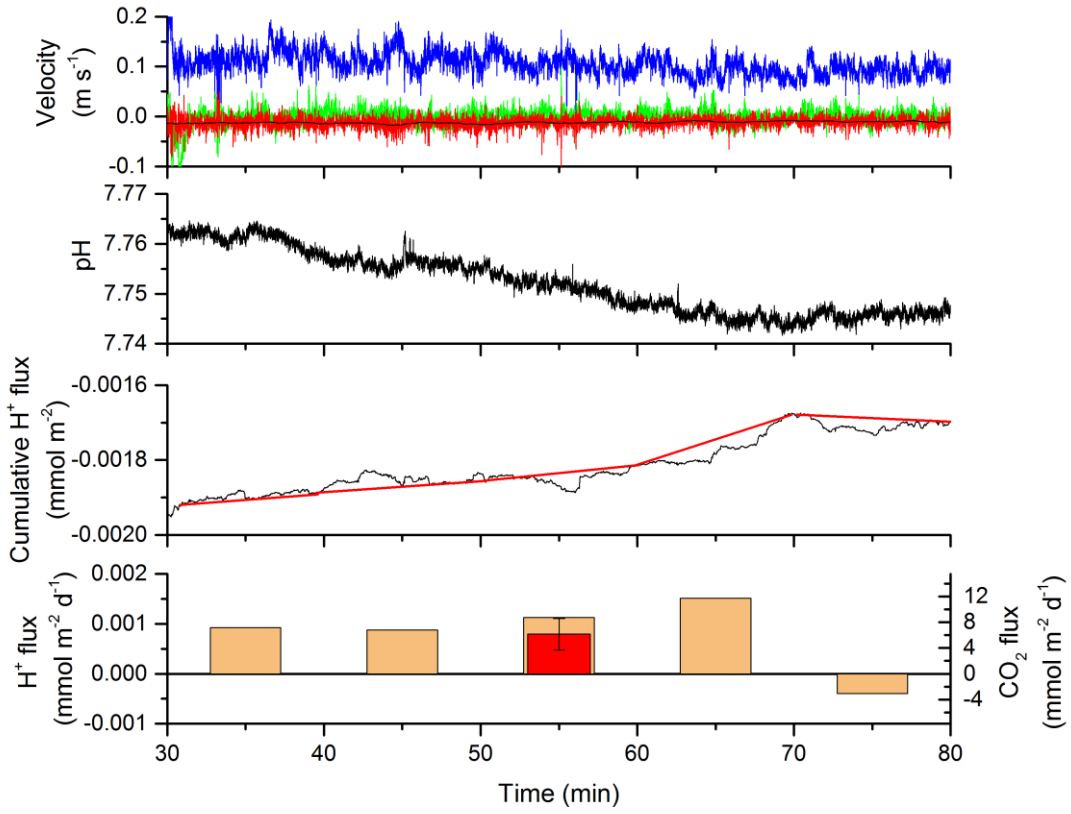

Fig. 37: The eddy covariance measurements of water velocity, pH, cumulative hydrogen ion flux, and benthic CO_2 fluxes for the deployment at Goldeneye. Positive fluxes correspond to benthic CO_2 production of close to 5 mmol of CO_2 m^{-2} d^{-1}.

6.3 Lander Measurements

Stefan Sommer, Peter Linke

Storms play an important, but as yet poorly quantified, role in the ecosystem dynamics of the ocean (Babin et al. 2004) and have a major impact on coastal management (Weisse et al. 2012). The physical response of the upper ocean to storms includes a decrease in sea surface temperature associated with an uplifted thermocline, deepening of the mixed layer, and transient upwelling induced by Ekman pumping (Shropshire et al. 2016 and references therein). Storms further strongly affects mixing of the water column as well as sediment suspension and transport (Glenn et al. 2008). Mixing events are especially significant on continental shelves, where storms can affect the full water column and the sediment bed below (Chang et al. 2001). Storms can be expected to affect oxygen and carbon turnover dynamics in the benthic boundary layer (BBL) and the seabed. Climate projections indicate longer stratification period and stronger thermocline stability in the North Sea (Nauw et al. 2015), which likely lead to an increasing O_2 depletion in the BBL and sediments (Rovelli et al. 2016 and references therein). Substantial turbulent O_2 fluxes from the thermocline to the otherwise isolated BBL caused by baroclinic near inertial waves were reported for the central North Sea (Rovelli et al. 2016). However, whether storm driven ventilation events might contribute to counteract the ongoing O_2 depletion (Queste et al. 2013) remains enigmatic.

There is no clear trend in the frequency and magnitude of storms in relation to proceeding global warming. The storm activity in the North Sea underwent considerable variability during the past decades but do not show a clear long-term trend (Weisse et al. 2012). Storm activity was low during the 1960s increased towards a maximum in the 1990s and decreased again. Most projections indicate a moderate increase in storm activity in the North Sea with corresponding changes in storm surge and wave climate (Weisse et al. 2012).

6.3.1 NOC Lander Measurements

Mario Esposito

The NOC lander's first deployment occurred on this cruise, in the early hours of the 16th of October. After deployment the lander was interrogated via hydrophone to verify all the sensors were correctly operating. The response was successful. On the 18th of October the lander was interrogated for the second time, however this time, strong currents precluded a successful communication. A second attempt was performed on the 20th of October and this time, despite the heavy weather conditions, a successful communication was established. Remote access to the lander data logger confirmed the lander was correctly operating and data from all the integrated devices were being recorded.

6.3.2 SLM Lander Measurements

Stefan Sommer, Peter Linke, Christine Utecht, Matthias Türk, Asmus Petersen

During this cruise, we had the opportunity to observe the impact of the hurricane "Ophelia" on water column hydrodynamics and benthic oxygen fluxes. During its northwards passage the hurricane "Ophelia" weakened and has been categorized as a very strong gale. It passed over the working area during the night from Monday 16. to Tuesday 17. October. Water column properties were recorded using a SLM lander for the time period of 16.10.17 07:35 to 22.10.17 13:35. The lander was equipped with an upward looking RDI ADCP (307.2 kHz), which sampled every 60.02 s with a bin size of 1 m starting from 3.21 m from the bottom, a SBE CTD for the measurement of physical properties, an O_2 optode sensor (Aanderaa Data Instruments AS, Bergen, Norway), which recorded BBL O_2 concentration at 5 min intervals, as well as with a fluorometric probe for turbidity measurements. Unfortunately, the turbidity sensor was not in operation during the deployment.

Bottom water O_2 levels recorded by the SLM lander varied between 223 and 233 µM, Fig. 38 (upper panel). Since the passage of the storm the O_2 concentrations slightly increased until midnight 19. Oct., where a sharp drop of O_2 was measured. Afterwards the O_2 concentration increased again. Whether this O_2 variability is related to the passage of lows and which effects on bottom water O_2 is induced by the passage of Ophelia awaits further analysis. This increase of oxygen could be caused by the Fair Isle Current, which transport saline oxygenated water (35.05 – 35.15) into the working area (Nauw et al. 2015). In October, when stratification was still present transport can to be enhanced (reduced) by North North Westerly (South South Easterly) winds blowing directly along the mean topography (Nauw et al. 2015), thereby contribute to modulate the bottom water O_2 levels.

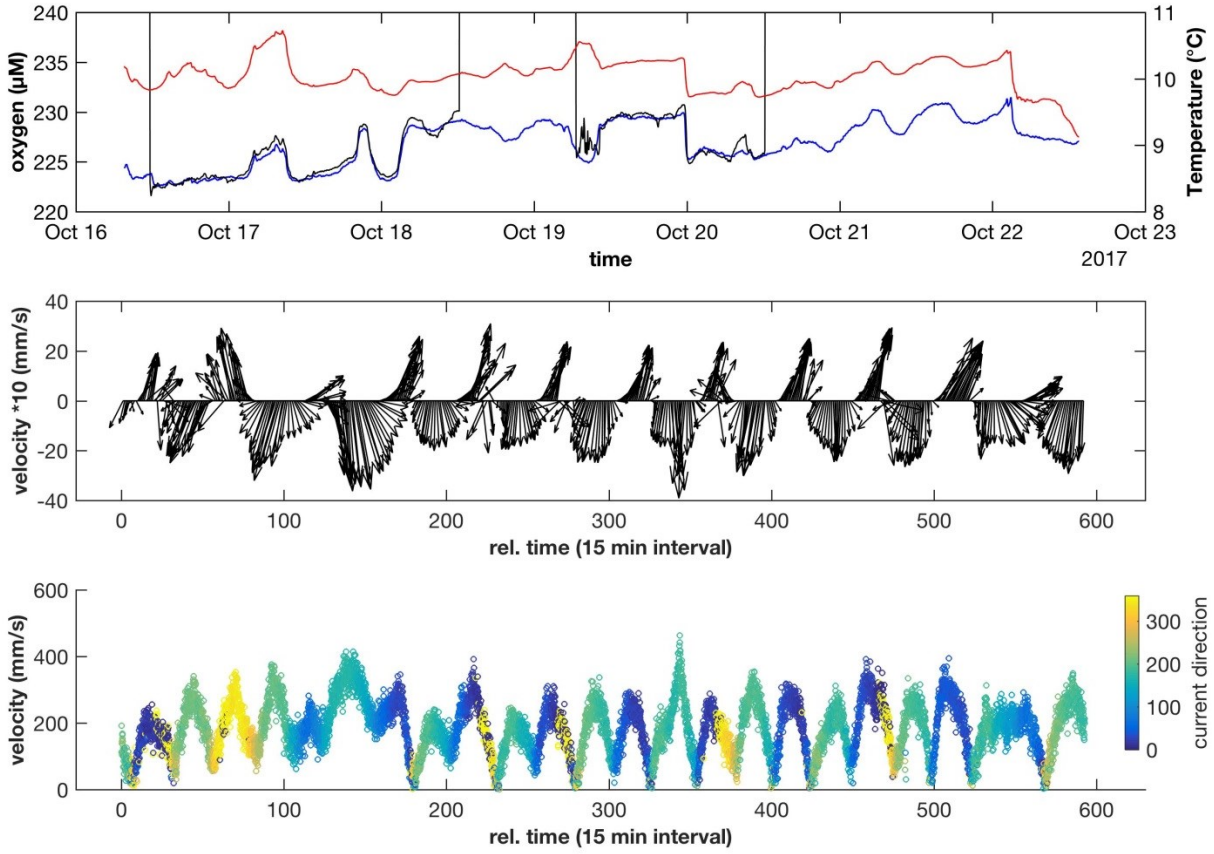

Fig. 38: upper panel, time series of O_2 levels (blue line) and temperature (red line) measured during the SLM3 lander deployment. The black lines indicate independent O_2 measurements recorded during the BIGO-I-l and BIGO-I-2 deployment using an optode mounted in a distance of ~50 cm above the seafloor. The vertical lines indicate the descend to seafloor and the ascend back to the sea surface of each deployment; **middle panel**, time series of current vectors, which were measured in a distance of about 4.5 m above the sea floor (2nd Bin of ADCP record); **lower panel**, time series of current velocity (Bin 2).

Further pronounced effects of the storm passage became apparent in distinct changes of the bottom water current regime. During and directly after the passage of Ophelia, the northeasterly component of the bottom water current regime typically characterized by a regular semidiurnal change between southerly and north-easterly current directions became almost suppressed (Fig. 38, middle panel). Instead, southerly currents with high velocities became predominant (Fig. 38, middle and lower panel). This results in an enhanced southward flow with maximum current velocities of more than 500 mm s^{-1} (data not shown in the reduced data set), whereas the tidally affected flow is directed into a southeasterly direction (Fig. 39). This apparently storm driven change in the current regime affects the entire water column (Fig. 40).

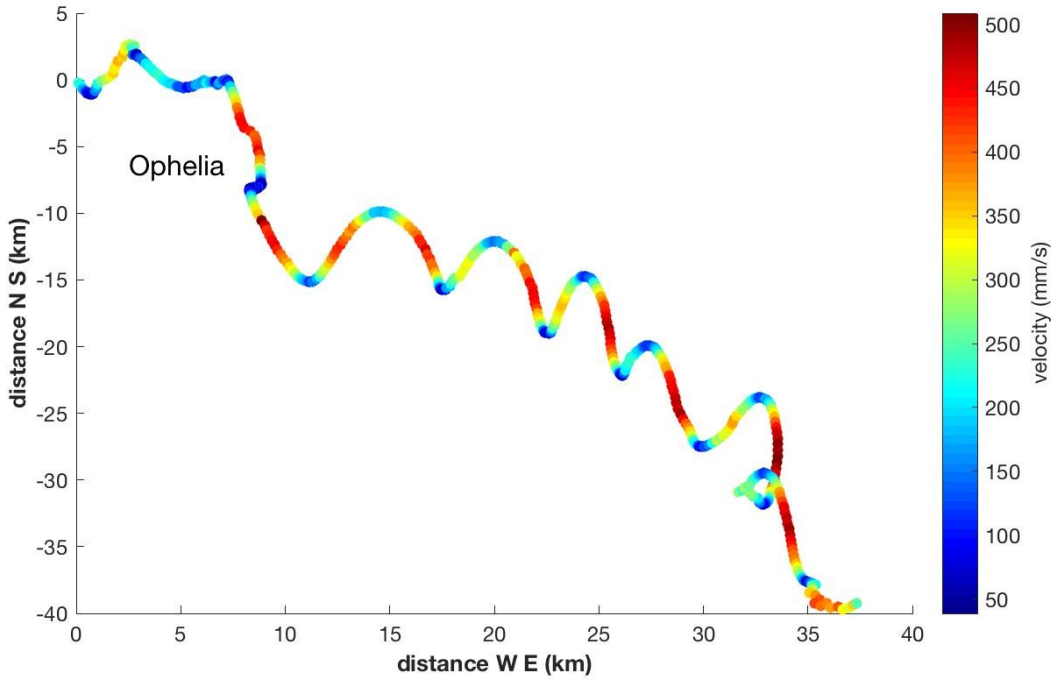

Fig. 39: Cummulative current vector measured at a distance of 4.5 m above the sea floor.

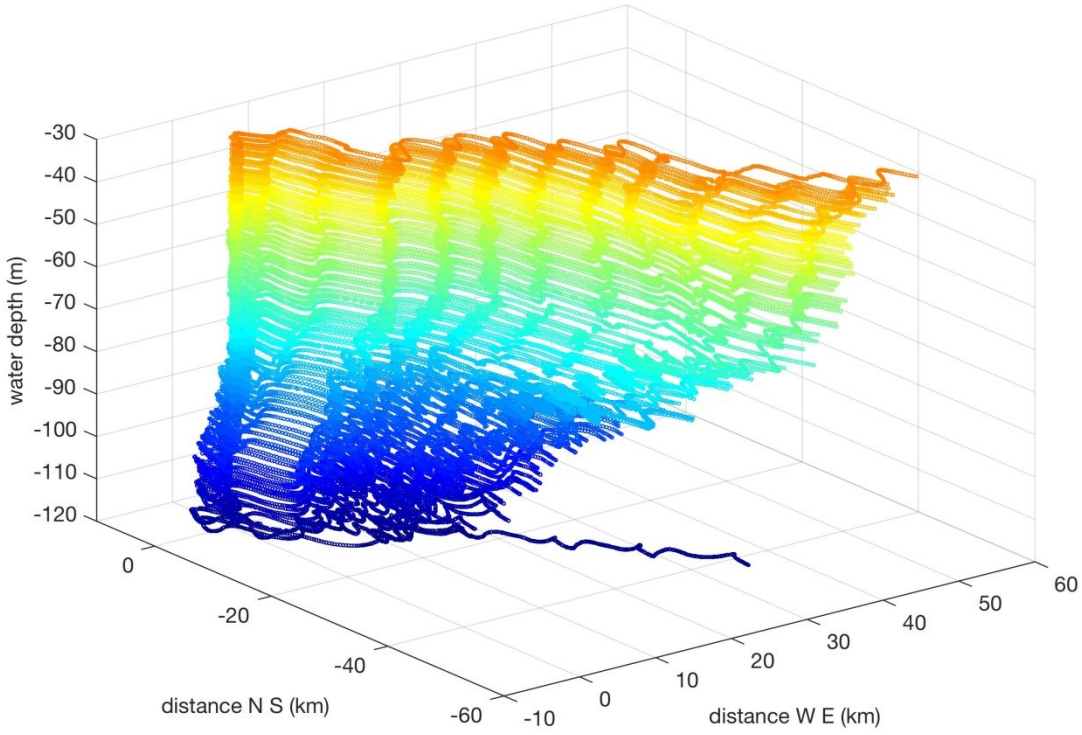

Fig. 40: Cummulative current vectors starting at position (0, 0) displayed for a depth range of 30 to 120 m.

6.3.3 In situ Benthic Flux Measurements

Stefan Sommer, Peter Linke, Christine Utecht, Matthias Türk, Asmus Petersen

Despite bad weather conditions we managed to conduct two deployments of the BIGO type lander (Biogeochemical Observatory) close to the Goldeneye platform (for details see station list). The deployments of BIGO-I-1 (16-18 Oct. 17) and BIGO-I-2 (19-20 Oct. 17) lasted for 33.8 and 21.8 hours as indicated by time period between the first and the last syringe. In addition to seabed fluxes, the sediments were sampled for pore water geochemistry, physical properties of the sediment (water content, porosity, element analysis). During the deployment of BIGO-I-1, in the night of Monday to Tuesday (16/17 Oct.), the former hurricane Ophelia, by then being categorized as a very strong gale, passed over the working area.

The BIGO lander deployments were successful nicely recording the change of O_2 over time allowing the determination of the TOU (Fig. 41).

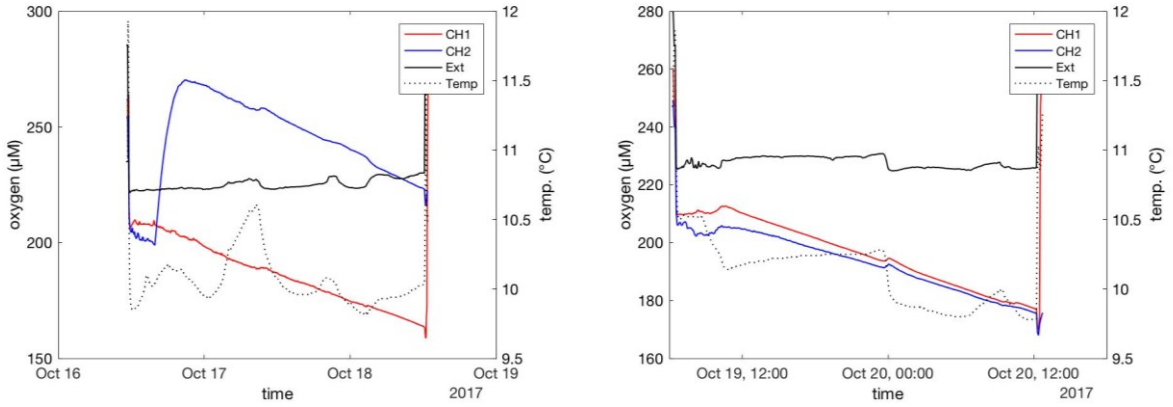

Fig. 41: Concentrations of O_2 over time inside chamber 1 (CH1), chamber 2 (CH2) and the ambient bottom water (Ext) during the deployment of BIGO-I-1 **(left panel)** and BIGO-I-2 **(right panel)**. Temperature (Temp) was recorded in the bottom water.

During the deployment of BIGO-I-1 the O_2 levels strongly increased in chamber 2 due to air bubbles trapped in the pump system of the integrated pH and CO_2 sensors. For the deployment BIGO-I-2 this problem was tackled by flushing the pump system prior to the insertion of the chamber into the sediment. However, still a slight offset of N_2 (~ 40 µM) compared to chamber 1 was measured indicating the dissolution of small air bubbles.

Nevertheless, seabed fluxes of the different geochemical parameters could be determined successfully (Table 5). The strong increase of O_2 of about 75 µM in chamber 2 during deployment BIGO-I-1 did not result in enhanced oxygen uptake indicating that O_2 is not limiting organic carbon degradation. The TOU rates determined during this leg are very similar to the oxygen uptake rates determined using eddy correlation technique of about 5 mmol m^{-2} d^{-1} during leg 1. The average TOU_{opt} to DIC ratio was high (1.9), which deviates from the traditional Redfield–Ketchum–Richards (1963) equation for the production (or respiration) of marine plankton as well as from the recently reported molar respiration ratio (O_2/C) of 1.45 (Hedges et al. 2002).

Dinitrogen fluxes indicate low denitrification and / or anammox taking place in the surface sediments. The dinitrogen flux almost matches the N-release during ammonification when the nitrate release indicative for nitrification is subtracted. Except DIC, the fluxes measured during both lander deployments do not differ distinctively, hence the passage of “Ophelia” had no measurable effect on seabed element turnover.

Table 5: Seabed fluxes of the different parameters determined during the deployments of BIGO-I-1 and BIGO-I-2. TOU was determined via O_2 measurements using the optodes (TOU_{opt}) and the MIMS (TOU_{MIMS}). All fluxes in mmol m^{-2} d^{-1}. Fluxes into the sediment are indicated by negative sign and vice versa. Please note these fluxes are preliminary.

Gear	TOU_{opt}	TOU_{MIMS}	DIC	N_2	Nitrate	Phosphate
BIGO-I-1						
CH1	-5.2	-5.4	2.4	0.2	0.07	0.03
CH2	-6.4	(-8.8)	2.1	n.d.	0.06	0.03
BIGO-I-2						
CH1	-6.7	-6.7	5.5	0.2	0,06	0.03
CH2	-6.4	-6.1	n.d.	n.d.	0,10	0.03

These results contribute to a baseline study, which is carried out within the framework of the project STEMM CCS to resolve natural seabed fluxes of TOU and DIC in the British sector of the North Sea where CO_2 injection into a submarine geological reservoir at Goldeneye has been planned. In concert with an upcoming CO_2 injection experiment these data are needed to develop a monitoring tool for the detection of small scale CO_2 leakages at CCS sites.

6.4 Sediment Geochemistry

Matthias Haeckel, Andrea Bodenbinder, Andy Dale, Anita Flohr

Geochemical analyses of the porewaters and sediments at Goldeneye and the Figge Maar aim at quantifying the biogeochemical fluxes and turnover rates associated with organic carbon remineralization.

Onboard, the collected porewater samples were analysed for their content of dissolved H_2S, NO_3^-, NO_2^-, NH_4^+, PO_4^{3-}, SiO_4^{4-}, and total alkalinity. Sub-samples were taken for further shore-based analyses of porewater DIC and DOC content, $\delta^{13}C$ signature of DIC, dissolved metal cations, SO_4^{2-}, Br^-, Cl^-, and I^- concentrations, isotopic ratios of Sr, Li, H, and O in the porewater as well as porosity, carbonate, POC, PON, and total sulfur content.

See Table 6 for a complete list of sub-samples and variables. A photo documentation of the sampled GCs and MUCs can be found in Appendix 8.3. **6.4.1 Sediment and Porewater Sampling**

Surface sediment samples were retrieved using push cores operated by the ROV (see Chapter 5.2) and a 3-m gravity corer (see Chapter 5.7). After core retrieval, the cores were processed at ambient temperatures in the core lab (since RV Poseidon does not possess a cold room). From the PCs sediment was extruded out of the plastic liners with a piston and cut into 1-2 cm thick slices, whereas the GC liners were cut into 1-m segments, divided length-wise with a saw into an archive and a working half. 3 to 5 sediment samples were taken from each 1-m working half segment. Subsequently, the

porewater was extracted out of the sediment samples using a low pressure-squeezer (argon at 3-5 bar). While squeezing, the porewater was filtered through 0.2 µm regenerated cellulose Whatman filters and collected in recipient vessels.

About 5 ml of wet sediment of each sediment slice was collected for porosity, carbonate and CNS element analyses at home. 3 ml of sediment were taken with a syringe and transferred into 20-ml headspace vials filled with 6 ml of a saturated NaCl solution for onshore gas chromatographic analysis of dissolved methane and higher hydrocarbons. Aliquots of the extracted porewater were sub-sampled for various onboard and further shore-based analyses. Subsamples for ICP-AES analysis were acidified with 30 µl of concentrated suprapure HNO_3 per 3 ml of porewater sample (i.e. pH<1) and ~1.8-ml subsamples for DIC/DOC were treated with 10 µl of $HgCl_2$ to inhibit further microbial degradation. All porewater samples for home-based analyses were stored refrigerated.

During Leg 2, porewaters were retrieved from 2 MUC liners and 1 GC. The gravity core was sampled as described above. Recovered sediments from the MUCs were immediately processed on board by sectioning with a depth resolution ranging from 1 cm at the surface to 4 cm in the deeper part of the cores. Porewaters were extracted from the sediment slices under gas pressure (4-6 bar) through 0.2 µm cellulose acetate filters and immediately analysed in the onboard laboratory. Subsamples of filtered samples were taken for additional analyses at the home laboratory (Table 6.3.2.). Sediment samples were also taken from each slice for the determination of water content and total C, N and S at home. The remaining sediment and porewater samples were stored refrigerated.

Porewater samples for DIC and $\delta^{13}C\_{DIC}$ analysis were filled into 4.5 mL glass bottles (LABCO). The samples were preserved with mercury (II) chloride (5 µL of saturated HgCl2 solution) directly after collection and stored cool and dark. The analysis of DIC, $\delta^{13}C\_{DIC}$ and $\delta^{13}C\_{DOC}$ will be performed using a TOC/TIC analyser (OI-Analytical, Aurora 1013W) in combination with a cavity ring-down spectrometer (PICARRO G2121-i) and the TA by titration (Metrohm, Titrino) both at the National Oceanography Centre in Southampton.

Samples for $\delta^{18}O\_{DIC}$, were filled into 4.5 mL Exetainer vials (LABCO) with no headspace and treated with 125 µL of a solution of 0.4 M $SrCl_2$ and 23 mM NaOH resulting in the precipitation of DIC as $SrCO_3$. The $\delta^{18}O\_{H2O}$ samples were filled into 2.2 mL borosilicate glass vials with no headspace. The $\delta^{18}O\_{DIC}$ and $\delta^{18}O\_{H2O}$ samples will be analysed at the Department of Earth Sciences in Oxford, England after the cruise.

On Leg 1 a total of 68 samples from 2 PCs and 4 GCs was collected for porewater and sediment analysis, whereas on Leg 2 a total of 131 samples from 2 BIGO, 2 MUC, and 1 GC deployments were processed (Table 7).

Additional GCs were taken during Leg 2 for colleagues on shore, 9-1 GC1 and 14-1 GC2 at Goldeneye (for Anna Lichtschlag, NOCS) as well as 18-1 GC4 at the Scanner Pockmark field (for Christoph Böttner, GEOMAR). These cores were only cut into 1-m segments, but were not opened. See station list 8.1 for coordinates.

6.4.2 Porewater Analyses

Analyses for the porewater solutes H_2S, NH_4^+, PO_4^{3-}, and SiO_4^{4-} were completed onboard using a Hitachi UV/VIS spectrophotometer. The respective chemical analytics

followed standard procedures (Grasshoff et al., 1999), i.e. hydrogen sulphide was measured as methylene blue, ammonium as indophenol blue, phosphate and silicate as molybdenum blue. NO_3^- and NO_2^- were analysed during leg 2 using an Autoanalyzer (subsamples taken on the first leg were kept frozen at -20 °C until processing). Total alkalinity of the porewater was determined by titration with 0.02 N HCl using a mixture of methyl red and methylene blue as indicator. The titration vessel was bubbled with argon to strip any CO_2 produced during the titration. The IAPSO seawater standard was used for calibration. Analytical precision and accuracy of each method are given in Table 6.

Table 6: Analytical methods of onboard geochemical analyses.

Parameter	Method	Detection limit	Analytical precision	Analytical Accuracy
NH_4^+	Photometer	1 µmol/l	5 %	-
PO_4^{3-}	Photometer	1 µmol/l	5 %	-
SiO_4^{4-}	Photometer	5 µmol/l	2 %	-
H_2S	Photometer	3 µmol/l	3 %	-
Alkalinity	Titration	0.05 meq/l	3 %	4 %
NO_3^-	Autoanalyzer	1 µmol/l	1 %	-
NO_2^-	Autoanalyzer	0.1 µmol/l	2 %	-
NH_4^+	Autoanalyzer	0.2 µmol/l	2 %	-
PO_4^{3-}	Autoanalyzer	0.05 µmol/l	2 %	-
SiO_4^{4-}	Autoanalyzer	1.7 µmol/l	2 %	-

6.4.3 Preliminary Results

a) Goldeneye Site

An overview of the distributions of selected geochemical species in sediment pore waters from GCs and MUCs at the Goldeneye site (Fig. 43) is given in Figure 42. Since the data from Goldeneye SE, E, and NW pockmark sites were virtually indistinguishable, all data are plotted together. The data show an increase in TA, NH_4^+, PO_4^{3-} and $Si(OH)_4$ with depth in the sediment due to degradation of organic matter. The concentration gradients of NH_4^+, PO_4^{3-} and $Si(OH)_4$ are steepest at the sediment surface, reflecting the mineralization of fresh organic detritus. For TA and $Si(OH)_4$, the data measured in the GCs (black curves) aligns nicely with the MUC data (red curves). (Note that the GC data have not been adjusted for loss of surface sediment). PO_4^{3-} concentrations at the top of GCs in two cores are lower than the deepest PO_4^{3-} concentrations in the MUCs, and similarly for NH_4^+. This is likely due to spatial heterogeneities in seafloor sedimentation and organic matter deposition. Nitrate is consumed within the top 4-5 cm, indicating an O_2 penetration depth of only 1-2 cm. However, H_2S concentrations were close to or below detection limit (and no smell could be sensed), despite the intense POC degradation as evident by the released high NH_4^+ concentrations.

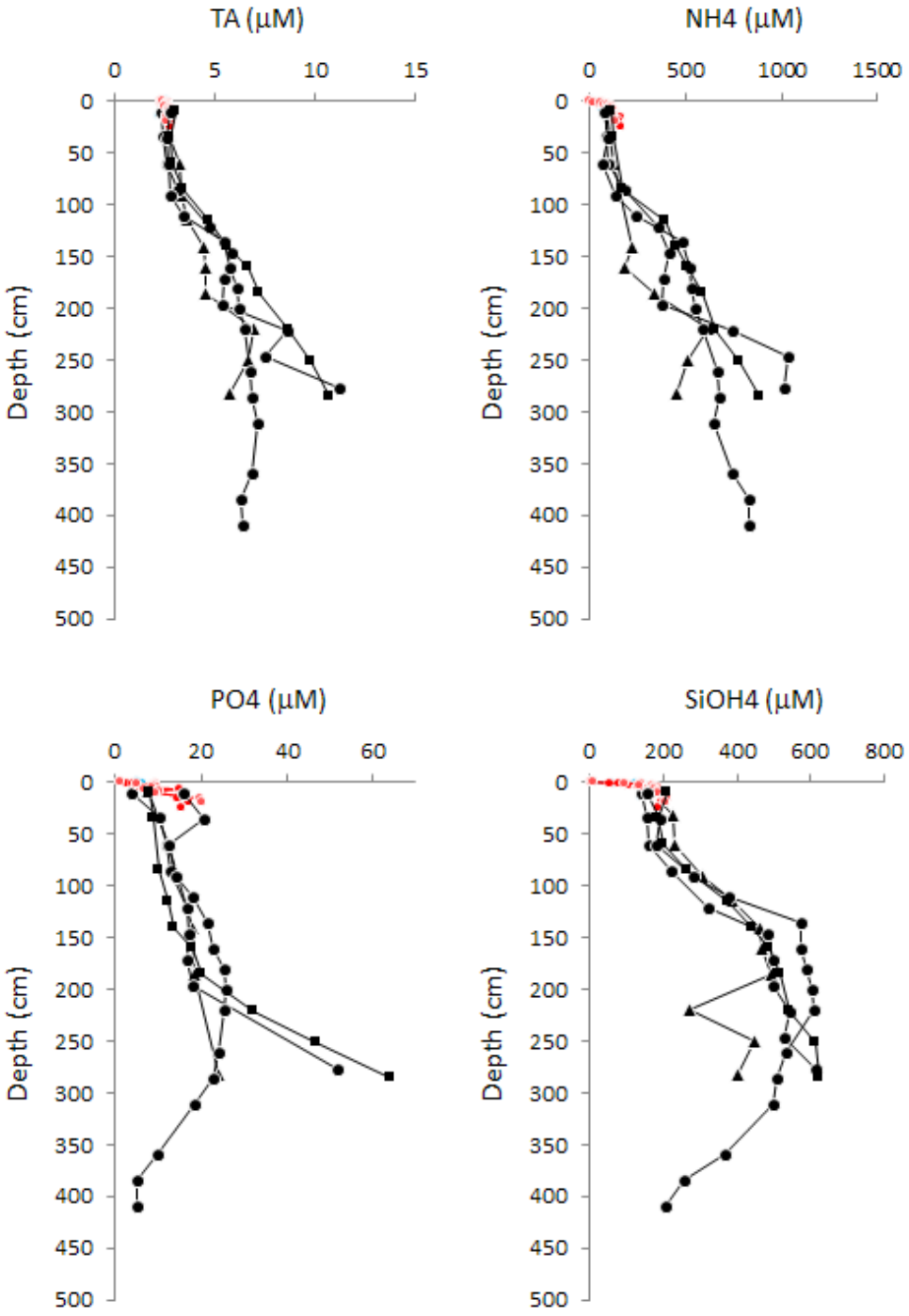

Fig. 42: Concentrations of TA, NH_4^+, PO_4^{3-} and $Si(OH)_4$ measured on board in sediment porewaters at the Goldeneye site (SE: ●; E: ▲; NW pockmark: ■). Data from gravity cores are shown in black, and from the multiple corer in red.

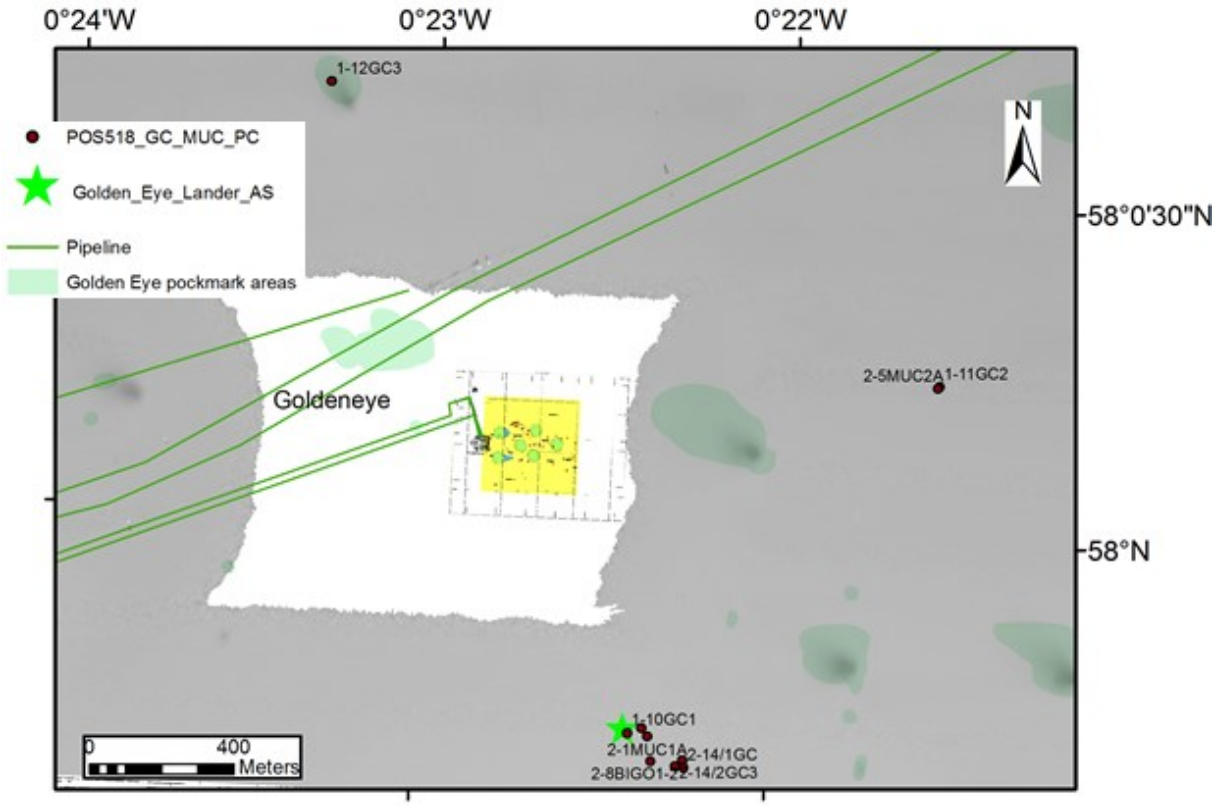

Fig. 43: Map of the Goldeneye area indicating the coring locations.

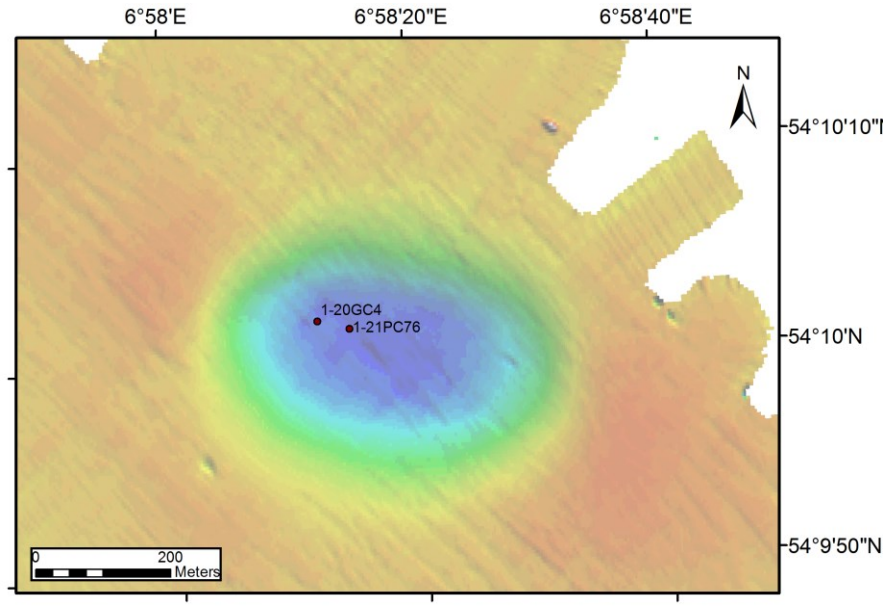

Fig. 44: Coring locations in the Figge Maar. Note: PC location is estimated based on ship's position.

b) Figge Maar

In the Figge Maar, a ROV-operated push core and a gravity core were taken (Fig. 44). Sediments show multiple lamination of silty-sandy and muddy layers, suggesting that the 15-m deep and 500-m wide depression acts as a sediment trap (see Section 8.3). Consequently, organic matter degradation is much stronger than at Goldeneye, reflected by steeply increasing NH_4^+ and TA values in the upper 50-70 cm that reach ~7400 µmol/l and ~85 meq/l, respectively (Fig. 45). In the push core $Si(OH)_4$ increases

to almost 1000 µmol/l at ~15 cm depth. However, in the gravity corer values stay below 500 µmol/l possibly reflecting spatial heterogeneities in the maar. PO_4^{3-} concentrations are quite variable in the upper meter of the sediment. Nitrate is consumed in the top 5-8 cm, indicating an O_2 penetration depth of only 1-2 cm. However, H_2S concentrations could not be detected or be smelled in the core, despite the sediment's intense black colour, particularly in the top meter.

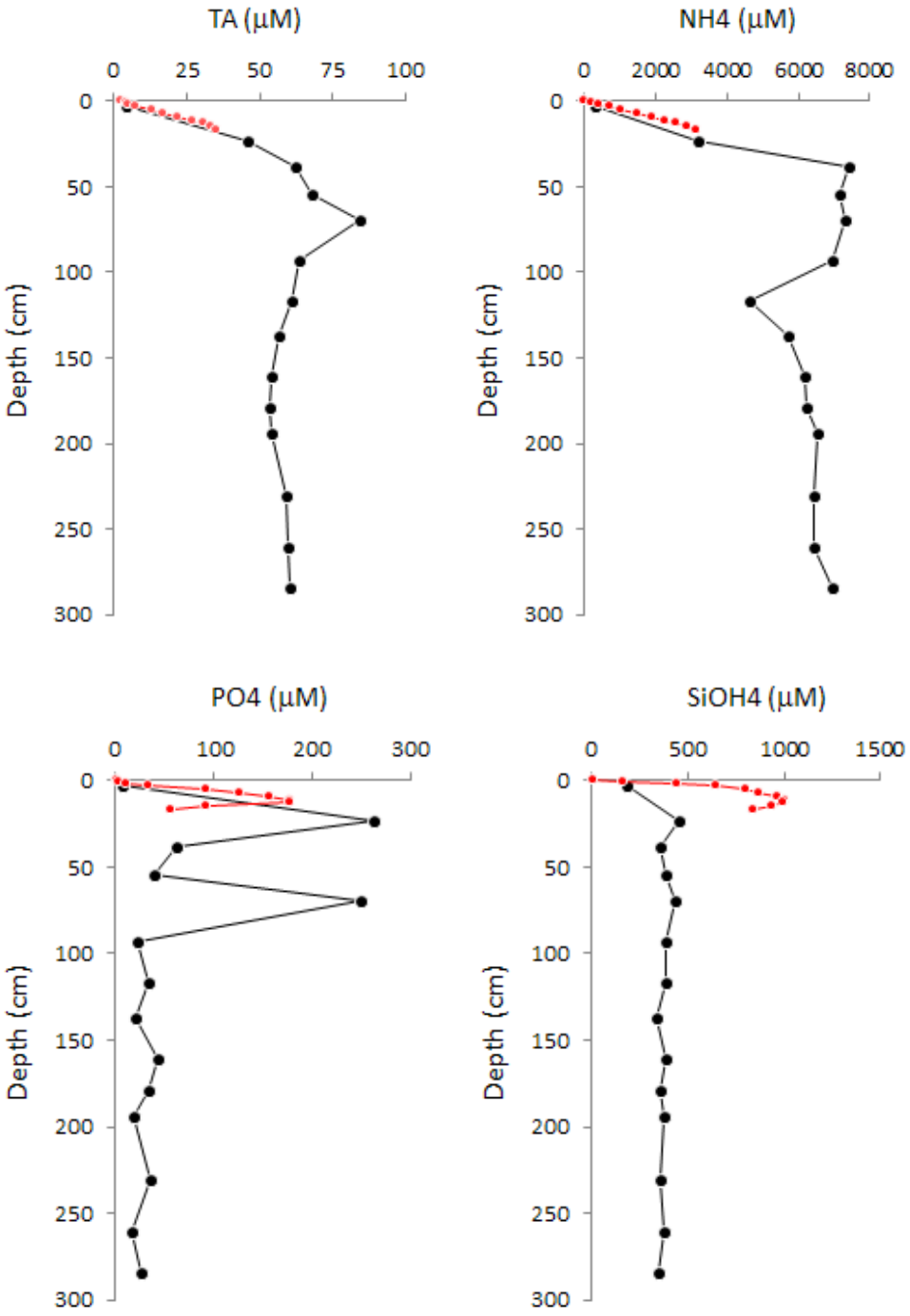

Fig. 45: Concentrations of TA, NH_4^+, PO_4^{3-} and $Si(OH)_4$ measured on board in sediment porewaters at of the Figge Maar. Data from the GC is shown in black, and from the MUC in red.

Table 7: List of sampled cores and collected sub-samples including BIGO syringe samples.

Station Device	Area	Latitude	Longitude	Water depth / m	PW	Poros / CNS	IC	ICP-AES	DIC / DOC	Iso PW	Core length / cm	No. samples
Leg 1												
10 GC1	Goldeneye	57° 59.694' N	000° 22.387' W	115.7	X	X	X	X	X	X	299	11
11 GC2	Goldeneye	58° 00.233' N	000° 21.555' W	117.0	X	X	X	X	X	X	287	11
12 GC3	Goldeneye	58° 00.644' N	000° 23.309' W	119.2	X	X	X	X	X	X	291	11
13 ROV1 PC29	Goldeneye	57° 59.702' N	000° 22.384' W	116.2	X	X	X	X	X	X	16	10
20 GC4	Figge Maar	54° 10.032' N	006° 58.197' E	38.6	X	X	X	X	X	X	289	14
21 ROV3 PC76 *	Figge Maar	54° 10.025' N	006° 58.240' E	44	X	X	X	X	X	X	19	11
Leg 2												
2/1 MUC1 A	Goldeneye	57° 59.691' N	00° 22.327' W	115	X	X	X	X	X	X	30	14
3 BIGO1-1 †	Goldeneye	57° 59.653' N	00° 22.317' W	117	-	-	X	X	X	X	-	26
3 BIGO1-1 (K2)	Goldeneye	57° 59.653' N	00° 22.317' W	117	X	X	X	X	X	X	12	10
5 MUC2A	Goldeneye	58° 00.23' N	00° 21.56' W	120	X	X	X	X	X	X	22	13
8 BIGO1-2 †	Goldeneye	57° 59.657' N	00° 22.228' W	115	-	-	X	X	X	X	-	26
8 BIGO1-2 (K2)	Goldeneye	57° 59.657' N	00° 22.228' W	115	X	X	X	X	X	X	13	26
9 GC1	Goldeneye	58° 00.224' N	00° 21.561' W	116	-	-	-	-	-	-	-	0
14/2 GC2	Goldeneye	57° 59.648' N	00° 22.247' W	117	X	X	X	X	X	X	435	16
18/1 GC3	Scanner Pockmark	58° 16.781’ N	00° 58.277’ E	150	-	-	-	-	-	-		0

PC = ROV-deployed push cores; GC = gravity corer; PW = porewater analyses of TA, H_2S, NO_3^-, NO_2^-, NH_4, PO_4, SiO_4; IC = ion chromatography (SO_4, Br, Cl, I); ICP-AES = inductively-coupled atomic emission spectroscopy (for various dissolved cations); Iso PW = O, H, Sr, Li isotope ratios of porewater; DIC/DOC = dissolved inorganic and organic carbon in porewater. † Syringe samples. * no ROV position available during dive: coordinates of 21 ROV3 PC76 are guessed based on ship position and cable length / direction.

7 References

Artioli Y., Blackford J.C., Nondal G., Bellerby R.G.J., Wakelin S.L., Holt J.T., Butenschön M., Allen J.I. (2014) Heterogeneity of impacts of high CO2 on the North Western European Shelf. Biogeosciences 11:601–612

Babin S.M., Carton J.A., Dickey T.D., Wiggert J.D. (2004) Satellite evidence of hurricane-induced phytoplankton blooms in an oceanic dessert. J. Geophys. Res., 109, C03043, doi:10.1029/2003JC001938, 2004.

Berg P., Røy H., Janssen F., Meyer V., Jørgensen B. B., Huettel M., de Beer D. (2003) Oxygen uptake by aquatic sediments measured with a novel non-invasive eddy-correlation technique. Marine Ecology Progress Series 261, 75-83.

Berg P., Røy H., Wiberg P.L. (2007) Eddy correlation flux measurements: The sediment surface area that contributes to the flux. Limnology and Oceanography 52, 1672-1684.

Blackford, J., Bull, J.M., Cevatoglu, M., Connelly, D., Hauton, C., James, R.H., Lichtschlag, A., Stahl, H., Widdicombe, S., Wright I.C. (2015) Marine baseline and monitoring strategies for carbon dioxide capture and storage (CCS). Int. J. Greenh. Gas Control 38, 221-229. http://dx.doi.org/10.1016/j.ijggc.2014.09.007

Chang, G.C., Dichey T.D., Williams III A.J. (2001) Sediment resuspension on the Middle Atlantic Bight continental shelf during Hurricanes Edouard and Hortense: September 1996. J. Geophys. Res. 106: 9517–9531.

Dickson A.G., Sabine C.L., Christian J.R. (2007) Guide to best practices for ocean CO_2 measurements. PICES Special Publication 3, 191 p.

Fettweis, M., Monbaliu, J., Baeye, M., Nechad, B., Van den Eynde, D. (2012) Weather and climate induced spatial variability of surface suspended particulate matter concentration in the North Sea and the English Channel. Methods in Oceanography (3–4), 25-39.

GEOMAR Helmholtz-Zentrum für Ozeanforschung Kiel (2017). Remotely Operated Vehicle “ROV PHOCA“. Journal of Large-scale Research Facilities 3, A118. http://dx.doi.org/10.17815/jlsrf-3-162.

Glenn S (2008) Glider observations of sediment resuspension in a Middle Atlantic Bight fall transition storm. Limnol Oceanogr., 55, 2180-2196.

Grasshoff K., Ehrhardt M., Kremling K. (1999) Methods of Seawater Analysis. Wiley-VCH, Weinheim.

Greinert J. (2008) Monitoring temporal variability of bubble release at seeps: The hydroacoustic swath system GasQuant. Journal of Geophysical Research Oceans 113(C7), 7048.

Hedges J.I., Baldock J.A., Gélinas Y., Lee C., Peterson M.L., Wakeham S.G. (2002) The biochemical and elemental compositions of marine plankton: A NMR perspective. Marine Chemistry, 78, 47-63.

Jordt A., Zelenka C., Schneider von Deimling J., Koch R., Köser K. (2015) The Bubble Box: Towards an Automated Visual Sensor for 3D Analysis and Characterization of Marine Gas Release Sites. Sensors 15, 30716-30735.

Lewis E., Wallace D.W.R. (1998) Program Developed for CO_2 System Calculations. ORNL/CDIAC-105. Carbon Dioxide Information Analysis Center, Oak Ridge National Laboratory, U.S. Department of Energy, Oak Ridge, Tennessee.

Linke P., Schmidt M., Rohleder M., Al-Barakati A., Al-Farawati R. (2015) Novel online digital video and high-speed data broadcasting via standard coaxial cable onboard marine operating vessels. Marine Technology Society Journal 49(1), 7-18.

Long M.H., Charette M.A., Martin W.R., McCorkle D.C. (2015) Oxygen metabolism and pH in coastal ecosystems: Eddy Covariance Hydrogen ion and Oxygen Exchange System (ECHOES). Limnology and Oceanography: Methods 13, 438-450.

Luff, R., Moll, A. (2004) Seasonal dynamics of the North Sea sediments using a three-dimensional coupled water-sediment model system. Cont. Shelf Res. 24, 1099–1127.

Nauw J., de Haas H., Rehder G. (2015) A review of oceanographic and meteorological controls on the North Sea circulation and hydrodynamics with a view to the fate of North Sea methane from well site 22/4b and other seabed sources. Mar Petr Geol., 68, 861-882.

Queste B.Y., Fernand L., Jickells T.D., Heywood K. J. (2013) Spatial extent and historical context of North Sea oxygen depletion in August 2010. Biogeochemistry, 113, 53–68, doi:10.1007/s10533-012-9729-9, 2013.

Redfield A.C., Ketchum B.H., Richards F.A. (1963) The influence of organisms on the composition of seawater. In: Hill M.N. (Ed) The Sea, Vol 2, Interscience, New York, 26-77.

Richier, S., Achterberg, E. P., Dumousseaud, C., Poulton, A. J., Suggett, D. J., Tyrrell, T., Zubkov, M. V., and Moore, C. M. (2014) Phytoplankton responses and associated carbon cycling during shipboard carbonate chemistry manipulation experiments conducted around Northwest European shelf seas, Biogeosciences, 11, 4733-4752. doi:10.5194/bg-11-4733-2014.

Rovelli L., Dengler M., Schmidt M., Sommer S., Linke P., McGinnis D.F. (2016) Thermocline mixing and vertical oxygen fluxes in the stratified central North Sea. Biogeosciences, 13, 1609-1620. doi:10.5194/bg-13-1609-2016.

Schmidt M., Linke P., Esser D. (2013) Recent development in IR-sensor technology for monitoring subsea methane discharge. Marine Technology Society Journal 47(3), 27-35.

Schmidt M., Linke P., Sommer S., Esser D., Cherednichenko S. (2015) Natural CO_2 seeps offshore Panarea – A test site for subsea CO_2 leak detection technology. Marine Technology Society Journal 49(1), 19-30.

Schneider von Deimling J., Greinert J., Chapman N.R., Rabbel W., Linke P. (2010) Acoustic imaging of natural gas seepage in the North Sea: Sensing bubbles controlled by variable currents. Limnology and Oceanography: Methods 8, 155.

Shropshire T., Li Y., He R. (2016) Storm impact on sea surface temperature and chlorophyll a in the Gulf of Mexico and Sargasso Sea based on daily cloud-free satellite data reconstructions. Geophys. Res. Lett., 43, doi:10.1002/ 2016GL071178.

Sommer S., Clemens D., Yücel M., Pfannkuche O., Hall P.O.J., Almroth-Rosell E., Schulz-Vogt H.N., Dale A.W. (2017) Major bottom water ventilation events do not significanty reduce basin-wide benthic N and P release in the eastern Gotland Basin (Baltic Sea). Marine Science 4, 18.

Sommer S., Gier J., Treude T., Lomnitz U., Dengler M., Cardich J., Dale A.W. (2016) Depletion of oxygen, nitrate and nitrite in the Peruvian oxygen minimum zone cause an imbalance of benthic fluxes. Deep-Sea Research I 112, 113-122.

Thatje S., Gerdes D., Rachor E. (19999 A seafloor crater in the German Bight and ist effect on the benthos. Helgol. Mar. Res. 53: 36-44.

Thomas, H., Schiettecatte, L.-S., Suykens, K., Koné, Y. J. M., Shadwick, E. H., Prowe, A. E. F., Bozec, Y., de Baar, H. J. W., and Borges, A. V. (2009) Enhanced ocean carbon storage from anaerobic alkalinity generation in coastal sediments, Biogeosciences 6, 267-274. doi:10.5194/bg-6-267-2009.

Turrell W.R., Henderson E.W., Slesser G., Payne R., Adams R.D. (1992) Seasonal changes in the circulation of the northern North Sea. Continental Shelf Research 12(2), 257-286.

Vielstädte, L., Karstens, J., Haeckel, M., Schmidt, M., Linke, P., Reimann, S., Liebetrau, V., McGinnis, D.F., Wallmann, K., 2015. Quantification of methane emissions at abandoned gas wells in the Central North Sea. Marine and Petroleum Geology 68, 848-860.

Wakelin, S. L., Holt, J., Blackford, J. C., Allen, J. I., Butenschön, M., Artioli, Y. (2012) Modeling the carbon fluxes of the northwest European continental shelf: Validation and budgets, J. Geophys. Res. 117, C05020. doi:10.1029/2011JC007402.

Wallmann, K., Haeckel, M., Linke, P., Haffert, L., Schmidt, M., Buenz, S., James, R., Hauton, C., Tsimplis, M., Widdicombe, S., Blackford, J., Queiros, A. M., Connelly, D., Lichtschlag, A., Dewar, M., Chen, B., Baumberger, T., Beaubin, S., Vercelli, S., Proelss, A., Wildenborg, T., Mikunda, T., Nepveu, M., Maynard, C., Finnerty, S., Flach, T., Ahmed, N., Ulfsnes, A., Brooks, L., Moskeland, T. and Purcell, M. (2015) Best Practice Guidance for Environmental Risk Assessment for offshore CO2 geological storage. ECO2 Deliverable, D14.1, 53 pp. DOI 10.3289/ECO2_D14.1.

Weisse R., von Storch H., Niemeyer H.D., Knaack H. (2012) Changing North Sea storm surge climate: An increasing hazard? Ocean & Coastal Management, 68, 58 -68.

8 Appendices

8.1 Station Lists of Leg 1 and 2

POS518/1_ Station No.	Date Time UTC	Device	Action	Latitude	Longitude	Water Depth / m
1-1	27.09.2017 12:00	Multibeam echosounder	profile start	54° 00.228' N	007° 53.425' E	30.5
1-1	27.09.2017 12:08	Multibeam echosounder	alter course	54° 00.576' N	007° 53.129' E	30.7
1-1	27.09.2017 12:12	Multibeam echosounder	alter course	54° 00.616' N	007° 53.203' E	30.7
1-1	27.09.2017 12:23	Multibeam echosounder	alter course	54° 00.310' N	007° 53.073' E	30.7
1-1	27.09.2017 12:30	Multibeam echosounder	profile end	54° 00.563' N	007° 53.575' E	30.7
2-1	27.09.2017 18:01	CTD	in the water	54° 10.013' N	006° 58.899' E	31
2-1	27.09.2017 18:08	CTD	max depth / on ground	54° 10.007' N	006° 58.858' E	30.3
2-1	27.09.2017 18:10	CTD	on deck	54° 10.002' N	006° 58.845' E	30.7
3-1	27.09.2017 18:56	Multibeam echosounder	profile start	54° 09.855' N	006° 58.090' E	30.3
3-1	27.09.2017 19:02	Multibeam echosounder	alter course	54° 10.103' N	006° 57.720' E	30.3
3-1	27.09.2017 19:19	Multibeam echosounder	alter course	54° 09.791' N	006° 58.386' E	30.3
3-1	27.09.2017 19:31	Multibeam echosounder	alter course	54° 10.127' N	006° 57.750' E	30.3
3-1	27.09.2017 19:47	Multibeam echosounder	alter course	54° 09.788' N	006° 58.444' E	30.3
3-1	27.09.2017 19:59	Multibeam echosounder	alter course	54° 10.145' N	006° 57.774' E	30.3
3-1	27.09.2017 20:16	Multibeam echosounder	alter course	54° 09.790' N	006° 58.494' E	30.3
3-1	27.09.2017 20:28	Multibeam echosounder	alter course	54° 10.089' N	006° 57.685' E	30.3
3-1	27.09.2017 20:45	Multibeam echosounder	alter course	54° 09.805' N	006° 58.514' E	30.3
3-1	27.09.2017 20:57	Multibeam echosounder	alter course	54° 09.803' N	006° 57.983' E	30.3
3-1	27.09.2017 21:13	Multibeam echosounder	alter course	54° 10.254' N	006° 58.399' E	30.3
3-1	27.09.2017 21:27	Multibeam echosounder	alter course	54° 09.823' N	006° 57.951' E	30.3
3-1	27.09.2017 21:42	Multibeam echosounder	alter course	54° 10.246' N	006° 58.346' E	30.3
3-1	27.09.2017 21:55	Multibeam echosounder	alter course	54° 09.842' N	006° 57.920' E	30.3
3-1	27.09.2017 22:15	Multibeam echosounder	alter course	54° 10.203' N	006° 58.469' E	30.3
3-1	27.09.2017 22:32	Multibeam echosounder	alter course	54° 09.980' N	006° 57.734' E	30.3
3-1	27.09.2017 22:45	Multibeam echosounder	alter course	54° 10.264' N	006° 58.522' E	30.3
3-1	27.09.2017 23:04	Multibeam echosounder	alter course	54° 10.002' N	006° 57.726' E	30.3

POS518/1_ Station No.	Date Time UTC	Device	Action	Latitude	Longitude	Water Depth / m
3-1	27.09.2017 23:18	Multibeam echosounder	alter course	54° 10.259' N	006° 58.465' E	30.3
3-1	27.09.2017 23:37	Multibeam echosounder	alter course	54° 10.040' N	006° 57.726' E	30.3
3-1	28.09.2017 00:29	Multibeam echosounder	alter course	54° 09.966' N	006° 58.371' E	30.3
3-1	28.09.2017 00:39	Multibeam echosounder	alter course	54° 09.747' N	006° 58.178' E	30.3
3-1	28.09.2017 00:52	Multibeam echosounder	alter course	54° 09.959' N	006° 58.411' E	30.3
3-1	28.09.2017 01:00	Multibeam echosounder	alter course	54° 09.684' N	006° 57.998' E	30.3
3-1	28.09.2017 01:15	Multibeam echosounder	alter course	54° 09.974' N	006° 58.511' E	30.3
3-1	28.09.2017 01:27	Multibeam echosounder	alter course	54° 09.670' N	006° 58.135' E	30.3
3-1	28.09.2017 01:42	Multibeam echosounder	alter course	54° 09.891' N	006° 58.640' E	30.3
3-1	28.09.2017 01:57	Multibeam echosounder	alter course	54° 09.713' N	006° 58.355' E	30.3
3-1	28.09.2017 02:01	Multibeam echosounder	alter course	54° 09.798' N	006° 58.594' E	30.3
3-1	28.09.2017 02:15	Multibeam echosounder	alter course	54° 10.162' N	006° 58.104' E	30.3
3-1	28.09.2017 02:30	Multibeam echosounder	alter course	54° 09.848' N	006° 58.624' E	30.3
3-1	28.09.2017 02:46	Multibeam echosounder	alter course	54° 10.209' N	006° 58.159' E	30.3
3-1	28.09.2017 03:01	Multibeam echosounder	alter course	54° 09.880' N	006° 58.685' E	30.3
3-1	28.09.2017 03:17	Multibeam echosounder	alter course	54° 10.241' N	006° 58.236' E	30.3
3-1	28.09.2017 03:32	Multibeam echosounder	profile end	54° 09.916' N	006° 58.754' E	30.3
4-1	28.09.2017 18:10	Multibeam echosounder	profile start	55° 28.783' N	004° 30.948' E	27
4-1	28.09.2017 18:42	Multibeam echosounder	alter course	55° 28.266' N	004° 28.093' E	27
4-1	28.09.2017 19:45	Multibeam echosounder	profile end	55° 28.220' N	004° 30.676' E	27
5-1	29.09.2017 09:02	CTD	in the water	56° 57.129' N	002° 02.442' E	87.2
5-1	29.09.2017 09:14	CTD	max depth / on ground	56° 57.080' N	002° 02.354' E	87
5-1	29.09.2017 09:21	CTD	on deck	56° 57.078' N	002° 02.317' E	87.2
6-1	29.09.2017 10:00	Multibeam echosounder	profile start	56° 57.295' N	002° 02.987' E	87.2
6-1	29.09.2017 11:35	Multibeam echosounder	alter course	57° 00.108' N	002° 10.352' E	87.2
6-1	29.09.2017 11:49	Multibeam echosounder	alter course	57° 00.533' N	002° 09.453' E	87.2
6-1	29.09.2017 12:02	Multibeam echosounder	alter course	57° 00.541' N	002° 10.262' E	87.2

POS518/1_ Station No.	Date Time UTC	Device	Action	Latitude	Longitude	Water Depth / m
6-1	29.09.2017 12:17	Multibeam echosounder	alter course	57° 00.067' N	002° 09.476' E	87.2
6-1	29.09.2017 12:33	Multibeam echosounder	alter course	56° 59.849' N	002° 09.955' E	87.2
6-1	29.09.2017 14:05	Multibeam echosounder	alter course	56° 57.258' N	002° 03.125' E	87.2
6-1	29.09.2017 14:13	Multibeam echosounder	profile end	56° 57.536' N	002° 02.584' E	87.2
7-1	29.09.2017 18:33	Multibeam echosounder	profile start	56° 59.091' N	001° 08.576' E	81.2
7-1	29.09.2017 19:13	Multibeam echosounder	alter course	56° 59.614' N	001° 04.805' E	81.2
7-1	29.09.2017 19:27	Multibeam echosounder	alter course	57° 00.071' N	001° 05.812' E	81.2
7-1	29.09.2017 19:55	Multibeam echosounder	alter course	56° 58.719' N	001° 05.370' E	81.2
7-1	29.09.2017 20:17	Multibeam echosounder	alter course	56° 58.401' N	001° 07.271' E	81.2
7-1	29.09.2017 20:47	Multibeam echosounder	profile end	56° 59.887' N	001° 08.039' E	81.2
8-1	30.09.2017 07:10	CTD	in the water	58° 00.629' N	000° 23.286' W	120.2
8-1	30.09.2017 07:21	CTD	max depth / on ground	58° 00.632' N	000° 23.274' W	121.7
8-1	30.09.2017 07:22	CTD	max depth / on ground	58° 00.626' N	000° 23.278' W	121
8-1	30.09.2017 08:02	CTD	on deck	58° 00.671' N	000° 23.329' W	118
9-1	30.09.2017 10:03	CTD	in the water	57° 59.683' N	000° 22.419' W	117.5
9-1	30.09.2017 10:20	CTD	max depth / on ground	57° 59.692' N	000° 22.410' W	116.7
9-1	30.09.2017 10:41	CTD	on deck	57° 59.681' N	000° 22.247' W	116
10-1	30.09.2017 10:59	Gravity corer	in the water	57° 59.704' N	000° 22.386' W	116.2
10-1	30.09.2017 11:03	Gravity corer	information	57° 59.694' N	000° 22.387' W	115.7
10-1	30.09.2017 11:08	Gravity corer	on deck	57° 59.689' N	000° 22.404' W	115.7
11-1	30.09.2017 11:49	Gravity corer	in the water	58° 00.243' N	000° 21.500' W	118.2
11-1	30.09.2017 11:52	Gravity corer	max depth / on ground	58° 00.233' N	000° 21.555' W	117
11-1	30.09.2017 11:55	Gravity corer	on deck	58° 00.227' N	000° 21.548' W	117
12-1	30.09.2017 12:30	Gravity corer	in the water	58° 00.655' N	000° 23.295' W	119.5
12-1	30.09.2017 12:36	Gravity corer	max depth / on ground	58° 00.644' N	000° 23.309' W	119.2
12-1	30.09.2017 12:42	Gravity corer	on deck	58° 00.637' N	000° 23.293' W	121.5

POS518/1_ Station No.	Date Time UTC	Device	Action	Latitude	Longitude	Water Depth / m
13-1	30.09.2017 13:27	Remote Operated Vehicle	in the water	57° 59.704' N	000° 22.377' W	116.2
13-1	30.09.2017 13:34	Remote Operated Vehicle	information	57° 59.702' N	000° 22.384' W	116.2
13-1	30.09.2017 13:36	Remote Operated Vehicle	information	57° 59.706' N	000° 22.378' W	116.2
13-1	30.09.2017 15:32	Remote Operated Vehicle	at surface	57° 59.709' N	000° 22.396' W	116.2
13-1	30.09.2017 15:41	Remote Operated Vehicle	on deck	57° 59.671' N	000° 22.348' W	116.2
14-1	30.09.2017 17:00	Multibeam echosounder	profile start	58° 00.923' N	000° 20.029' W	116.2
14-1	30.09.2017 17:49	Multibeam echosounder	alter course	57° 58.860' N	000° 22.686' W	116.2
14-1	30.09.2017 18:12	Multibeam echosounder	alter course	57° 59.932' N	000° 23.756' W	116.2
14-1	30.09.2017 18:25	Multibeam echosounder	alter course	58° 00.554' N	000° 24.011' W	116.2
14-1	30.09.2017 18:41	Multibeam echosounder	alter course	58° 00.685' N	000° 22.545' W	116.2
14-1	30.09.2017 19:04	Multibeam echosounder	alter course	58° 01.831' N	000° 21.870' W	116.2
14-1	30.09.2017 20:11	Multibeam echosounder	alter course	57° 58.919' N	000° 19.647' W	116.2
14-1	30.09.2017 21:01	Multibeam echosounder	alter course	57° 59.568' N	000° 23.744' W	116.2
14-1	30.09.2017 21:14	Multibeam echosounder	alter course	58° 00.214' N	000° 23.702' W	116.2
14-1	30.09.2017 21:40	Multibeam echosounder	alter course	58° 01.476' N	000° 22.839' W	116.2
14-1	30.09.2017 22:22	Multibeam echosounder	alter course	58° 01.310' N	000° 19.998' W	116.2
14-1	30.09.2017 22:52	Multibeam echosounder	profile end	58° 01.524' N	000° 22.869' W	116.2
15-1	01.10.2017 02:35	Multibeam echosounder	profile start	57° 57.526' N	000° 35.482' E	116.2
15-1	01.10.2017 03:19	Multibeam echosounder	alter course	57° 58.953' N	000° 38.288' E	116.2
15-1	01.10.2017 03:53	Multibeam echosounder	alter course	57° 59.425' N	000° 38.598' E	116.2
15-1	01.10.2017 04:43	Multibeam echosounder	alter course	57° 57.864' N	000° 35.891' E	116.2
15-1	01.10.2017 05:00	Multibeam echosounder	profile end	57° 57.510' N	000° 35.920' E	116.2
16-1	07.10.2017 01:06	CTD	in the water	58° 03.437' N	000° 50.182' E	145.5
16-1	07.10.2017 01:14	CTD	information	58° 03.431' N	000° 50.097' E	1518

POS518/1_ Station No.	Date Time UTC	Device	Action	Latitude	Longitude	Water Depth / m
16-1	07.10.2017 01:23	CTD	on deck	58° 03.396' N	000° 50.075' E	146.5
17-1	07.10.2017 01:57	Multibeam echosounder	profile start	58° 03.579' N	000° 50.435' E	145.2
17-1	07.10.2017 03:05	Multibeam echosounder	alter course	58° 06.936' N	000° 50.990' E	147.8
17-1	07.10.2017 03:18	Multibeam echosounder	alter course	58° 06.494' N	000° 51.538' E	150.3
17-1	07.10.2017 03:32	Multibeam echosounder	alter course	58° 05.827' N	000° 51.525' E	147.6
17-1	07.10.2017 03:47	Multibeam echosounder	alter course	58° 05.319' N	000° 50.545' E	146.4
17-1	07.10.2017 04:15	Multibeam echosounder	alter course	58° 03.975' N	000° 50.522' E	144.7
17-1	07.10.2017 04:29	Multibeam echosounder	alter course	58° 04.120' N	000° 50.247' E	144.7
17-1	07.10.2017 05:23	Multibeam echosounder	alter course	58° 05.892' N	000° 52.026' E	145.7
17-1	07.10.2017 05:47	Multibeam echosounder	alter course	58° 06.187' N	000° 50.081' E	146.2
17-1	07.10.2017 05:57	Multibeam echosounder	alter course	58° 06.640' N	000° 50.245' E	147.6
17-1	07.10.2017 06:11	Multibeam echosounder	profile end	58° 06.567' N	000° 51.362' E	146.4
18-1	07.10.2017 07:34	Multibeam echosounder	profile start	58° 03.871' N	001° 08.897' E	133.8
18-1	07.10.2017 08:29	Multibeam echosounder	alter course	58° 03.089' N	001° 14.297' E	127.6
18-1	07.10.2017 09:13	Multibeam echosounder	alter course	58° 02.402' N	001° 10.616' E	129.5
18-1	07.10.2017 09:16	Multibeam echosounder	alter course	58° 02.333' N	001° 10.847' E	131.4
18-1	07.10.2017 09:31	Multibeam echosounder	alter course	58° 03.067' N	001° 10.416' E	131.2
18-1	07.10.2017 09:40	Multibeam echosounder	alter course	58° 03.460' N	001° 09.960' E	132
18-1	07.10.2017 09:49	Multibeam echosounder	alter course	58° 03.943' N	001° 10.101' E	133.4
18-1	07.10.2017 10:36	Multibeam echosounder	alter course	58° 03.357' N	001° 13.731' E	127.5
18-1	07.10.2017 10:45	Multibeam echosounder	alter course	58° 03.044' N	001° 13.373' E	127.8
18-1	07.10.2017 11:04	Multibeam echosounder	alter course	58° 02.930' N	001° 12.490' E	129.6
18-1	07.10.2017 11:13	Multibeam echosounder	profile end	58° 02.540' N	001° 12.772' E	128.4
19-1	07.10.2017 12:14	Multibeam echosounder	profile start	57° 56.814' N	001° 26.030' E	98.9
19-1	07.10.2017 12:48	Multibeam echosounder	alter course	57° 55.722' N	001° 25.163' E	96.9
19-1	07.10.2017 13:00	Multibeam echosounder	alter course	57° 55.743' N	001° 25.965' E	96.5
19-1	07.10.2017 13:20	Multibeam echosounder	alter course	57° 56.123' N	001° 25.316' E	98

POS518/1_ Station No.	Date Time UTC	Device	Action	Latitude	Longitude	Water Depth / m
19-1	07.10.2017 13:48	Multibeam echosounder	alter course	57° 56.835' N	001° 26.685' E	97.1
19-1	07.10.2017 14:41	Multibeam echosounder	alter course	57° 57.097' N	001° 21.170' E	101.8
19-1	07.10.2017 14:57	Multibeam echosounder	alter course	57° 57.129' N	001° 21.353' E	102
19-1	07.10.2017 15:21	Multibeam echosounder	alter course	57° 56.782' N	001° 23.270' E	99.3
19-1	07.10.2017 15:28	Multibeam echosounder	alter course	57° 56.454' N	001° 23.325' E	98.6
19-1	07.10.2017 16:46	Multibeam echosounder	alter course	57° 52.787' N	001° 29.277' E	90.9
19-1	07.10.2017 17:07	Multibeam echosounder	alter course	57° 53.109' N	001° 29.384' E	91.1
19-1	07.10.2017 17:25	Multibeam echosounder	profile end	57° 52.473' N	001° 29.027' E	90
20-1	09.10.2017 06:01	Gravity corer	in the water	54° 10.032' N	006° 58.175' E	38.8
20-1	09.10.2017 06:05	Gravity corer	max depth / on ground	54° 10.032' N	006° 58.197' E	38.6
20-1	09.10.2017 06:09	Gravity corer	on deck	54° 10.033' N	006° 58.205' E	39.3
21-1	09.10.2017 07:28	Remote Operated Vehicle	in the water	54° 10.015' N	006° 58.198' E	38.1
21-1	09.10.2017 07:40	Remote Operated Vehicle	max depth / on ground	54° 10.058' N	006° 58.211' E	38.1
21-1	09.10.2017 07:53	Remote Operated Vehicle	on deck	54° 10.111' N	006° 58.205' E	38.1
21-2	09.10.2017 08:56	Remote Operated Vehicle	in the water	54° 09.997' N	006° 58.077' E	38.1
21-2	09.10.2017 09:06	Remote Operated Vehicle	max depth / on ground	54° 09.998' N	006° 58.066' E	38.1
21-2	09.10.2017 16:30	Remote Operated Vehicle	on deck	54° 10.090' N	006° 58.354' E	38.1
22-1	09.10.2017 17:02	Multibeam echosounder	profile start	54° 10.057' N	006° 57.815' E	30.7
22-1	09.10.2017 17:33	Multibeam echosounder	alter course	54° 10.022' N	006° 58.392' E	65
22-1	09.10.2017 18:38	Multibeam echosounder	alter course	54° 10.011' N	006° 58.608' E	29.2
22-1	09.10.2017 18:58	Multibeam echosounder	alter course	54° 09.987' N	006° 58.471' E	60.2
22-1	09.10.2017 19:08	Multibeam echosounder	alter course	54° 10.077' N	006° 58.008' E	49.8
22-1	09.10.2017 19:20	Multibeam echosounder	alter course	54° 09.991' N	006° 58.393' E	64.8
22-1	09.10.2017 19:35	Multibeam echosounder	alter course	54° 10.064' N	006° 57.996' E	29.2

POS518/1_ Station No.	Date Time UTC	Device	Action	Latitude	Longitude	Water Depth / m
22-1	09.10.2017 19:48	Multibeam echosounder	alter course	54° 09.942' N	006° 58.437' E	34.4
22-1	09.10.2017 19:59	Multibeam echosounder	alter course	54° 10.074' N	006° 57.924' E	30
22-1	09.10.2017 20:12	Multibeam echosounder	alter course	54° 09.892' N	006° 58.439' E	30.9
22-1	09.10.2017 20:23	Multibeam echosounder	alter course	54° 09.792' N	006° 58.170' E	30.7
22-1	09.10.2017 20:38	Multibeam echosounder	alter course	54° 10.087' N	006° 58.477' E	52.6
22-1	09.10.2017 20:51	Multibeam echosounder	alter course	54° 09.932' N	006° 57.983' E	30.5
22-1	09.10.2017 21:00	Multibeam echosounder	alter course	54° 10.083' N	006° 58.403' E	33.4
22-1	09.10.2017 21:14	Multibeam echosounder	alter course	54° 09.937' N	006° 57.932' E	30.6
22-1	09.10.2017 21:25	Multibeam echosounder	alter course	54° 10.122' N	006° 58.408' E	56.4
22-1	09.10.2017 21:38	Multibeam echosounder	alter course	54° 09.971' N	006° 57.909' E	31.1
22-1	09.10.2017 21:49	Multibeam echosounder	alter course	54° 10.131' N	006° 58.424' E	52.2
22-1	09.10.2017 22:04	Multibeam echosounder	alter course	54° 10.043' N	006° 58.362' E	42.5
22-1	09.10.2017 22:27	Multibeam echosounder	alter course	54° 10.118' N	006° 58.233' E	37.1
22-1	09.10.2017 23:33	Multibeam echosounder	alter course	54° 10.279' N	006° 57.707' E	31.6
22-1	09.10.2017 23:59	Multibeam echosounder	alter course	54° 10.097' N	006° 58.336' E	33.8
22-1	10.10.2017 00:11	Multibeam echosounder	alter course	54° 09.996' N	006° 58.139' E	38.8
22-1	10.10.2017 00:27	Multibeam echosounder	alter course	54° 10.088' N	006° 58.553' E	32.1
22-1	10.10.2017 00:43	Multibeam echosounder	alter course	54° 09.945' N	006° 58.070' E	37.2
22-1	10.10.2017 00:57	Multibeam echosounder	alter course	54° 10.010' N	006° 58.537' E	33.3
22-1	10.10.2017 01:04	Multibeam echosounder	alter course	54° 09.914' N	006° 57.982' E	31.6
22-1	10.10.2017 01:35	Multibeam echosounder	alter course	54° 10.061' N	006° 58.730' E	32
22-1	10.10.2017 02:39	Multibeam echosounder	profile end	54° 10.004' N	006° 58.064' E	39.4
23-1	10.10.2017 04:00	CTD	in the water	54° 10.071' N	006° 58.132' E	39.4
23-1	10.10.2017 04:39	CTD	max depth / on ground	54° 09.944' N	006° 58.344' E	37.6
23-1	10.10.2017 05:53	CTD	on deck	54° 09.953' N	006° 58.395' E	37.6

POS518/2_ Station No.	Date Time UTC	Device	Action	Latitude	Longitude	Water Depth / m
1-1	16.10.2017 04:22	CTD	in the water	57° 59.765' N	00°22.382' W	114.5
1-1	16.10.2017 04:38	CTD	max depth / on ground	57° 59.713' N	00° 22.383' W	115.2
1-1	16.10.2017 04:49	CTD	on deck	57° 59.708' N	00° 22.395' W	115.0
1-2	16.10.2017 05:01	NOC-Lander	in the water	57° 59.698' N	00° 22.391' W	115.0
1-2	16.10.2017 05:11	NOC-Lander	max depth / on ground	57° 59.699' N	00° 22.419' W	115.2
1-3	16.10.2017 06:48	SLM-Lander	in the water	57° 59.666' N	00° 22.387' W	115.2
1-3	27.09.2017 07:04	SLM-Lander	max depth / on ground	57° 59.660' N	00° 22.400' W	115.2
1-3	16.10.2017 07:16	SLM-Lander	Launcher on deck	57° 59.699' N	00° 22.327' W	116.5
2-1	16.10.2017 07:22	Multi Corer	in the water	57° 59.699' N	00° 22.330' W	116.2
2-1	16.10.2017 07:26	Multi Corer	max depth / on ground	57° 59.691' N	00° 22.327' W	115.7
3-1	16.10.2017 11:24	BIGO-Lander	in the water	57° 59.647' N	00° 22.303' W	116.7
3-1	16.10.2017 11:36	BIGO-Lander	max depth / on ground	57° 59.653' N	00° 22.320' W	116.0
3-1	16.10.2017 11:41	BIGO-Lander	Launcher on deck	57° 59.644' N	00° 22.304	116.0
4-1	18.10.2017 11:22	CTD	in the water	57° 59.639' N	00° 22.277' W	116.0
4-1	18.10.2017 11:30	CTD	max depth / on ground	57° 59.627' N	00° 22.246' W	117.7
4-1	18.10.2017 11:40	CTD	on deck	57° 59.651' N	00° 22.192' W	118.0
5-1	18.10.2017 11:57	Multi Corer	in the water	58° 00.219' N	00° 21.553' W	118.2
5-1	18.10.2017 12:01	Multi Corer	max depth / on ground	58° 00.228' N	00° 21.555' W	119.0
5-1	18.10.2017 12:06	Multi Corer	on deck	58° 00.237' N	00° 21.568' W	118.5
6-1	18.10.2017 12:23	BIGO-Lander	released	57° 59.529' N	00° 22.253' W	116.2
6-1	18.10.2017 12:35	BIGO-Lander	on deck	57° 59.505' N	00° 22.347' W	117.2

POS518/2_ Station No.	Date Time UTC	Device	Action	Latitude	Longitude	Water Depth / m
7-1	18.10.2017 13:02	CTD	in the water	58° 00.226' N	00° 21.542' W	117.7
7-1	18.10.2017 13:09	CTD	max depth / on ground	58° 00.232' N	00° 21.596' W	117.2
7-1	18.10.2017 13:14	CTD	on deck	58° 00.264' N	00° 21.556' W	119.0
8-1	19.10.2017 06:21	BIGO-Lander	in the water	57° 59.665' N	00° 22.216' W	115.7
8-1	19.10.2017 06:34	BIGO-Lander	max depth / on ground	57° 59.657' N	00° 22.230' W	115.2
8-1	19.10.2017 06:41	BIGO-Lander	Launcher on deck	57° 59.652' N	00° 22.238' W	114.0
9-1	19.10.2017 07:13	Gravity corer	in the water	58° 00.231' N	00° 21.583' W	115.5
9-1	19.10.2017 07:20	Gravity corer	max depth / on ground	58° 00.224' N	00° 21.561' W	116.7
9-1	19.10.2017 07:25	Gravity corer	on deck	58° 00.233' N	00° 21.574' W	117.7
10-1	20.10.2017 08:01	CTD	in the water	57° 59.660’ N	00° 22.609’ W	117.9
10-1	20.10.2017 08:07	CTD	max depth / on ground	57° 59.644’ N	00° 22.581’ W	116.0
10-1	20.10.2017 08:16	CTD	on deck	57° 59.632’ N	00° 22.563’ W	115.5
11-1	20.10.2017 08:56	CTD	in the water	57° 59.761’ N	00° 22.493’ W	115.6
11-1	20.10.2017 09:02	CTD	max depth / on ground	57° 59.738’ N	00° 22.506’ W	115.7
11-1	20.10.2017 09:08	CTD	on deck	57° 59.736’ N	00° 22.508’ W	116.1
11-2	20.10.2017 10:01	CTD	in the water	57° 59.720’ N	00°22.513’ W	116.0
11-2	20.10.2017 10:08	CTD	max depth / on ground	57° 59.668’ N	00° 22.454’ w	116.0
11-2	20.10.2017 10:15	CTD	on deck	57° 59.669‘ N	00° 22.518’ W	116.0
12-2	20.10.2017 11:05	NOC-Lander	Hydrophone in the water	57° 59.693’ N	00° 22.454’ W	116.8
12-2	20.10.2017 11:56	NOC Lander	Hydrophone on deck	57° 59.691’ N	00° 22.422’ W	118.0
13-1	20.10.2017 12:15	BIGO Lander	Hydrophone in the water	57° 59.563’ N	00° 22.478’ W	118.0
13-1	20.10.2017 12:20	BIGO Lander	released	57° 59.533’ N	00° 22.436’ W	118.0
13-1	20.10.2017 12:29	BIGO-Lander	on deck	57° 59.523’ N	00° 22.203’ W	118.0
14-1	20.10.2017 13:02	Gravity corer	in the water	57° 57.645’ N	00° 22.238’ W	116.9

POS518/2_ Station No.	Date Time UTC	Device	Action	Latitude	Longitude	Water Depth / m
14-1	20.10.2017 13:05	Gravity corer	max depth / on ground	57° 59.646' N	00° 22.223' W	117.5
14-1	20.10.2017 13:10	Gravity corer	on deck	57° 59.635' N	00° 22.174' W	117.8
14-2	20.10.2017 13:21	Gravity corer	in the water	57° 59.649' N	00° 22.252' W	117.9
14-2	20.10.2017 13:23	Gravity corer	max depth / on ground	57° 59.647' N	00° 22.246' W	117.9
14-2	20.10.2017 13:30	Gravity corer	on deck	57° 59.658' N	00° 22.241' W	118.6
15-1	22.10.2017 14:13	SLM-Lander	Hydrophone in the water	57° 59.541' N	00° 22.741' W	
15-1	22.10.2017 14:14	SLM-Lander	released	57° 59.523' N	00° 22.743' W	
15-1	22.10.2017 14:26	SLM-Lander	on deck	57° 59.522' N	00° 22,332' W	
16-1	20.10.2017 14:40	CTD	in the water	57° 59.305' N	00° 22.073' W	116.5
16-1	22.10.2017 14:49	CTD	max depth / on ground	57° 59.172' N	00° 21.875' W	115.9
16-1	22.10.2017 14:59	CTD	on deck	57° 59.051' N	00° 21.683' W	
17-1	23.10.2017 06:30	CTD	in the water	58° 16.794' N	00° 58.303' E	
17-1	23.10.2017 06:37	CTD	max depth / on ground	58° 16.796' N	00° 58.276' E	152.2
17-1	23.10.2017 06:45	CTD	on deck	58° 16.794' N	00° 58.273' E	
18-1	23.10.2017 06:51	Gravity corer	in the water	58° 16.783' N	00° 58.285' E	152.5
18-1	23.10.2017 06:54	Gravity corer	max depth / on ground	58° 16.781' N	00° 58.277' E	150.7
18-1	23.10.2017 07:02	Gravity corer	on deck	58° 16.788' N	00° 58.253' E	151.7

8.2 ROV PHOCA Dive Protocols

8.2.1 13 ROV-Dive1 (Goldeneye) Date: 30.09.2017

Tools: 4 pushcores, MPI Eddy Correlation Device

Responsible Scientist: Dirk Koopmans

Protocol Scientists: Mark Schmidt + Tim Weiß

ROV in the water: 13:33:59 UTC

Descent

ROV at the bottom

UTC time	ship lat	ship lon	sub lat	sub lon	water depth
13:37:28	57 59.7018	-0 22.3737	58.0026696	-0.3588111	116.2 m

Martin reported difficulty with precise GPS location of ROV, ship coordinates are more accurate.

Orientation at the seafloor for 10.5 minutes.

Manuever to location for placing eddy correlation instruments, 13 minutes.

Action 1: Deployment of Eddy Correlation Device

UTC time	ship lat	ship lon	sub lat	sub lon	water depth
14:01:06			57.9950074	-0.3730713	116.2 m

14:02 – 14:03 three photos taken of eddy correlation frame

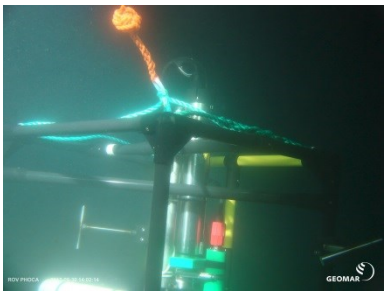
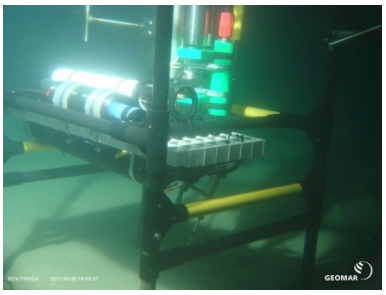


Action 2: Sampling of 2 pushcores about 50 m downstream away from the Eddy; PCs separated by 5-10 m from each other

UTC time	ship lat	ship lon	sub lat	sub lon	water depth
14:17:28			57.995484	-0.3730352	116.2 m

PC 25 recovery at 14:17:28 UTC

PC 2 recovery at 14:40:31 UTC

only time for one PC to attempt an additional core recovery. Heavy sediment resuspension at the seafloor restricted the time available for manuevering to a second site. Instead we stayed at the site of initial core recovery.

14:38 – 14:39: four photos taken of core retrieval, core did not make it back to holder. Attempted again.




14:46 additional photo taken of core retrieval

Action 3: Video Survey of seafloor around "seafloor start point" (incl. time for training PCs)

This time was cut short due to the weather delay of the start of the dive. Instead of conducting a video survey, training of the PCs focused on the more challenging core recovery, which was successful.

Action 4: Pick-up of Eddy Correlation Device

Eddy correlation frame retrieval at 15:08:38

ROV off of the bottom 15:22:29

Ascent (accomplished in 00:18:25)

ROV on deck: 15:40:57 UTC

Time On Deck: 15:41 UTC ROV secured / ready for next station

8.2.2 21 ROV-Dive2&3 (Figge Maar) Date: 09.10.2017

Tools: 2 push cores, Gas sampler, GasQuant (Dive-2), Bubble Box (Dive-3)

Responsible Scientists: Tim Weiss (7-12 UTC), Mark Schmidt (12-16 UTC)

Protocol Scientists: Dirk Koopmans (7-12 UTC), Christoph Böttner (12-16 UTC)

ROV in the water: 07:29 UTC

Descent.

ROV at the bottom: 07:40

Sub-position of ROV does not work.

Action 1: Deployment of GasQuant next to bubble streams

UTC time	ship lat	ship lon	sub lat	sub lon	water depth
07:40	54.167608	6.970187			41.0 m

Red LED light on Battery of GasQuant indicates error 07:41

ROV off the Bottom: 07:44:26

Ascent

ROV on deck

UTC time	ship lat	ship lon	sub lat	sub lon	water depth
07:53	54.161718	6.960353			41.0 m

End of 21 ROV Dive-2

exchanged GasQuant lander with BubbleBox

ROV in the water: 08:56

Descent

ROV at the bottom

UTC time	ship lat	ship lon	sub lat	sub lon	water depth
09:06	54.167608	6.970187			41.7 m

Action 2: start of bubble survey

UTC time	ship lat	ship lon	sub lat	sub lon	water depth
09:19	54.1670036	6.9677119			38.9 m

Due to bad visual conditions only single bubbles were found. Strong currents and no navigation were additional factors which had a strong influence on the survey strategy.

Turn on HD camera: 10:28:54

Small flare detected

UTC time	ship lat	ship lon	sub lat	sub lon	water depth
14:29	54.167342	6.969813			44 m

Action 4: Take reference push core (PC 79)

UTC time	ship lat	ship lon	sub lat	sub lon	water depth
13:25:36	54.1671753	6.9698601			38.1 m

Photos of PC79 (13:26:01):

Action 5: Take gas sample at a bubble stream

UTC time	ship lat	ship lon	sub lat	sub lon	water depth
14:50	54.167475	6.969908			43.8 m

Place bubble box next to ROV, so the robotic arm can be used for the gas sampling.

Push funnel into sediment and move around with ROV arm to initiate release of gas to be collected. This took several minutes, but was successful for retrieving sufficient amounts of gas.

During the recovery of the gas sampler, the ROV was pulled away from the sampling site due to changing current direction while tide changed and ship could not hold position. The bubble box got out of sight of the ROV.

Due to the changing tide, the ship and the ROV were maneuvered to new positions.

Action 6: Search for Bubble box with acoustic beacon using ROV sonar 15:19

Bubble box found and picked up

UTC time	ship lat	ship lon	sub lat	sub lon	water depth
16:10	54.1674652	6.9711022			43.3 m

ROV off the Bottom: 16:18

Ascent

ROV on deck

UTC time	ship lat	ship lon	sub lat	sub lon	water depth
16:30	54.1681595	6.972558			38.1 m

End of ROV Dive-3

8.3 Core Photos

Leg1: 10 GC1SE Goldeneye (NOCS lander position) 0 – 299 cm

0-99

99-199

199-299

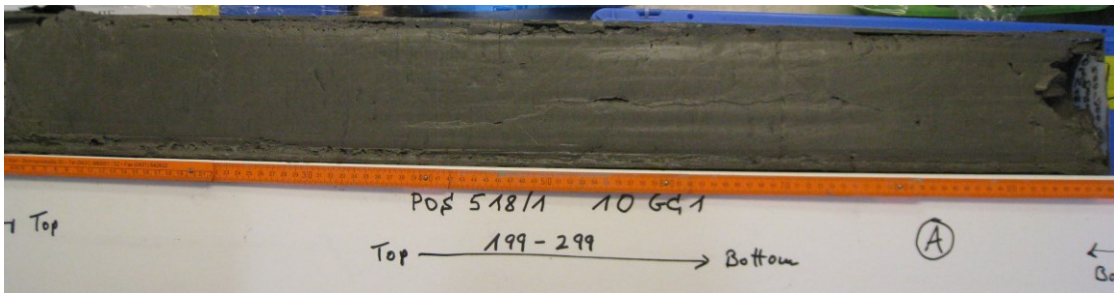

Leg 1: 11 GC2 **E Goldeneye** 0 – 287 cm

0-100

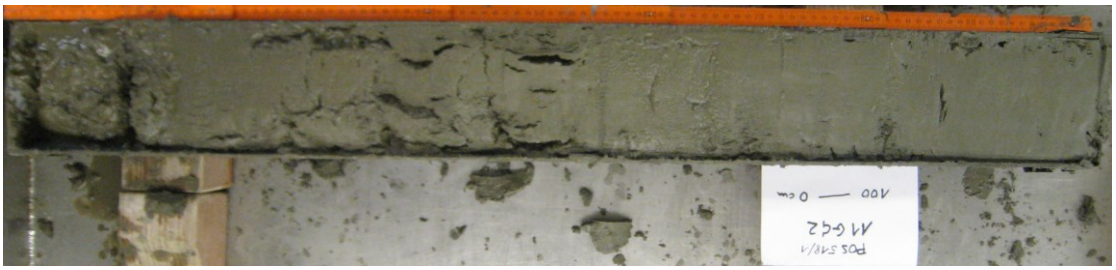

100-200

200-287

Leg 1: 12 GC3 **NW Goldeneye Pockmark** 0 – 291 cm

0-100

100-200

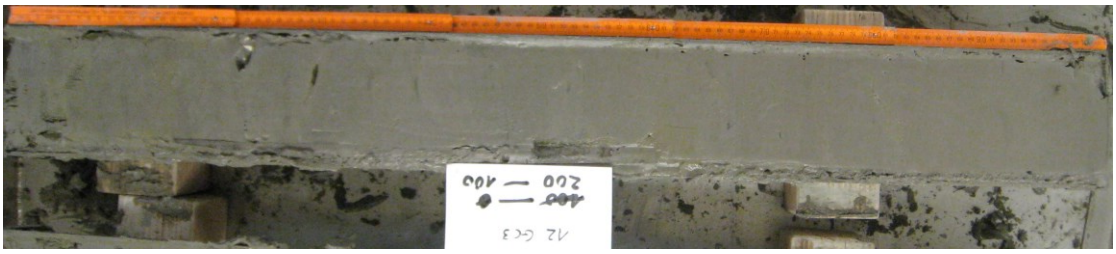

200-291

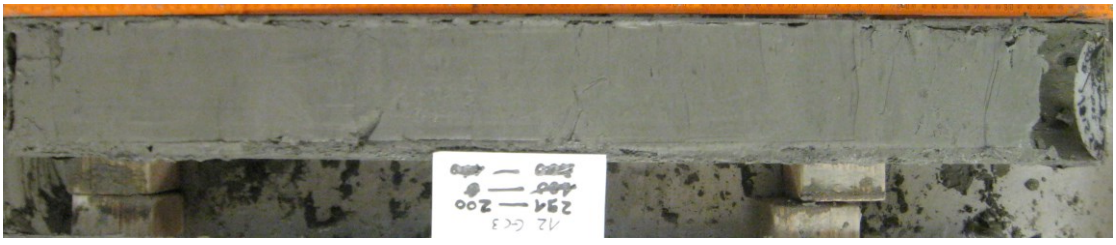

Leg 1: 20 GC4 Figge Maar 0 – 289 cm

0-100

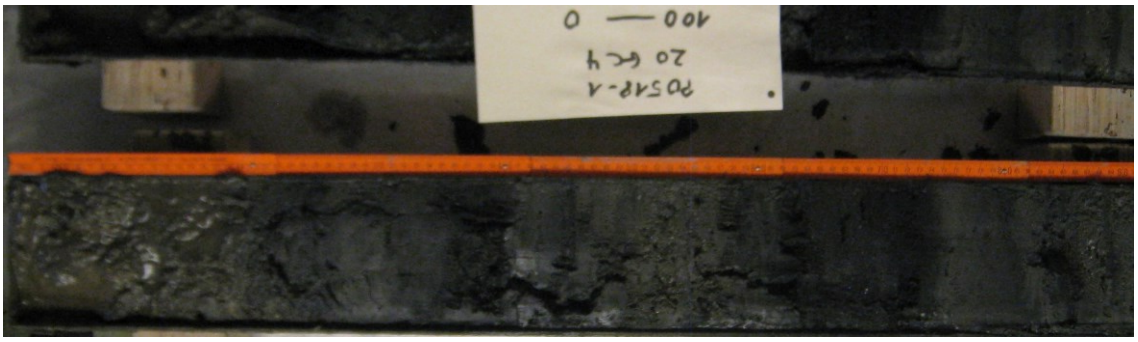

100-200

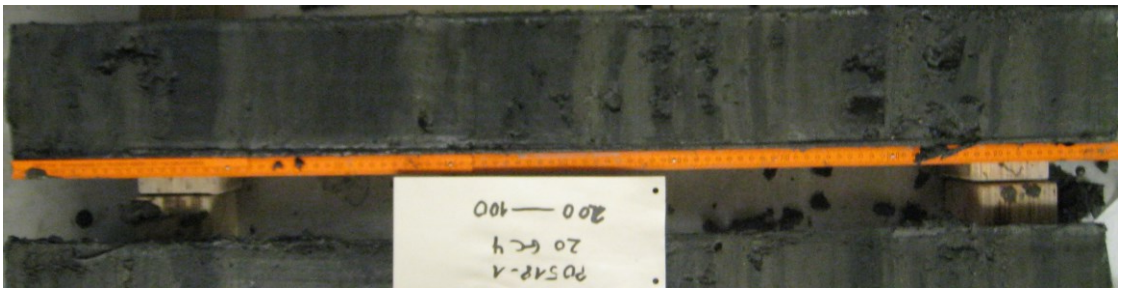

200-289

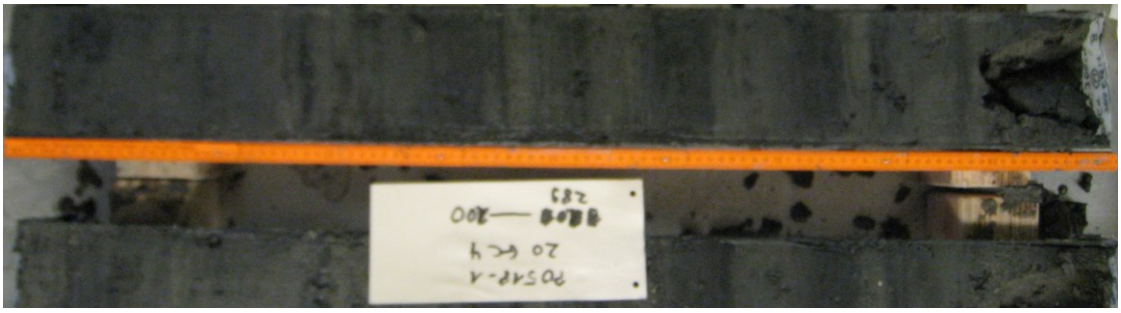

Leg 2: 14/2 GC 3 SE Goldeneye (NOCS lander position) 0 – 435 cm

0-50

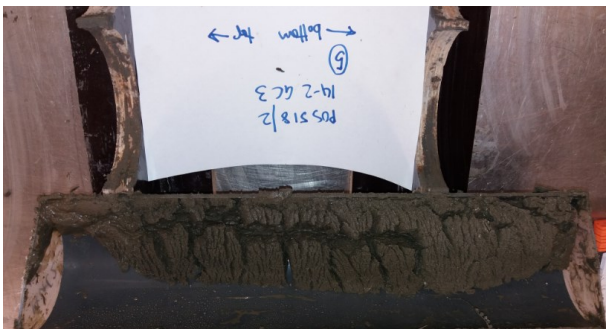

50-150

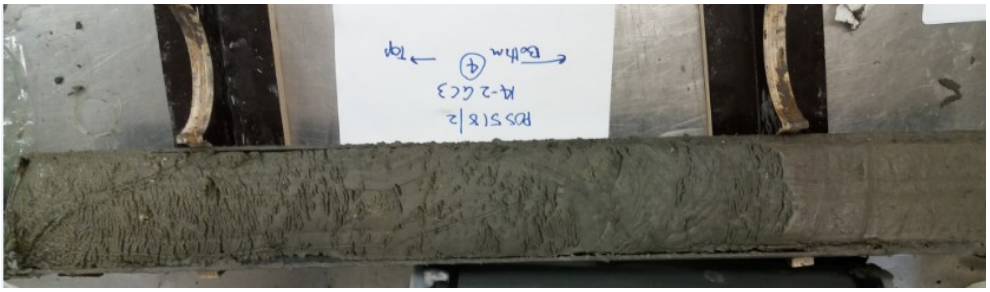

150-235

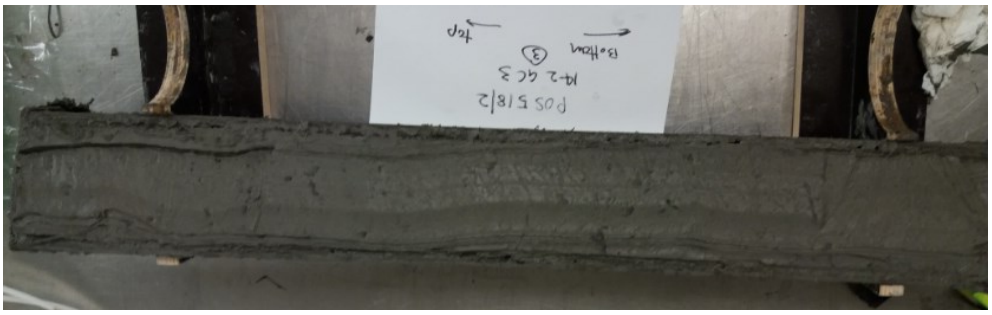

235-335

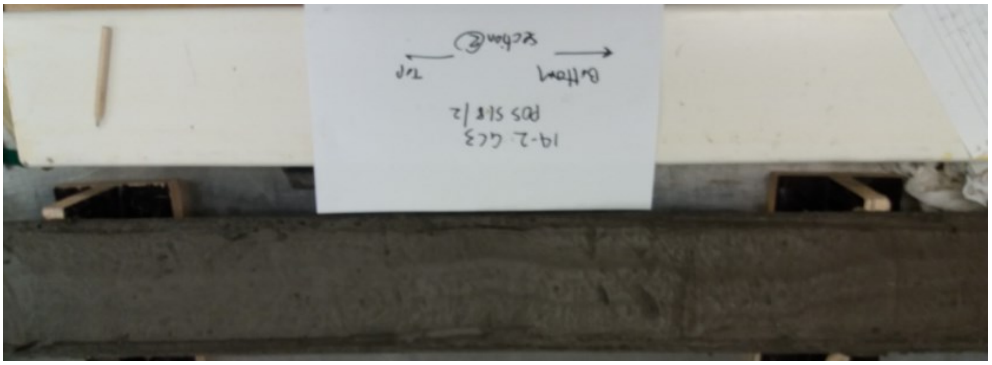

335-435

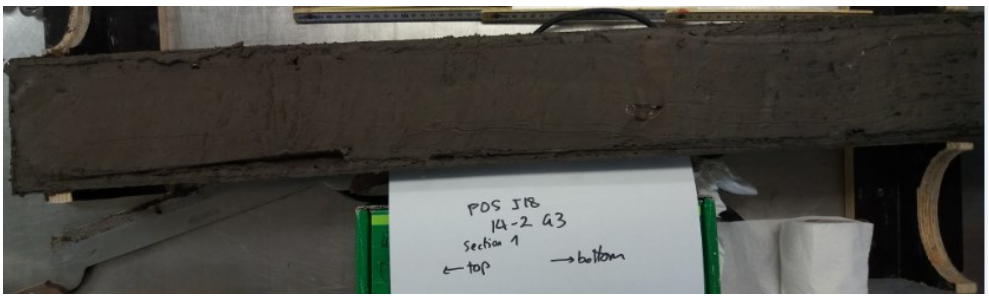

Leg 2: 14/2 GC 3 Complete working halves 0 – 435 cm

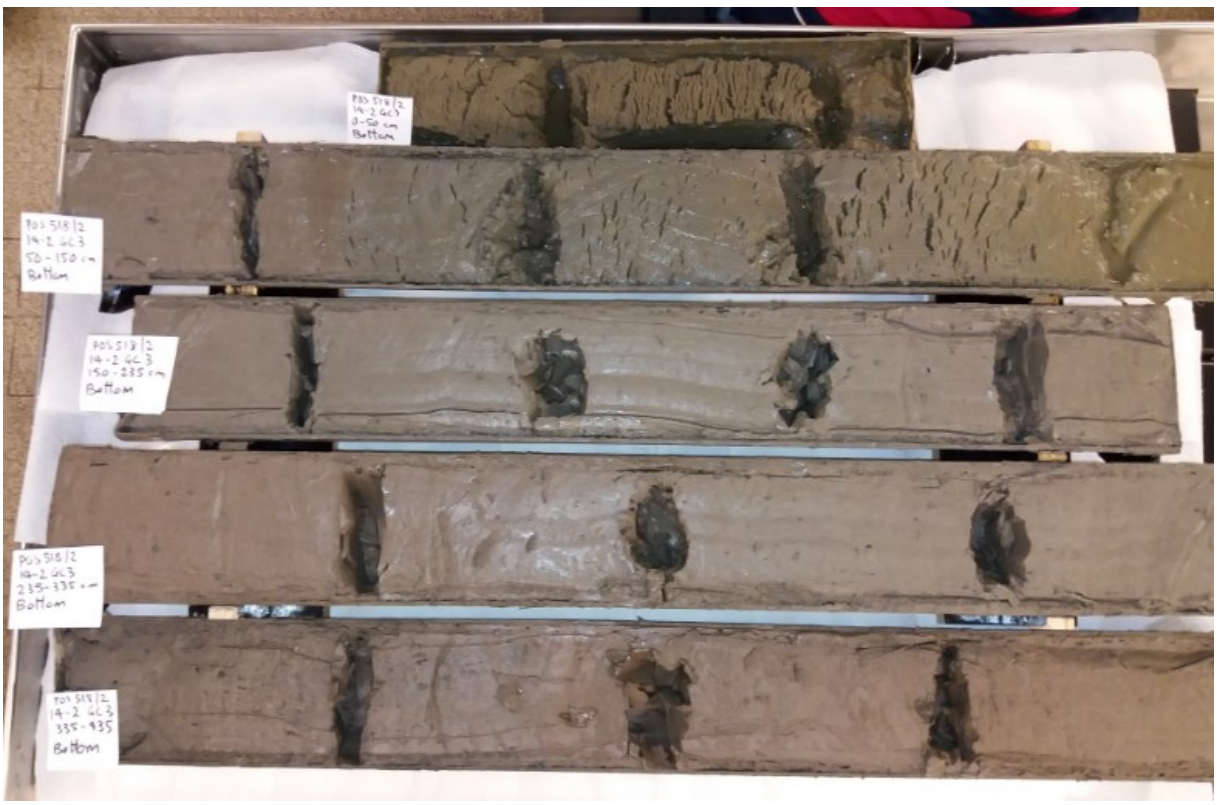

Leg 2: 2/1 MUC 1A SE Goldeneye (NOCS lander position) 30 cm long


Leg 2: 5 MUC 2A E Goldeneye 21 cm long


8.4 Multibeam Data

Survey: POS 518, Vessel: Poseidon, Acquisition system: Imagenex Delta T , Zone/Leg: Central North Sea, Operator: T. Weiß

Date	Time	File name	Line	Latitude	Longitude	Latitude	Longitude	Speed	Course	Depth	Remarks
28.09.17	17:56	28sep2017-175434.837		55° 28.93	4° 31.71	55.48216667	4.5285	3.3	243		START SURVEY Judd site
	18:10		1	55° 28.78	4° 30.95	55.47966667	4.515833333	2.9	259	31.61	sol1
	18:42			55° 28.27	4° 28.09	55.47116667	4.468166667	3	261	31.6	eol1, back to auto ping rate, persistent noise signal
	19:23	28sep2017-185928.837	2	55° 29.34	4°30.36	55.489	4.506	2.8	172	31.58	sol2
	19:45	28sep2017-193325.837		55° 28.27	4° 30.66	55.47116667	4.511	3.4	169	31.82	eol2, stop logging multibeam
29.09.2017	09:55			56° 57.15	2° 2.40	56.9525	2.04	0.2	103	80	START SURVEY
	09:59	29sep2017-100023.837	1	56° 57.26	2° 02.91	56.95433333	2.0485	3.3	55	80	sol1
flare	10:30	29sep2017-103021.837		56° 58.20	2° 05.3244	56.97	2.08874	2.8	55	81	flare
flare	10:30			56° 58.2247	2° 05.3667	56.97041167	2.089445	3.1	53	81	flare
	10:39	29sep2017-103612.837		56° 58.4779	2° 06.0408	56.97463167	2.10068	3	54	81	possible flare
flare	11:20	29sep2017-111503.837		56° 59.6655	2° 09.1621	56.994425	2.152701667	3	54	79	small flare
flare	11:22	29sep2017-112033.837		56° 59.7388	2° 09.3489	56.99564667	2.155815	3	54	79	flare on starboard side
	11:35	29sep2017-113018.837		57° 00.13	2° 10.39	57.00216667	2.173166667	3.3	16	84.89	eol1
	11:38		2	57° 00.23	2° 10.18	57.00383333	2.169666667	3.1	288	84.13	sol2
	11:46			57° 00.43	2° 09.53	57.00716667	2.158833333	3.3	308	84.55	eol2
	11:47	29sep2017-114602.837		56° 00.4459	2° 09.5103	56.00743167	2.158505	3	305	82	fish swarm?
	12:00	29sep2017-115546.837		57° 00.6219	2° 10.2499	57.010365	2.170831667	1	135	81	strong echos in watercolumn on starboard side
	12:02	29sep2017-120104.837		57° 00.55548	2° 10.2984	57.009258	2.17164	1	210	81	strong echos in watercolumn on port side (possible flare)
	12:04		3	57° 00.46	2° 10.11	57.00766667	2.1685	2.5	227	83.86	sol3
	12:05			57° 00.44220	2° 10.08462	57.00737	2.168077	2	221	80	strong echos in watercolumn
	12:10	29sep2017-120656.837		57° 00.30342	2° 09.86490	57.005057	2.164415	2	217	80	strong echos in watercolumn
	12:15			57° 00.10	2° 09.51	57.00166667	2.1585	3.2	224	85.42	eol3
flare	12:17	29sep2017-121406.837		57° 00.06288	2° 09.47292	57.001048	2.157882	1	186	85	big flare
	12:20		4	57° 00.06	2° 09.65	57.001	2.160833333	2.6	122	85.32	sol4

Date	Time	File name	Line	Latitude	Longitude	Latitude	Longitude	Speed	Course	Depth	Remarks
flare	12:20	29sep2017-122007.837		57° 00.06090	2° 09.64740	57.001015	2.16079	2	118	85	probably flare
flare	12:23			56° 59.9433	2° 09.8808	56.999055	2.16468	3	123	85	probably flare
flare	12:24			56° 59.92002	2° 09.95010	56.998667	2.165835	3	123	85	probably flare
	12:33			56° 59.8551	2° 09.96462	56.997585	2.166077	2	211	85	fish swarm?
	12:26			56° 59.88	2° 10.08	56.998	2.168	3.1	118	86.3	eol4
	12:32		5	56° 59.88	2° 09.98	56.998	2.166333333	2.6	196	86.36	sol5
	13:50	29sep2017-134121.837		56° 57.71	2° 04.30	56.96183333	2.071666667	3.4	231	91.35	Continuing line 5
	14:06	29sep2017-135341.837	6	56° 57.28	2° 03.06	56.95466667	2.051	3.2	318	90.01	eol5, sol6
	14:14	29sep2017-140900.837		56° 57.56	2° 02.54	56.95933333	2.042333333	3.4	316	90.77	eol6, END SURVEY
29.09.2017	17:55	20170929175438_079		56° 57.90	01° 12.51E	56.965	1.2085	8.7	293		START SURVEY
	18:32		1	56° 59.08	01° 08.61	56.98466667	1.1435	3.3	288		sol1
flare	18:42			56° 59.22	01° 7.69	56.987	1.128166667	2.9	286		flare on port side
	19:04			56° 59.5	01° 5.68	56.99166667	1.094666667	3.1	284		29/01c-9Z, no flare
	19:12		2	56°59.62	01° 05.2	56.99366667	1.086666667	3.2	284		eol1, sol2
	19:30		3	57° 0.06	1° 5.93	57.001	1.098833333	3	133		eol2, sol3
	19:40			56° 59.48	01° 05.67	56.99133333	1.0945	3	187		29/01c-9Z, no flare
	19:57		4	56° 58.633	1°05.402	56.97721667	1.090033333	2.8	125		eol3,sol4
	20:18		5	56° 58.409	1° 07.373	56.97348333	1.122883333	3	26		eol4,sol5
flare	20:34			56° 59.234	1° 7.739	56.98723333	1.128983333	3.3	5		29/01c-4, flare
	20:47			56° 59.881	1° 0.804	56.99801667	1.0134	3.5	355		END SURVEY

GEOMAR
Helmholtz-Zentrum für Ozeanforschung Kiel

GEOMAR Reports

No.	Title
1	FS POSEIDON Fahrtbericht / Cruise Report POS421, 08. – 18.11.2011, Kiel - Las Palmas, Ed.: T.J. Müller, 26 pp, DOI: 10.3289/GEOMAR_REP_NS_1_2012
2	Nitrous Oxide Time Series Measurements off Peru – A Collaboration between SFB 754 and IMARPE –, Annual Report 2011, Eds.: Baustian, T., M. Graco, H.W. Bange, G. Flores, J. Ledesma, M. Sarmiento, V. Leon, C. Robles, O. Moron, 20 pp, DOI: 10.3289/GEOMAR_REP_NS_2_2012
3	FS POSEIDON Fahrtbericht / Cruise Report POS427 – Fluid emissions from mud volcanoes, cold seeps and fluid circulation at the Don-_Kuban deep sea fan (Kerch peninsula, Crimea, Black Sea) – 23.02. – 19.03.2012, Burgas, Bulgaria - Heraklion, Greece, Ed.: J. Bialas, 32 pp, DOI: 10.3289/GEOMAR_REP_NS_3_2012
4	RV CELTIC EXPLORER EUROFLEETS Cruise Report, CE12010 – ECO2@NorthSea, 20.07. – 06.08.2012, Bremerhaven – Hamburg, Eds.: P. Linke et al., 65 pp, DOI: 10.3289/GEOMAR_REP_NS_4_2012
5	RV PELAGIA Fahrtbericht / Cruise Report 64PE350/64PE351 – JEDDAH-TRANSECT -, 08.03. – 05.04.2012, Jeddah – Jeddah, 06.04 - 22.04.2012, Jeddah – Duba, Eds.: M. Schmidt, R. Al-Farawati, A. Al-Aidaroos, B. Kürten and the shipboard scientific party, 154 pp, DOI: 10.3289/GEOMAR_REP_NS_5_2013
6	RV SONNE Fahrtbericht / Cruise Report SO225 - MANIHIKI II Leg 2 The Manihiki Plateau - Origin, Structure and Effects of Oceanic Plateaus and Pleistocene Dynamic of the West Pacific Warm Water Pool, 19.11.2012 - 06.01.2013 Suva / Fiji – Auckland / New Zealand, Eds.: R. Werner, D. Nürnberg, and F. Hauff and the shipboard scientific party, 176 pp, DOI: 10.3289/GEOMAR_REP_NS_6_2013
7	RV SONNE Fahrtbericht / Cruise Report SO226 – CHRIMP CHatham RIse Methane Pockmarks, 07.01. - 06.02.2013 / Auckland – Lyttleton & 07.02. – 01.03.2013 / Lyttleton – Wellington, Eds.: Jörg Bialas / Ingo Klaucke / Jasmin Mögeltönder, 126 pp, DOI: 10.3289/GEOMAR_REP_NS_7_2013
8	The SUGAR Toolbox - A library of numerical algorithms and data for modelling of gas hydrate systems and marine environments, Eds.: Elke Kossel, Nikolaus Bigalke, Elena Piñero, Matthias Haeckel, 168 pp, DOI: 10.3289/GEOMAR_REP_NS_8_2013
9	RV ALKOR Fahrtbericht / Cruise Report AL412, 22.03.-08.04.2013, Kiel – Kiel. Eds: Peter Linke and the shipboard scientific party, 38 pp, DOI: 10.3289/GEOMAR_REP_NS_9_2013
10	Literaturrecherche, Aus- und Bewertung der Datenbasis zur Meerforelle (Salmo trutta trutta L.) Grundlage für ein Projekt zur Optimierung des Meerforellenmanagements in Schleswig-Holstein. Eds.: Christoph Petereit, Thorsten Reusch, Jan Dierking, Albrecht Hahn, 158 pp, DOI: 10.3289/GEOMAR_REP_NS_10_2013
11	RV SONNE Fahrtbericht / Cruise Report SO227 TAIFLUX, 02.04. – 02.05.2013, Kaohsiung – Kaohsiung (Taiwan), Christian Berndt, 105 pp, DOI: 10.3289/GEOMAR_REP_NS_11_2013
12	RV SONNE Fahrtbericht / Cruise Report SO218 SHIVA (Stratospheric Ozone: Halogens in a Varying Atmosphere), 15.-29.11.2011, Singapore - Manila, Philippines, Part 1: SO218- SHIVA Summary Report (in German), Part 2: SO218- SHIVA English reports of participating groups, Eds.: Birgit Quack & Kirstin Krüger, 119 pp, DOI: 10.3289/GEOMAR_REP_NS_12_2013
13	KIEL276 Time Series Data from Moored Current Meters. Madeira Abyssal Plain, 33°N, 22°W, 5285 m water depth, March 1980 – April 2011. Background Information and Data Compilation. Eds.: Thomas J. Müller and Joanna J. Waniek, 239 pp, DOI: 10.3289/GEOMAR_REP_NS_13_2013

GEOMAR
Helmholtz-Zentrum für Ozeanforschung Kiel

GEOMAR Reports

No.	Title
14	RV POSEIDON Fahrtbericht / Cruise Report POS457: ICELAND HAZARDS Volcanic Risks from Iceland and Climate Change:The Late Quaternary to Anthropogene Development Reykjavík / Iceland – Galway / Ireland, 7.-22. August 2013. Eds.: Reinhard Werner, Dirk Nürnberg and the shipboard scientific party, 88 pp, DOI: 10.3289/GEOMAR_REP_NS_14_2014
15	RV MARIA S. MERIAN Fahrtbericht / Cruise Report MSM-34 / 1 & 2, SUGAR Site, Varna – Varna, 06.12.13 – 16.01.14. Eds: Jörg Bialas, Ingo Klaucke, Matthias Haeckel, 111 pp, DOI: 10.3289/GEOMAR_REP_NS_15_2014
16	RV POSEIDON Fahrtbericht / Cruise Report POS 442, "AUVinTYS" High-resolution geological investigations of hydrothermal sites in the Tyrrhenian Sea using the AUV "Abyss", 31.10. – 09.11.12, Messina – Messina, Ed.: Sven Petersen, 32 pp, DOI: 10.3289/GEOMAR_REP_NS_16_2014
17	RV SONNE, Fahrtbericht / Cruise Report, SO 234/1, "SPACES": Science or the Assessment of Complex Earth System Processes, 22.06. – 06.07.2014, Walvis Bay / Namibia - Durban / South Africa, Eds.: Reinhard Werner and Hans-Joachim Wagner and the shipbord scientific party, 44 pp, DOI: 10.3289/GEOMAR_REP_NS_17_2014
18	RV POSEIDON Fahrtbericht / Cruise Report POS 453 & 458, "COMM3D", Crustal Structure and Ocean Mixing observed with 3D Seismic Measurements, 20.05. – 12.06.2013 (POS453), Galway, Ireland – Vigo, Portugal, 24.09. – 17.10.2013 (POS458), Vigo, Portugal – Vigo, Portugal, Eds.: Cord Papenberg and Dirk Klaeschen, 66 pp, DOI: 10.3289/GEOMAR_REP_NS_18_2014
19	RV POSEIDON, Fahrtbericht / Cruise Report, POS469, "PANAREA", 02. – 22.05.2014, (Bari, Italy – Malaga, Spain) & Panarea shallow-water diving campaign, 10. – 19.05.2014, Ed.: Peter Linke, 55 pp, DOI: 10.3289/GEOMAR_REP_NS_19_2014
20	RV SONNE Fahrtbericht / Cruise Report SO234-2, 08.-20.07.2014, Durban, -South Africa - Port Louis, Mauritius, Eds.: Kirstin Krüger, Birgit Quack and Christa Marandino, 95 pp, DOI: 10.3289/GEOMAR_REP_NS_20_2014
21	RV SONNE Fahrtbericht / Cruise Report SO235, 23.07.-07.08.2014, Port Louis, Mauritius to Malé, Maldives, Eds.: Kirstin Krüger, Birgit Quack and Christa Marandino, 76 pp, DOI: 10.3289/GEOMAR_REP_NS_21_2014
22	RV SONNE Fahrtbericht / Cruise Report SO233 WALVIS II, 14.05-21.06.2014, Cape Town, South Africa - Walvis Bay, Namibia, Eds.: Kaj Hoernle, Reinhard Werner, and Carsten Lüter, 153 pp, DOI: 10.3289/GEOMAR_REP_NS_22_2014
23	RV SONNE Fahrtbericht / Cruise Report SO237 Vema-TRANSIT Bathymetry of the Vema-Fracture Zone and Puerto Rico TRench and Abyssal AtlaNtic BiodiverSITy Study, Las Palmas (Spain) - Santo Domingo (Dom. Rep.) 14.12.14 - 26.01.15, Ed.: Colin W. Devey, 130 pp, DOI: 10.3289/GEOMAR_REP_NS_23_2015
24	RV POSEIDON Fahrtbericht / Cruise Report POS430, POS440, POS460 & POS467 Seismic Hazards to the Southwest of Portugal; POS430 - La-Seyne-sur-Mer - Portimao (7.4. - 14.4.2012), POS440 - Lisbon - Faro (12.10. - 19.10.2012), POS460 - Funchal - Portimao (5.10. - 14.10.2013), POS467 - Funchal - Portimao (21.3. - 27.3.2014), Ed.: Ingo Grevemeyer, 43 pp, DOI: 10.3289/GEOMAR_REP_NS_24_2015
25	RV SONNE Fahrtbericht / Cruise Report SO239, EcoResponse Assessing the Ecology, Connectivity and Resilience of Polymetallic Nodule Field Systems, Balboa (Panama) – Manzanillo (Mexico), 11.03. -30.04.2015, Eds.: Pedro Martínez Arbizu and Matthias Haeckel, 204 pp, DOI: 10.3289/GEOMAR_REP_NS_25_2015

GEOMAR
Helmholtz-Zentrum für Ozeanforschung Kiel

GEOMAR Reports

No.	Title
26	RV SONNE Fahrtbericht / Cruise Report SO242-1, JPI OCEANS Ecological Aspects of Deep-Sea Mining, DISCOL Revisited, Guayaquil - Guayaquil (Equador), 29.07.-25.08.2015, Ed.: Jens Greinert, 290 pp, DOI: 10.3289/GEOMAR_REP_NS_26_2015
27	RV SONNE Fahrtbericht / Cruise Report SO242-2, JPI OCEANS Ecological Aspects of Deep-Sea Mining DISCOL Revisited, Guayaquil - Guayaquil (Equador), 28.08.-01.10.2015, Ed.: Antje Boetius, 552 pp, DOI: 10.3289/GEOMAR_REP_NS_27_2015
28	RV POSEIDON Fahrtbericht / Cruise Report POS493, AUV DEDAVE Test Cruise, Las Palmas - Las Palmas (Spain), 26.01.-01.02.2016, Ed.: Klas Lackschewitz, 17 pp, DOI: 10.3289/GEOMAR_REP_NS_28_2016
29	Integrated German Indian Ocean Study (IGIOS) - From the seafloor to the atmosphere - A possible German contribution to the International Indian Ocean Expedition 2 (IIOE-2) programme – A Science Prospectus, Eds.: Bange, H.W. , E.P. Achterberg, W. Bach, C. Beier, C. Berndt, A. Biastoch, G. Bohrmann, R. Czeschel, M. Dengler, B. Gaye, K. Haase, H. Herrmann, J. Lelieveld, M. Mohtadi, T. Rixen, R. Schneider, U. Schwarz-Schampera, J. Segschneider, M. Visbeck, M. Voß, and J. Williams, 77pp, DOI: 10.3289/GEOMAR_REP_NS_29_2016
30	RV SONNE Fahrtbericht / Cruise Report SO249, BERING – Origin and Evolution of the Bering Sea: An Integrated Geochronological, Volcanological, Petrological and Geochemical Approach, Leg 1: Dutch Harbor (U.S.A.) - Petropavlovsk-Kamchatsky (Russia), 05.06.2016-15.07.2016, Leg 2: Petropavlovsk-Kamchatsky (Russia) - Tomakomai (Japan), 16.07.2016-14.08.2016, Eds.: Reinhard Werner, et al., DOI: 10.3289/GEOMAR_REP_NS_30_2016
31	RV POSEIDON Fahrtbericht/ Cruise Report POS494/2, HIERROSEIS Leg 2: Assessment of the Ongoing Magmatic-Hydrothermal Discharge of the El Hierro Submarine Volcano, Canary Islands by the Submersible JAGO, Valverde – Las Palmas (Spain), 07.02.-15.02.2016, Eds.: Hannington, M.D. and Shipboard Scientific Party, DOI: 10.3289/GEOMAR_REP_NS_31_2016
32	RV METEOR Fahrtbericht/ Cruise Report M127, Extended Version, Metal fluxes and Resource Potential at the Slow-spreading TAG Midocean Ridge Segment (26°N, MAR) – Blue Mining@Sea, Bridgetown (Barbados) – Ponta Delgada (Portugal) 25.05.-28.06.2016, Eds.: Petersen, S. and Shipboard Scientific Party, DOI: 10.3289/GEOMAR_REP_NS_32_2016
33	RV SONNE Fahrtbericht/Cruise Report SO244/1, GeoSEA: Geodetic Earthquake Observatory on the Seafloor, Antofagasta (Chile) – Antofagasta (Chile), 31.10.-24.11.2015, Eds.: Jan Behrmann, Ingo Klaucke, Michal Stipp, Jacob Geersen and Scientific Crew SO244/1, DOI: 10.3289/GEOMAR_REP_NS_33_2016
34	RV SONNE Fahrtbericht/Cruise Report SO244/2, GeoSEA: Geodetic Earthquake Observatory on the Seafloor, Antofagasta (Chile) – Antofagasta (Chile), 27.11.-13.12.2015, Eds.: Heidrun Kopp, Dietrich Lange, Katrin Hannemann, Anne Krabbenhoeft, Florian Petersen, Anina Timmermann and Scientific Crew SO244/2, DOI: 10.3289/GEOMAR_REP_NS_34_2016
35	RV SONNE Fahrtbericht/Cruise Report SO255, VITIAZ – The Life Cycle of the Vitiaz-Kermadec Arc / Backarc System: from Arc Initiation to Splitting and Backarc Basin Formation, Auckland (New Zealand) - Auckland (New Zealand), 02.03.-14.04.2017, Eds.: Kaj Hoernle, Folkmar Hauff, and Reinhard Werner with contributions from cruise participants, DOI: 10.3289/GEOMAR_REP_NS_35_2017

GEOMAR
Helmholtz-Zentrum für Ozeanforschung Kiel

GEOMAR Reports

No.	Title
36	RV POSEIDON Fahrtbericht/Cruise Report POS515, CALVADOS - CALabrian arc mud VolcAnoes: Deep Origin and internal Structure, Dubrovnik (Croatia) – Catania (Italy), 18.06.-13.07.2017, Eds.: M. Riedel, J. Bialas, A. Krabbenhoeft, V. Bähre, F. Beeck, O. Candoni, M. Kühn, S. Muff, J. Rindfleisch, N. Stange, DOI: 10.3289/GEOMAR_REP_NS_36_2017
37	RV MARIA S. MERIAN Fahrtbericht/Cruise Report MSM63, PERMO, Southampton – Southampton (U.K.), 29.04.-25.05.2017, Eds.: Christian Berndt and Judith Elger with contributions from cruise participants C. Böttner, R.Gehrmann, J. Karstens, S. Muff, B. Pitcairn, B. Schramm, A. Lichtschlag, A.-M. Völsch, DOI: 10.3289/GEOMAR_REP_NS_37_2017
38	RV SONNE Fahrtbericht/Cruise Report SO258/1, INGON: The Indian - Antarctic Break-up Engima, Fremantle (Australia) - Colombo (Sri Lanka), 07.06.-09.07.2017, 29.04.-25.05.2017, Eds.: Reinhard Werner, Hans-Joachim Wagner, and Folkmar Hauff with contributions from cruise participants, DOI: 10.3289/GEOMAR_REP_NS_38_2017
39	RV POSEIDON Fahrtbericht/Cruise Report POS509, ElectroPal 2: Geophysical investigations of sediment hosted massive sulfide deposits on the Palinuro Volcanic Complex in the Tyrrhenian Sea, Malaga (Spain) – Catania (Italy), 15.02.-03.03.2017, Ed.: Sebastian Hölz, DOI: 10.3289/GEOMAR_REP_NS_39_2017
40	RV POSEIDON Fahrtbericht/Cruise Report POS518, Baseline Study for the Environmental Monitoring of Subseafloor CO_2 Storage Operations, Leg 1: Bremerhaven – Bremerhaven (Germany), 25.09.-11.10.2017, Leg 2: Bremerhaven – Kiel (Germany), 12.10.-28.10.2017, Eds.: Peter Linke and Matthias Haeckel, DOI: 10.3289/GEOMAR_REP_NS_40_2018

For GEOMAR Reports, please visit:
https://oceanrep.geomar.de/view/series/GEOMAR_Report.html

Reports of the former IFM-GEOMAR series can be found under:
https://oceanrep.geomar.de/view/series/IFM-GEOMAR_Report.html

GEOMAR
Helmholtz-Zentrum für Ozeanforschung Kiel

Das GEOMAR Helmholtz-Zentrum für Ozeanforschung Kiel ist Mitglied der Helmholtz-Gemeinschaft Deutscher Forschungszentren e.V.

The GEOMAR Helmholtz Centre for Ocean Research Kiel is a member of the Helmholtz Association of German Research Centres

Helmholtz-Zentrum für Ozeanforschung Kiel / Helmholtz Centre for Ocean Research Kiel
GEOMAR
Dienstgebäude Westufer / West Shore Building
Düsternbrooker Weg 20
D-24105 Kiel
Germany

Helmholtz-Zentrum für Ozeanforschung Kiel / Helmholtz Centre for Ocean Research Kiel
GEOMAR
Dienstgebäude Ostufer / East Shore Building
Wischhofstr. 1-3
D-24148 Kiel
Germany

Tel.: +49 431 600-0
Fax: +49 431 600-2805
www.geomar.de